Investigating Novel Cerebrovascular Therapies for Neurodegenerative Disease

Naomi King

A thesis submitted in partial fulfilment of the requirements for the degree of

Doctor of Philosophy

March 2025

Acknowledgements

This PhD has truly been a journey, and I have so many people to thank for helping me reach this point.

Firstly, a huge thank you to my supervisors. Jason, your unrelenting enthusiasm and positivity towards the research is truly infectious. Your ability to be patient and understanding while also making sure to give me the kick I needed at times has kept this whole PhD on track, made it a great experience, and allowed me to develop not just my scientific skills but confidence in my own abilities, and I will forever be grateful for that.

Clare, you have truly been a rock. You have always answered my questions, and always been willing to chat, whether about stats, life, or myriad other PhD questions. You were always there with motivation and inspiration (and chocolate when the situation called for it). Thank you for always making time and being a true inspiration.

Ivan, your drive has kept the project going, and kept everyone fully invested, even at the times it seemed nothing would work.

Everyone in the Sheffield Neurovascular Lab, you have kept this experience fun, even through the days stuck in a darkened room for hours on end. Our office chats provided much needed breaks (and often nonsense) and thank you to everyone for putting up with my venting sessions when things weren't quite going to plan, and for your artistic input to this thesis!

Of course, this PhD couldn't have happened without my collaborators and fellow dark room inmates. Tom and Spencer, through the highs and lows you kept me sane, with ridiculous puns, and DnD chats. Our experimental days (with all that came with them) make up some of my best memories from this whole experience. We really did make a pretty cool team.

To the friends I have made in Sheffield, I truly wouldn't have made it without you. Nick, for the coffees, lunches, and generally always being up for a venting session or much needed distraction. L'udka, for our hot chocolate dates, for matching my weirdness, and always being an inspiration to me, even when far away. I love you and will forever be grateful to Sheffield for bringing us together.

To the friends who have been there from the beginning, thank you for putting up with my lack of conversational diversity over the last few years, and for always seeming to know when I need a pick-me-up. Yasmin, I can't imagine telling the 16-year-old versions of us laughing over chemistry squares that this is where we'd end up, and I can't imagine making it to this point without you being there, every step of the way, to remind me that I truly do love science, even when it's determined to go wrong!

To my family, what do I even say? You always supported me and accepted all my idiosyncrasies. Mum and Dad, even from afar your support and willingness to listen to me prattle on about my projects, and everything else besides has been invaluable. Ben and Josh, you inspired my love of science, and even now are showing me the way through life.

Phoebe, you are the best sister anyone could ask for, and made sure I know that great things can happen when you don't leave writing to the last minute!

Angus, my goose. You have supported me every step of the way, even when it meant being stuck in different countries. You have taken care of me, providing hugs, home cooked meals, and motivation when I needed it the most. You have listened to every presentation, talked through every scientific problem, and invested in every experiment with me. Thank you for being here through all the highs and the lows, and for always believing that I can do anything I set my mind to, even when I don't believe it myself. I truly couldn't have done this without you.

Finally, to my laptop, for surviving long enough to write this thesis, to Sarah and Simon for your constant warm support, to the hundreds of cups of tea, coffee, and hot chocolate that kept me going, and to me, for never giving up.

We did it!

Abbreviations

2D-OIS	Dimensional Optical Imaging Spectroscopy
4-AP	4-Aminopyridine
AD	Alzheimer's disease
AEDs	Anti-epileptic drugs
APOE2	Apolipoprotein E 2
APOE4	Apolipoprotein E 4
APP	Amyloid Precursor protein
ASM	anti-seizure medication
ATP	Adenosine Triphosphate
BBB	Blood Brain Barrier
CBF	Cerebral blood flow
CNS	Central nervous System
CO2	Carbon Dioxide
COX-2	Cyclooxygenase-2
CSF	Cerebrospinal fluid
DBS	Deep brain stimulation
EEG	Electroencephalogram
ELISA	enzyme-linked immunosorbent assay
fMRI	functional MRI
GFAP	glial fibrillary astrocytic protein
GWAS	Genome wide Association Study

HbO	Oxygenated Haemoglobin
HBOT	hyperbaric oxygen therapy
HbR	Deoxygenated Haemoglobin
HbT	Total Haemoglobin
HR-EEG	High-resolution electroencephalogram
IBA1	ionized calcium-binding adapter molecule 1
ILAE	International League Against Epilepsy
LFP	Local Field potential
LITT	Laser Interstitial Thermal Therapy
LPGE1	lipo-prostaglandin E1
MABP	Mean Arterial Blood Pressure
MCA	middle cerebral artery
MCI	Mild Cognitive Impairment
mGluRs	Metabotropic glutamate receptors
MRI	magnetic resonance imaging
MST	Multiple subpial transections
NFT	Neurofibrillary Tangle
nNOS	neuronal Nitric Oxide Synthase
NO	Nitrous Oxide
NVC	Neurovascular coupling
NVU	neurovascular unit
PET	positron emission tomography
PSEN1	Presenilin-1

PSEN2	Presenilin-2
PUFAs	polyunsaturated fatty acids
RNS	Responsive neurostimulation
SE	Status Epilepticus
SHL	sudden hearing loss
SMCs	Smooth Muscle Cells
SMRs	standardised mortality ratios
SPECT	single-photon emission computed tomography
SUDEP	Sudden Unexpected Death in Epilepsy
TEC	thermoelectric cooler
TRPA1	transient receptor potential ankyrin 1
TRPM8	transient receptor potential melastatin 8
VNS	Vagus Nerve Stimulation
WHO	World Health Organisation

Contents

Declaration of Contribution

I Naomi King, declare that the work presented in this thesis is my own. The work has not been previously submitted at this university or others for the award of a higher degree.

This thesis includes work performed in collaboration with others:

1) **Chapter 3** – All surgeries and experiments described in chapter 3 were performed by Dr Jason Berwick and Dr Luke Boorman. All data analysis and writing was undertaken by myself.
2) **Chapter 4** – All surgeries and experiments described in chapter 4 were performed by myself and Dr Thomas Paterson. Design and manufacture of the implant was performed by Dr Spencer Moore. Data analysis and writing was undertaken by myself.
3) **Chapter 5 –** All experiments and data collection were performed by myself. Methoxy-XO4 staining and perfusions were performed by both myself and Llywelyn Lee. All data analysis and writing was undertaken by myself.

Abstract

This research aimed to investigate novel cerebrovascular therapies for neurodegenerative diseases, with a particular focus on epilepsy and Alzheimer's Disease.

Background: Epilepsy is one of the most common neurological conditions worldwide, affecting roughly 50 million people. Of those diagnosed with epilepsy 30-40% do not respond to pharmacological treatment and rely on surgical or dietary interventions to attempt to control their seizures. These interventions are not appropriate for all patients, and there are a number of risks associated with uncontrolled seizures, including increased risk of injury and sudden death.

Alzheimer's disease (AD) is the most common cause of dementia, with approximately 50 million people currently diagnosed, and this number expected to double every 5 years. Current treatments focus on symptom management, targeting acetylcholine or glutamate levels within the brain to improve cognitive function, though they are not able to alter the disease course. The newest treatments (lecanemab and donanemab) target amyloid plaques, reducing levels within the brain and slowing cognitive decline, though they are only effective for patients early in the disease course, and are not available on the NHS.

Blood flow is known to be altered in both epilepsy and AD. Epileptic seizures result in significant alterations to the cerebral blood flow, resulting in post-ictal hypoxia, which is postulated to contribute to continuing epileptogenesis. Cerebrovascular alterations are also identified in over 50% of clinically diagnosed AD cases with blood flow alterations likely occurring even before cognitive symptoms develop. As such, therapies that target cerebral blood flow could provide breakthroughs in treatment for both epilepsy and AD patients.

Cooling for the reduction of neuronal seizure activity has been considered as a potential therapy for epilepsy patients for many years, however, the impact of cooling on haemodynamic activity has not been thoroughly investigated. The difficulties of creating a cooling device suitable for translation into patients have also prevented progression of this therapeutic approach, but new technological advances have allowed reconsideration of cooling as a therapy. Research into increasing blood flow in AD has identified positive effects of hyperbaric oxygen treatment, increasing cerebral blood flow and potentially decreasing cognitive deficits. This treatment requires patients to travel to clinics, while an in home gas treatment could reduce the disruption for patients. Carbogen gas (95% O_2, 5% CO_2) combines the positive impact of oxygen, with the vasodilatory effects of CO_2, potentially increasing the benefit that could be gained from breathing pure oxygen in a standard environment.

Aims: 1) To investigate the impact of cortical cooling on neural and haemodynamic activity induced by 4-AP seizures. 2) To test a novel cooling implant, investigating the impact of its cooling on 4-AP induced seizure activity. 3) To investigate carbogen gas as a potential therapy for Alzheimer's disease.

Cooling was investigated using an anaesthetised 4-AP model of seizures, with cooling being supplied by either a skull-attached chamber over a thinned cranial window, or a novel cooling device positioned within a craniotomy. Carbogen treatment was applied in the APP/PSEN1 mouse model of AD for 1 hour a day over 2 months.

Results: Cooling from both a skull-attached chamber and novel cooling implant was capable of reducing neuronal activity induced by 4-AP. Cooling from a skull-attached chamber altered the haemodynamic activity during 4-AP induced seizures, with a novel finding showing

differing impact of cooling in the middle cerebral artery (MCA), compared to the surrounding cortical tissue. Cooling to 25°C with the novel cooling implant was sufficient to reduce neuronal activity, compared to cooling to 10°C being required with the skull attached chamber. Carbogen gas treatment did not affect amyloid plaque load, but there was a lesser plaque burden in cortex surrounding major branches of the MCA. This novel finding suggests an important role of blood flow in amyloid accumulation.

Conclusions: These results provide novel insights into the impact of cooling on both neural and haemodynamic activity. They also demonstrate how cooling can be converted into a feasible therapeutic device for patients with drug resistant epilepsy. They show a novel finding supporting the role of blood flow in the clearance of amyloid plaques in an AD model. Finally, they demonstrate the importance of cerebrovascular approaches to novel therapies for neurodegenerative diseases.

Chapter 1

Introduction

1.1 Summary

The work in this thesis was conducted with the aim of exploring novel vascular therapies for neurodegenerative diseases. Chapters 3 and 4 focus on the utility of cooling as a therapy for drug resistant focal epilepsy, building on previous experimental work conducted within the Sheffield Neurovascular Lab, while chapter 5 explores the potential for Carbogen to be used as a therapeutic for Alzheimer's disease. This literature review will examine epilepsy and Alzheimer's disease as neurodegenerative diseases, introduce the neurovascular unit and neurovascular coupling, and identify the ways in which we can exploit the neurovasculature to treat these diseases.

1.2 Neurovascular coupling

Before exploring the defects in blood flow that occur in disease, and discussing the potential for exploiting the cerebrovasculature for therapeutic purposes, we must first understand the mechanisms responsible for controlling cerebral blood flow within the healthy brain.

1.2.1 Background of Neurovascular coupling

The brain is the most complex organ of the human body and uses 20% of the body's metabolic reserves (Garlick 1992; Howarth et al 2012; Padamsey and Rochefort 2023). However, despite its complex metabolic needs the brain lacks the ability to store its own energy, instead receiving energy substrates (namely oxygen and glucose) from the blood supply. This means that the smallest changes in supply could have serious consequences for the brain's metabolism and function, with a reduction in flow potentially causing chronic brain injury, and cessation of flow resulting in irreparable brain damage and potentially death (Iadecola 2013).

For many years it was believed that the brain had no control over its blood supply, and that the supply was controlled purely by the systemic circulatory system (Friedland and Iadecola 1991), however we now understand that the brain plays a much more active role, as any change in neuronal activity is coupled with a change in blood flow.

Neurovascular coupling (NVC) is the mechanism linking neural activity to changes in cerebral blood flow, and is responsible for autoregulation and hyperemia within the brain (Attwell et al 2010). Autoregulation is the process which maintains cerebral blood flow constant between 50-120mmHg and protects the brain from increases in blood flow during physiological processes such as exercise and pathology like cardiogenic shock (Paulson et al 1990; Silverman and Petersen 2024). This occurs at a macro level throughout the brain. By contrast hyperemia functions at the micro level, changing delivery of blood and energy substrates to fit the level of activity in specific activated areas. This was first described by Roy and Sherrington (1890), and has since been found to occur during activity such as reading, calculating and mental exercise, as well as during seizures when one area requires an increased supply (Nippert et al 2018).

1.2.2 The Neurovascular Unit

The concept of the neurovascular unit (NVU) was formally introduced by the Stroke Progress Review Group meeting in 2001 (Iadecola 2017), and since then research has elucidated the role of many aspects of the NVU in NVC in both health and disease.

The NVU was defined by Harder (2002) as “a structure formed by neurons, interneurons, astrocytes, basal lamina covered with smooth muscular cells, and pericytes, endothelial cells, and extracellular matrix”. Every component of the NVU is intricately linked to establish an anatomical and functional whole thus creating a highly efficient system for the regulation

of cerebral blood flow. Communication occurs via gap junctions between components, adhesion molecules and ionic channels facilitating influx and efflux of ions as well as action of neuromodulators. Each component of the NVU plays a specific and active role in maintaining the reciprocal dynamic linkages under physiologic conditions.

1.2.3 Neurons

Neurons have previously been referred to as the "pacemakers" of the NVU, due to their role communicating both directly and indirectly with local blood vessels. Glutamatergic activity is key in the regulation of blood flow, as it acts on post-synaptic NMDA and AMPA receptors thereby leading to increased levels of neuronal intracellular calcium ($[Ca^{2+}]i$) and activation of Ca2+ dependent enzymes. These enzymes include nNOS and COX-2 which produce the potent vasodilators NO and prostanoids (Attwell et al 2010; Lecrux et al 2011). NO will diffuse into the vascular smooth muscle cells, activating soluble guanylyl cyclase, which in turn forms cyclic guanosine monophosphate, inhibiting constriction and thereby promoting vasodilation (Krawutschke et al 2015; Ahmad et al 2018). Prostanoids act via specific prostaglandin receptors within vascular endothelium to increase levels of cyclic adenosine monophosphate and trigger vasodilation (Murray 1990; Chen et al 2014). Adenosine (produced from ATP) also acts as a potent vasodilator, with a role for ATP being theorised in the neocortex and the retina through action on purinergic receptors (Iadecola 1993; O'Regan 2005). Studies have also found unique roles depending on the specific neuronal subtype studied (Iadecola 2017) demonstrating the vast array of neuronal vasomodulatory actions.

1.2.4 Astrocytes

The position of astrocytes with their close connections to both synapses and microvessels means they are well situated to link neuronal activity with microvascular function. Astrocytic

endfeet make contact with both vascular smooth muscle cells and pericytes providing a large source of contact that can act as a fast and efficient surface facilitating the action of neurotransmitters and neuromodulators. Early investigation into the role of astrocytes in NVC identified the role of metabotropic glutamate receptors (mGluRs) (Zonta et al 2003). These G-protein coupled receptors are involved in the release of Ca2+ from the endoplasmic reticulum, and it was found that increasing [Ca2+]i levels directly or via mGluR agonist was sufficient to induce arteriole dilation in cortical slices. This astrocytic control of blood flow has been strongly linked to the production and release of arachidonic acid metabolites due to increases in astrocytic [Ca2+]i (Attwell et al 2010), and it was later found that the effect of increased astrocytic [Ca2+]i was mediated by multiple different physiological factors to situationally produce both constriction and dilation (Iadecola 2017). However, despite a strong understanding of mechanisms of Ca2+ release in astrocytes, the downstream mechanisms remain unclear, with many studies stating that the Ca2+ release is too slow, or even occurs after a vascular response has already been initiated (Iadecola 2017).

1.2.5 Endothelial cells

It is well known that endothelial cells play a vital role in regulation of CBF, producing both vasoactive and trophic factors which control vascular tone in response to mechanical and chemical inputs (Andresen et al 2006; Iadecola 2017). Upon dilation at a specific site within the brain it is necessary for this dilation to spread to upstream vessels in order to facilitate the increased flow without harming the flow to neighbouring vascular territories (Segal 2015). Endothelial cells have been shown to play a vital role in this process, with lesioning studies demonstrating that endothelial lesions markedly affected the amplitude and temporal dynamics of the haemodynamic response (Chen et al 2014). Endothelial cells have

therefore been shown to play a vital role in both the temporal coordination and full expression of haemodynamic responses to neuronal activation.

1.2.6 Pericytes and Myocytes

The signals generated by neurons, astrocytes, and endothelial cells all take action on the vasomotor apparatus of the vasculature. Within the majority of blood vessels this vasomotor apparatus is composed of smooth muscle cells, while in the capillaries they are replaced by pericytes (Iadecola 2017). Smooth muscle cells will contract and relax in response to a number of vasoactive agents, and in response to vasodilatory stimuli originating from downstream vessels (Ngai et al 1988; Longden et al 2017). Smooth muscle cells are also able to respond to changes in intravascular pressure, allowing blood pressure increases and decreases to trigger vasoconstriction and vasodilation respectively (Koller and Toth 2012; Longden et al 2016). This is especially common in penetrating arterioles, and these changes in resistance (known as cerebrovascular autoregulation) act to keep CBF relatively stable during changes in arterial pressure.

Pericytes are known to play a role in establishing and maintaining vascular structure and the BBB, but their role in regulating blood flow is less established. Certain studies have found pericytes to be contractile, responding to brain-generated vasoactive signals, and altering capillary diameter (Hall et al 2014; Peppiatt et al 2006). However, other studies have failed to establish a relationship between pericytes and flow regulation, or suggest that any impact of pericyte contractility on flow is not significant (Hill et al 2015; Fernandez-Klett et al 2010). This seeming contradiction in the current literature is possibly a result of the highly heterogeneous morphology of pericytes, as it is still unknown what functional significance this heterogeneity may have.

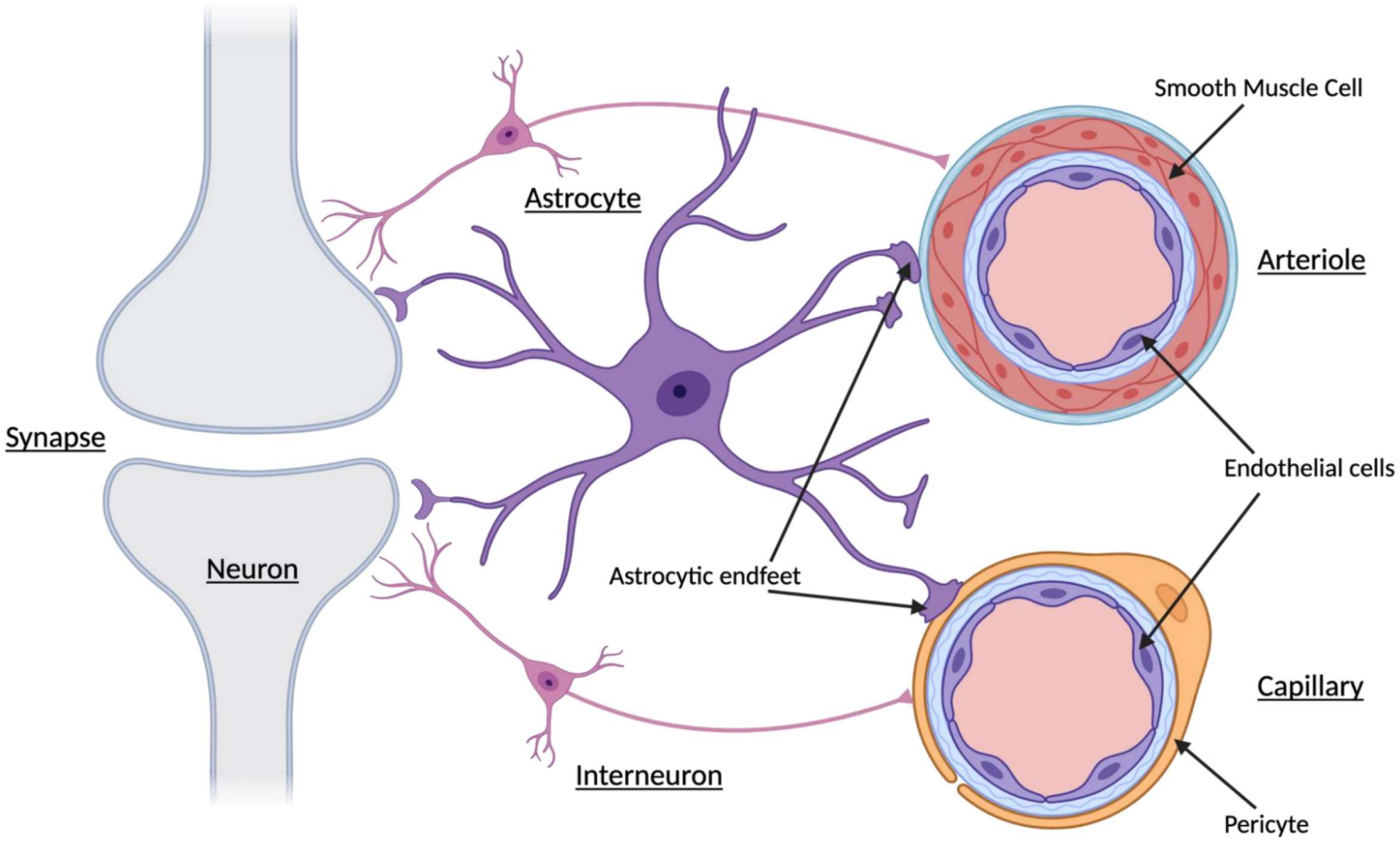

Figure 1.1 – The Neurovascular Unit

NVC occurs thanks to the complex relationships between numerous cells, including neurons, interneurons, astrocytes, endothelial cells, pericytes, and smooth muscle cells. The complex signalling mechanisms (described above) result in

1.2.7 Summary

The NVU plays a vital role in maintaining cerebral homeostasis, with all elements of the NVU working together to react to the changing environment and metabolic requirements of the brain. This therefore provides an important area of investigation when NVC breaks down or is impacted by a disease state. This thesis investigates novel therapeutic approaches to neurodegenerative disorders, with a focus on cerebral blood flow and NVC.

1.3 Epilepsy

1.3.1 Definition and general background

Epilepsy is one of the most common neurological conditions worldwide, characterised by disruptions in network activity within the brain that manifest as seizures (Fisher et al 2005). Seizures are paroxysmal events occurring because of abnormal synchronous neuronal firing within a section of the brain, or throughout its entirety (Falco-Walter 2020). They can be the result of irregularly formed networks, or networks being disrupted by structural, infectious, or metabolic disturbances.

A clinical epileptic seizure is defined as abnormal synchronised neuronal activity in the brain that causes transient clinical signs or symptoms, it is a transient event, and should have a clear start and stop, though termination of seizure activity is often less clinically obvious due to the postictal period (Fisher et al 2005).

Though seizures are the defining symptom of epilepsy it is possible to experience seizures without receiving an epilepsy diagnosis, with febrile seizures occurring in roughly 3% of children under the age of 5 (Shinnar and Glauser 2002), and in adults hypoglycaemia can result in non-epileptic seizures. Epilepsy is therefore defined as a disease in which one has either: One or more unprovoked or reflex seizures greater than 24 hours apart; an epilepsy syndrome; or a single unprovoked or reflex seizure in a person who has a ≥60% risk of having another seizure over the next 10 years (Fisher et al 2014).

20-30% of Epilepsy cases have a clear extrinsic or acquired cause, such as head trauma or stroke (Jallon et al 2001). The remaining 70% of cases have strong genetic components, whether that be as a causal factor, or through conferring increased susceptibility (Hildebrand et al 2013).

1.3.2 Prevalence and incidence

The likelihood of having a single seizure in one's lifetime is 10%, and most people who have a single seizure will not develop epilepsy. Despite this epilepsy is one of the most common neurological diseases, affecting roughly 50 million people worldwide (WHO epilepsy, 2019). Epilepsy has an incidence of 50.4 to 81.7 per 100,000 people per year (Beghi et al, 2019). However, there is significant incongruity in prevalence and incidence of epilepsy between high and low-income countries. Low and middle-income countries are found to be greatly more affected, with the WHO stating that nearly 80% of people living with epilepsy come from low or middle-income countries, and with incidence rates sometimes climbing to as many as 139 per 100,000. This discrepancy is likely multifactorial with factors including higher rates of parasitic infections, increased rates of head trauma, lack of available treatment and potentially genetic factors, though this effect is still undetermined.

There is no prevalence difference by gender, but differing aetiologies by age group do result in a bimodal distribution of prevalence. The first peak occurs as a result of genetic and developmental disturbances at around the ages of 5-9 years, and the second occurs around the age of 80 years as a result of accumulated injury to the brain (Falco-Walter 2020).

1.3.3 Epilepsy and Seizure Classification

Before treatment can be started, and to aid in the selection of appropriate treatments, both the seizures and epilepsy type must be classified (Falco-Walter 2020).

Seizures can be classified using either basic or expanded classification. This separation allows those in need of a more rigorous classification to receive one, while also preventing non-specialist practitioners and patients from becoming overwhelmed by classification (Fisher et

al 2017). The basic classification system can be broken down into 3 main components: onset, awareness level, motor involvement. Onset can be classified as focal - starting from a specific focus, generalised - both hemispheres are involved at onset, or unknown - insufficient data to classify onset. Awareness is then used to subclassify focal or unknown onset seizures, with awareness necessarily being impaired in generalised onset seizures. Finally, the motor component is considered. If motor symptoms are present, they can be described as “tonic-clonic” (involving both stiffening and twitching/jerking) or “other motor”. These components would then lead to a description of the specific seizure type, e.g. “focal aware seizure” or “generalised tonic-clonic seizure”.

Once the seizure type has been determined the epilepsy itself can be classified, considering all types of seizures present for the patient. These types break down to: focal, generalised, combined, and unknown (Scheffer et al 2017).

1.3.4 Prognosis and treatments

Recurrent seizures carry a number of risks, with seizure-related injuries occurring in up to 43% of patients (Asiri et al 2022), while studies find standardised mortality ratios (SMRs) to be significantly elevated, with a collection of 17 population and clinic based studies including all ages finding SMRs ranging from 1.6 to 7.5, with the highest SMRs occurring in studies looking solely at children (Thurman et al 2017).

Epilepsy is deemed resolved if no seizures have occurred for at least 10 years, and no medications have been taken to treat epilepsy for at least the past 5 years, or if one had an age dependent epilepsy syndrome, and has now passed the age above which it resolves (Falco-Walter 2020).

Studies have shown that 55-68% of newly diagnosed patients will achieve prolonged seizure freedom (Beghi et al 2015). This will however differ depending on the underlying aetiology, with idiopathic epilepsies showing more favourable rates of remission than symptomatic epilepsies, and patients with neurological dysfunction present at birth showing the lowest rates of seizure freedom (Annegers et al 1979).

1.3.5 Pharmacological treatments

The frontline treatment for epilepsy is pharmacological intervention with anti-seizure medication (ASM). There are currently 30 ASMs available, with nearly all being indicated as potential treatments for focal epilepsy, while fewer are indicated for treatment of generalised or unclassified epilepsy (Löscher and Klein 2021).

Once a patient's seizure type has been accurately identified, an appropriate ASM will be selected for use as a monotherapy. Treatment is started at a low dose and is increased to a moderate dose in order to minimise potential for adverse effects. If another seizure occurs, the dose is gradually increased until there are no more subsequent seizures, the maximal dose is reached, or adverse events occur. When assessing ASMs the primary outcome measures are often median reduction in seizure frequency, and proportion of patients achieving >50% reduction in seizure frequency (often referred to as responders).

Most ASMs result in 20-30% median seizure frequency reduction, and a 30-50% responder rate, with some newer studies finding 20% of patients achieving >75% reduction in seizure frequency (Löscher and Klein 2021).

If the selected ASM does not prevent persistent seizures, the maximal dose is reached, or adverse events occur, a second ASM will be trialled in similar manner to the first.

In the event that two appropriately selected ASMs are not successful in preventing persistent seizures, treatment with more than one ASM may be considered. There is still comparatively little information regarding the selection of optimal ASMs for polytherapy, and this course of treatment increases the risk of the patient experiencing adverse events or drug-drug interactions, thereby reducing rates of compliance (Guberman 1998).

1.4 Drug Resistant Epilepsy

Despite a near annual release of new ASMs, a number of patients will not respond to pharmacological interventions and will be diagnosed with intractable or treatment-resistant epilepsy.

A patient will be classified as having intractable epilepsy if they continue to experience persistent seizures following trials of 2 appropriately selected ASMs at optimal doses (administered either as single or multidrug therapies) (Kwan et al 2010).

Long-term outcome studies have found that following failure of two well-tolerated ASM schedules the chance of success with future drug regimens becomes progressively less likely (Kwan and Brodie 2000, Mohanraj and Brodie 2006). As a result, refractory epilepsy can often be identified early in the course of treatment, and it is possible that drug resistance is present from the beginning in a number of patients.

Drug resistant epilepsy occurs in roughly 30-40% of patients, but is more common in focal epilepsy at a rate of 40%, while in generalised epilepsy remission rates vary by syndrome (92% for tonic-clonic seizures alone, 59-90% for juvenile myoclonic epilepsy, 37-84% for childhood and juvenile absence epilepsy) (Kanner and Bicchi 2022).

1.4.1 Consequences of Uncontrolled Epilepsy

Drug resistance in epilepsy means that seizures will continue to occur, and this is associated with a number of risks to the patient. Ongoing seizures (particularly tonic-clonic seizures) are the most significant risk factor for sudden unexplained death in epilepsy (SUDEP (Ryvlin et al 2019)) , while also increasing the risks of other negative consequences of seizures, ranging from higher potential for mild injury such as scrapes and bruises, to a higher risk of drowning (Mahler et al 2018, Watila et al 2018). In total mortality rates for patients with drug resistant epilepsy have been found to be as high as 7 times those of the general population (Strzelczyk et al 2017).

Separate from the physical risks however there are also a number of personal consequences including loss of independence resulting from being unable to drive, and loss of employment opportunities. The impact of this loss of independence can be demonstrated by the estimated annual cost of epilepsy, which in Europe has been estimated to be €15.5 billion per annum (Pugliatti et al 2007).

Patients with drug resistant epilepsy have a number of non-pharmacological options available to assist in controlling their seizures.

1.4.2 Surgical interventions

Surgical interventions for epilepsy fall into three main categories: resection, palliative procedures, and neuromodulation. This section will focus on resective and palliative surgical procedures, with neuromodulatory techniques being discussed in greater detail below.

Surgical resection involves removal of the area of the brain from which the seizures are originating, known as the epileptogenic zone. The epileptogenic zone can be understood as a region of tissue “necessary and sufficient for initiating seizures” (Jehi, 2018). There are

multiple forms of resection depending on the location of the epileptogenic zone, and the functionality of the overlying cortical tissues, but generally resections are classified as either temporal, or extratemporal. More recently laser interstitial thermal therapy has been introduced as a minimally invasive approach, utilising MRI guided laser heat ablation to lesion epileptogenic cortical zones. Palliative procedures occur where a single seizure focus cannot be identified, or is located in eloquent cortical areas not suitable for resection. The aim of palliative procedures is to reduce seizure burden in order to improve quality of life, and they include procedures such as corpus callosotomy, hemispherectomy, and multiple subpial transection (Milovanović et al, 2020).

Eligibility criteria

Only a certain portion of epilepsy patients are eligible for surgical treatment, and one of the most important factors to consider is aetiology. A number of patients will be deemed unsuitable for surgical treatment as it is unlikely to provide long-term relief or control. For example, if seizures are the result of pathology that causes multiple epileptogenic lesions, or the pathology would continue even after surgical resection of the lesion (Milovanovic et al, 2020). Surgery is therefore only indicated in roughly 30-40% of those with medically refractory epilepsy.

Pre-surgery localisation

Prior to surgical resection the epileptogenic zone must be identified through use of multiple different imaging modalities, including magnetic resonance imaging (MRI), High-resolution electroencephalogram (HR-EEG), positron emission tomography (PET) and single-photon emission computed tomography (SPECT). These non-invasive techniques allow for identification and localisation of any structural or electrical abnormalities that would

indicate the location of seizure focus. Once an epileptogenic zone has been identified, multiple techniques are utilised such as functional MRI (fMRI), the wada test, and tractography to determine eloquent cortical areas, dominant hemisphere for language and memory, and locations of white matter tracts in order to minimise post-surgical deficits. Surgeons may also employ electrocorticography, in an attempt to more precisely determine the boundaries of the epileptogenic zone and reduce the volume of tissue to be resected (Milovanovic et al 2020, Ahmad et al 2020). Following localisation of the epileptogenic zone in relation to eloquent cortical areas surgeons must then decide whether surgical intervention is appropriate, or guide patients towards management techniques such as vagus nerve stimulation or responsive neurostimulation. The outcomes associated with surgical management and neuromodulation techniques will be discussed below.

Outcomes

The outcomes of surgical intervention for epilepsy are judged using the Engel Surgical Outcome Scale (Engel et al 1993). This scale defines 4 classes of seizure outcome, each with subclasses adding specificity to the classification. The 4 main classes are: class 1 - free of disabling seizures, class 2 - rare disabling seizures (almost seizure free), class 3 - worthwhile improvement (a significant reduction in seizures, or increase in time between seizures), class 4 - no worthwhile improvement. This scale is widely used, but was simplified and clarified by the International League Against Epilepsy (ILAE) to create their own outcome scale consisting of 6 classes of outcome. Class 1 - freedom from seizures and aura, class 2 - auras with no other seizures, class 3 - 1 to 3 seizure days per year, class 4 - between 4 seizure days and 50% reduction in baseline seizure days, class 5 - less than 50% reduction in seizure days, class 6 - greater than 100% increase in baseline seizure days (Wieser et al 2001). Either of these

classification systems may be used to describe patients' surgical outcomes, and they demonstrate the wide range of outcomes that are possible for those undergoing surgical treatments.

1.4.3 Resection Surgeries

Temporal lobectomy

Temporal lobectomy outcomes are superior to those for prolonged pharmacological intervention, with systematic reviews suggesting seizure freedom occurs in 66 to 70% of patients followed up between 1- and 5-years post-surgery (Engel et al 2012, Spencer and Huh 2008). Some studies even reported seizure freedom rates of up to 84% after 1 year (Jeong et al 1999). It is however also noted that in patients with greater than 5 years follow up seizure freedom rates are recorded at between 41 and 79%. This discrepancy is possibly due to lower numbers of patients reporting for long term follow up after the 5-year mark (Spencer and Huh, 2008).

Extratemporal resections

Extratemporal seizure foci are found in roughly 20% of medically refractory epilepsy cases. A longitudinal study of 58 patients with frontal extratemporal epilepsy (Lazow et al 2012) found that 57% of patients achieved an Engel class 1 outcome, however, only 24% were completely seizure free without auras (Engel class 1A) for the entire follow-up period (79.3 months). Meta-analysis of 1,200 patients reported that 45.1% of patients with frontal lobe epilepsy achieved seizure freedom following surgery, and this increased to 46% of patients with parietal-occipital epilepsy (Englot et al 2012). Due to the variety in pathologies treated with extratemporal resection the outcomes tend to be more varied than those for temporal

lobectomies, but generally those patients' receiving treatment for focal pathologies (e.g. tumours) have more favourable outcomes (Ahmad, Khanna and Sani 2020).

Laser Interstitial Thermal Therapy (LITT)

As LITT is a relatively new technique there is limited availability of outcome data. However, a recent systematic review of 21 articles found averages of roughly 56% Engel class 1, 19% Engel class 2, 17% Engel class 3, and 10% Engel class 4 (Alomar et al 2023).

Palliative procedures

Palliative procedures have become less common following the introduction of neuromodulatory technologies (Ahmad, Khanna and Sani 2020), yet they nevertheless play a vital role in epilepsy management, and can significantly improve quality of life in carefully chosen patients.

Multiple subpial transections (MST)

MST is frequently used in conjunction with resection in non-eloquent areas, and as such limited data is available on outcome measures. A 2018 review of patient data (Rolston et al 2018) found that when non-eloquent resection was combined with MST the seizure freedom rate was 55.2%, while MST alone provided a seizure freedom rate of just 23.9%. However, studies of radiating MST (where the transections are performed from a singular cortical entry point) found seizure freedom rates between 42-67% (Ntsambi-Eba et al 2013, Finet et al 2019)This suggests that modified MST could be highly beneficial for those ineligible for traditional resective procedures, while traditional MST is most effective when used as an additional treatment in combination with resection of non-eloquent areas.

Corpus callosotomy

Corpus callosotomy refers to a procedure whereby the corpus callosum of the patient is sectioned. There is still debate surrounding corpus callosotomy surgeries and whether partial or complete disconnections are most beneficial for patients, particularly considering the risk of patients developing split-brain syndrome. First described by Sperry in 1958, this is a phenomenon whereby the two hemispheres of the brain process information entirely separately from one another. When studied it is found that when a participant is presented with an image solely to the left visual field (processed in the right hemisphere) they are unable to verbally identify having seen the stimulus (the speech centre occurring primarily in the left hemisphere). However, when asked to point with the left arm (controlled by the right hemisphere) towards the object represented in the image, the participant will successfully identify the object, even while the left hemisphere reports having not seen anything at all.

One systematic review of paediatric patients (Graham, Tisdall and Gill 2016) found that transient disconnection syndrome (a milder, temporary occurrence of split-brain syndrome) occurred in 12.5% of total callosotomy patients. However, the same systematic review found that 88.2% of patients undergoing total callosotomy had a worthwhile reduction in seizure frequency, compared to 58.6% of patients receiving anterior callosotomy. A later meta-analysis of 58 studies and 1,742 patients including both adults and children found that only 18.8% of patients achieved seizure freedom (Chan et al 2018).

Hemispherectomy

Hemispherectomy involves disconnection of the cortex of one hemisphere from that of the contralateral hemisphere. This is generally performed in young children due to the severe nature of the indicating symptoms. Published results of hemispherectomy present seizure freedom rates ranging between 54% and 90% (Lew 2014). A systematic review finding of

seizure freedom rates of 73.4% after 1 year of follow-up (Griessenauer 2015) makes hemispherectomy one of the most successful forms of epilepsy surgery. However, the high rate of seizure freedom must be balanced against the severe side effects that can occur as a result of the procedure, with over 20% of patients requiring hydrocephalus treatment following hemispherectomy (Lew et al 2013).

1.4.4 Neuromodulation

Vagus nerve stimulation

For patients whose seizures are not adequately controlled, they may consider neuromodulation-based interventions, with the most well-known option being Vagus Nerve Stimulation (VNS). VNS has been used since 1997 (Ahmad et al 2020) and has been approved for use in both focal and generalised epilepsy. The VNS system consists of a battery powered device that resembles a cardiac pacemaker, and a pulse generator, which is implanted below the collarbone with a lead being wrapped around the left vagus nerve where it lies within the carotid sheath. It is still unclear the precise mechanism of action for VNS, but it has been hypothesised that it is a peripheral form of thalamic stimulation, with stimulation propagating to the locus coeruleus which has been implicated as playing a major role in the antiseizure properties of VNS. This hypothesis is backed by the remarkably similar results from the two treatment modalities (Ben-Menachem 2012).

A secondary hypothesis is stimulation causing upregulation of noradrenaline in the amygdala and $GABA_A$ receptor density in the hippocampus, with responders being found to have significantly increased $GABA_A$ receptor density compared to both controls and non-responders (Marrosu et al 2003).

Randomised controlled trials examining the short-term efficacy of VNS have found that 23%-57% of patients achieve 50% reduction in seizure frequency (termed as 'responders'). Long-term studies have found that response to VNS can also increase with duration of treatment. These studies followed up for periods of 3-64 months and found that 21%-54% of patients achieved a 50% reduction in seizure frequency (González et al 2019). One group (Englot et al 2016) conducted a review of patient outcome registry data (5554 patients) and a literature review (2698 patients). The registry data review concluded that, at 0-4 months post implantation, 49% of patients were responders and 2.6% were seizure free, while at 24-48 months 63% were responders with 8.2% being seizure free. The literature review found that 40% were responders at 0-4 months (2.6% seizure free) and at last follow-up, 60.1% were responders with 8.0% being seizure free. They also found an important correlation between age of epilepsy onset and rates of seizure freedom. 11.3% of those over 12 years of age at epilepsy onset achieved seizure freedom compared with 7.3% of those under 12 at epilepsy onset.

Responsive neurostimulation

Responsive neurostimulation is designed to treat those with up to two seizure foci who are not eligible for resective surgery. It involves a closed-loop intracranial electrical stimulation system that both detects seizures and provides stimulation as required, prior to the onset of seizures. Up to two surface or depth electrode arrays are implanted within the seizure foci and connected to a cranially implanted generator (Ahmad et al 2020). The major RNS study first published results in 2011, then in 2014 after 2-year follow-up, and many patients were then followed up for 7 years in a long-term treatment study. After 1 and 2 years of follow-up, responder rates were 44% and 55% respectively (Heck et al 2014). The long-term treatment

study results showed that after 9 years 73% of patients were classed as responders (with 30% achieving ≥90% reduction in seizure frequency), and median seizure reduction was 75% (Nair et al 2020).

Deep brain stimulation

Deep brain stimulation is more frequently used to treat movement disorders, such as Parkinson's disease, but has recently been introduced as a potential therapy for refractory epilepsy. Treatment requires implantation of 4 contact electrodes into the anterior nucleus of the thalamus. These electrodes are connected to a chest implanted pulse generator that is controlled by a clinician to provide personalised pulse stimulation. A randomised, double-blind study of 110 patients was performed to examine the efficacy of DBS in epilepsy (Fisher et al 2010), and found that treatment resulted in a 40.4% decrease in seizure frequency compared to 14.5% in the control group, after 4 months. Follow up after 2 years showed a 56% median reduction in seizure frequency, with 54% of patients achieving ≥ 50% reduction in seizure frequency, and 14 patients becoming completely seizure free for the 6 months prior to follow up. The study also found that DBS showed greater efficacy in those with temporal lobe epilepsy compared to frontal, and those without anatomic abnormalities.

1.4.5 Dietary interventions

With surgical intervention not being appropriate for a number of patients with refractory epilepsy, and bearing the potential for severe adverse effects, a number of patients prefer dietary interventions to control their seizures.

The ketogenic diet is the oldest dietary treatment for epilepsy, first being introduced in 1921. It consists of high fat content (80-90%), and low protein (6-8%) and carbohydrate (2-4%)

intake, with the aim of inducing ketosis in the patient (Verrotti et al 2020). Since the inception of the ketogenic diet, a number of different variations have arisen, with the aim of making it less restrictive and better tolerated, as well as improving growth in young children, where the reduced intake of fruits, vegetables, milk, and other vital nutrients can have a much greater impact.

The precise mechanism behind the efficacy of the ketogenic diet in treating epilepsy is unknown, but the most widely accepted hypothesis is that increasing ketone bodies and polyunsaturated fatty acids (PUFAs) plays a vital role in reducing seizure activity. It is thought that ketone bodies may induce an upregulation of inhibitory neurotransmitters, as well as activating potassium channels and increasing energy production within the brain, while PUFAs inhibit voltage gated sodium and calcium channels, and activate potassium channels, among a number of other potentially protective actions (Barzegar et al 2021).

The ketogenic diet has not been well studied in an adult population. One meta-analysis provided evidence of efficacy, with 13% of patients becoming seizure free, and 53% showing greater than 50% reduction in seizure frequency (Liu et al 2018). However, the study only included those patients who completed all trials and follow-ups, introducing the possibility for bias, as it is possible those who responded well were more likely to stay on until the end of studies. Additionally, further research is required to examine the different efficacies and adverse effects from the major subgroups of the ketogenic diet in adults.

The efficacy of ketogenic diets in children with epilepsy has been well studied. A review and meta-analysis by Sourbron et al (2020) found that in 5 randomised controlled trials 35-56.1% of patients (children and adolescents ≤18 years) achieved ≥50% reduction in seizure frequency. Generally, the research agrees that the classic ketogenic diet can be highly

beneficial for children with refractory epilepsy, and that for many children starting the ketogenic diet, their seizures are so severe or frequent, and have such a profound impact on quality of life, that any reduction in seizure frequency can have a meaningful positive impact, even if seizure freedom is not achieved.

While there are many reasons for a patient or family to choose a particular form of ketogenic diet over the others, Sourbron et al (2020) found that no one form of ketogenic diet is universally effective, or better than any of the others. A 10-year retrospective study of ketogenic diet therapies in 48 children found that neither the type of diet, nor the diet duration was predictive of seizure frequency reduction (Wibisono et al 2015).

Despite the promising results from a number of treatments for refractory epilepsy, there is still a population of patients who do not see relief, and are not eligible for a number of the treatment options. As such it is imperative that we continue to develop novel therapeutic approaches to reduce both seizure frequency, and the impact of seizures on patients' quality of life.

1.4.6 Conclusions/summary

Uncontrolled epilepsy can have devastating consequences for patients, increasing risks of injury and serious harm from seizure events, and current treatments are not able to help every patient.

Much of the general discourse surrounding epilepsy focuses on the neurological symptoms that occur as a result of seizure activity, however, it is of equal importance to understand the impact that this neurological activity has on cerebral blood flow, and what consequences this may have for patients, extending beyond the impact of acute seizure events.

1.5 Epilepsy and Neurovascular Coupling

1.5.1 Postictal hypoxia and hypoperfusion

It is well established that seizures cause dramatic changes in local blood flow and oxygen saturation levels. However, there is mixed evidence from patients (Fong et al 2000, Farrell et al 2016) and animal studies (Wolff et al 2020, Prager et al 2019) around whether seizures cause hyper- or hypo-perfusion.

Wolff et al (2020) examined alterations in cerebral oxygenation levels both during kainic acid induced status epilepticus, and self-generated seizures post status epilepticus. In this study they utilised the perforant path stimulation model, whereby the main excitatory input to the hippocampus is electrically stimulated (Kelsey et al 2000). This stimulation leads to kindling, whereby the repeated stimulation leads to an increase in the severity and frequency of seizures, and eventually spontaneous seizure activity without stimulation (Goddard et al 1969).

They found that hippocampal partial pressure of O2 (pO2) increased following seizure onset, and continued to increase for the duration of the seizure by roughly 0.8mmHg every 10 minutes, remaining high for up to 90 minutes post infusion. Using the perforant path stimulation model they also found that pO2 levels increased to beyond normoxic range 1.5 hours after stimulation was initiated, remaining high for the duration of stimulation. However, once kindling had been achieved and animals were experiencing self-generated seizure activity, these seizures induced a period of mild pO2 increase, followed by a sustained state of postictal hypoxia.

It has been hypothesised that the state of hyperoxia generated by prolonged status epilepticus contributes to damage induced by seizure activity. The periods of status epilepticus in these models cause sufficient damage to produce future self-generated seizures, and it is well known that the brain is particularly vulnerable to oxidative damage.

One study (Prager et al 2019) looked at capillary diameter changes, and pO2 in cortical slices, and examined the changes occurring over the course of multiple seizures. They found that initially, seizure activity resulted in a diameter increase of ~20%, but after 5 seizures capillaries failed to dilate, and no increase in diameter was seen in response to the increased neuronal activity. pO2 was found to be low for the entire duration of the seizures, but increased to normal levels within 5 minutes of cessation, with no difference in pO2 response between the first and the fourth seizure event. Later In Vivo studies of CBF found that changes in arteriole diameter varied over the time-course of a seizure. In the first 30 minutes a dilation was found of ~60%, but this decreased to ~35% over the course of 4 hours with no change in seizure severity. This shows a marked neurovascular decoupling to prolonged seizure activity, potentially resulting in permanent alterations to the process of NVC.

Clinical studies of epilepsy patients have historically shown similarly mixed results. Fong et al (2000) investigated blood flow in patients exhibiting postictal psychosis, and found that it was associated with hyperperfusion, in contrast to results from other patient studies demonstrating postictal hypoxia.

Farrell et al (2016) examined 10 patients with intractable epilepsy using arterial spin labelling scans. Cerebral blood flow (CBF) was quantified at baseline and in the postictal period, and maximal changes in blood flow quantified in ml/100g/min. The brain areas showing significant changes were compared to EEGs to determine concordance between activity and

perfusion. Maximal postictal CBF reductions of at least 10ml/100g/min were seen in 8 of the 10 patients, with the magnitude of hypoperfusion correlated with seizure duration. In the 2 patients who did not show hypoperfusion, seizure durations were notably shorter. In the 8 where hypoperfusion was seen, the area of maximal hypoperfusion overlapped with a brain structure related to the seizure activity suggesting that this hypoperfusion was a phenomenon localised to the seizure focus.

1.5.2 Mechanisms of post-ictal hypoxia

Much research has focussed on the potential mechanisms underlying postictal hypoxia. The widespread expression of COX-2, and its established role in neurovascular coupling made it a popular candidate for control of post-ictal hypoxia and hypoperfusion. Farrell et al (2016) found that behavioural alterations resulting from postictal hypoxia and hypoperfusion could be ameliorated through treatment with COX-2 or l-type calcium channel antagonists, without altering seizure intensity or duration. Further to this, they determined that while l-type calcium channel antagonists are effective when given immediately following seizure termination, COX-2 antagonists are only effective when given as a pre-treatment. As a result of these findings, a theory was proposed to explain the mechanisms that may result in postictal hypoperfusion. The model states that following sustained synaptic activity, neuronal COX-2 oxygenates its substrates to vasoactive products which then translocate to act on receptors located on vascular smooth muscle cells. This action then facilitates l-type calcium channel conductance, enabling extracellular calcium to enter the vascular SMCs. Elevated calcium levels engage the molecular machinery responsible for vasoconstriction, thereby leading to reduced flow, and consequent hypoperfusion, and localised hypoxia.

1.5.3 Impact of hypoperfusion and hypoxia

The impact of postictal hypoxia and hypoperfusion has been well established in the literature, with neuronal and behavioural impairments often occurring following a seizure event (Farrell et al 2016). One such behavioural impairment, Todd's Paresis, has symptoms so similar to an ischemic stroke (moderate to severe motor weakness) that it is often misdiagnosed as such (Masterson et al 2009). Further to this, Farrell et al (2016) conducted a study using a kindling model of seizures in rats, and found that when exposed to post-ictal hypoxic conditions during memory training (using the novel object recognition test) the rats were unable to distinguish between a familiar and novel object upon testing. This suggests that postictal hypoxia can have a profound effect on memory function. In addition to behavioural impairments, researchers are investigating anatomical changes that arise following seizures. These changes include enhanced BBB permeability, central inflammation, neuronal loss, and increased astrocyte size and count (van Vliet et al 2007, Vezzani et al 2011, Seifart et al 2010, Dingledine et al 2014). These anatomical changes are very similar to those occurring in ischemic stroke, and have been positively correlated with seizure frequency, and suggested to play a role in further epileptogenesis (Farrell et al 2017). Finally, a recent study (George et al 2023) utilised a kainic acid mouse model of SUDEP, and blocked postictal hypoxia using either COX-2 or l-type calcium channel antagonists. They found that blocking postictal hypoxia prolonged life, suggesting that it may play a causative role in SUDEP. As such, investigating haemodynamic responses to seizure activity and finding therapies that target not only neuronal activity but blood flow, may prove vital to improving both quality and length of life for those with drug resistant epilepsy.

1.6 Cooling in epilepsy

Cooling has been studied as a potential therapeutic for over half a century, with early research suggesting a clinical utility of cooling for head trauma and intractable pain (Fay 1959). Since then, multiple controlled studies have been conducted that have found benefits to patients after acute head trauma or asphyxia when treated with a temperature reduction of no more than 4°C (Azzopardi et al 2000, Inder et al 2004, Shankaran et al 2005).

The first indication that cooling could act as a potential therapeutic in epilepsy came in 1956, with generalised hypothermia preventing epileptiform activity in primates (Baldwin et al 1956). Further to this, in 1963 a study was published demonstrating the effects of local brain cooling on epileptiform activity, including termination of status epilepticus in one patient, and reduction in seizure frequency for two other patients, following application of cold Elliotts B solution (a buffered intrathecal electrolyte solution) to the exposed cortex (Ommaya and Baldwin 1963).

Application of iced saline to the neocortex during cortical mapping surgery has also been found to terminate focal spiking activity (Sartorius et al 1998, Karkar et al 2002). Earlier experiments (Sourek et al 1970) chilled patients under general anaesthesia to 29°C and used iced saline to cool their cortical temperatures to below 24°C. Follow up after 1 year found that 11 showed a marked decrease in seizure frequency, and 4 had been seizure free.

1.6.1 The theory of cooling for epilepsy

There are multiple theories for why cooling would reduce neuronal activity, though as yet there is no consensus on what specific mechanisms are involved in reducing epileptic discharges in response to cooling.

Evidence suggests that the effect of cooling on neuronal firing may depend on alterations in multiple different systems. Early studies into neuronal firing patterns found that threshold current and threshold potential values were dramatically decreased at 7°C compared to 26°C (Guttman 1962), and resting input resistance of the neurons was significantly increased during cooling (Thompson et al 1985). A more recent study (Yang et al 2006) showed that cooling to 5°C induced reversible blebbing of dendrite shafts, and loss of dendritic spines, and the same lab found that cooling of rat hippocampal slices between 33°C and 20°C dramatically reduced transmitter release in a way that could not be accounted for by reduced axonal conduction (Yang et al 2005). This is in keeping with findings in the rat visual cortex, whereby cooling from 33°C to 23°C reduced the probability of glutamate release from the synapse (Volgushev et al 2004), and in clinical populations where levels of glutamate, glycerol and lactate were all reduced during focal cooling (Nomura et al 2014). A recent study also found that activation of transient receptor potential melastatin 8 (TRPM8), which is an ion channel that detects cold temperatures and is activated at 15°C, reduced epileptiform spike activity in anaesthetised rats (Moriyama et al 2019).

These findings suggest that combined alterations of neuronal electrical properties, dendritic spines, neurotransmitter release, and ion channel activation all contribute to the reduction in epileptiform activity in response to cooling, though further research is required to fully elucidate the therapeutic mechanisms of focal cooling.

1.6.2 Cooling as a neurovascular therapy

Previous work within the Sheffield Neurovascular Lab has established that alterations in temperature can have profound effects on haemodynamic responses to neuronal activity (Boorman et al 2023). The study found that changes in cortical temperature significantly

altered both the timing and magnitude of haemodynamic responses, with cooling increasing the time between neuronal activation and subsequent peak in total haemoglobin levels. This built on work examining neurovascular responses to stimulation during seizure activity (Harris et al 2013) which found significant alterations in those haemodynamic responses. During seizure activity, increases in both total and oxygenated haemoglobin levels (in response to stimulation) were decreased, and responses in surrounding regions were also altered. This demonstrates that cooling is not only capable of altering neuronal activity, but also the vascular responses, potentially ameliorating the alterations found during seizure activity. Studies examining the effect of cooling in epilepsy have also demonstrated a correlation between cooling and blood flow, with one study (Nomura et al 2014) showing that cooling during epilepsy surgery reduced blood flow to the seizure focus in tandem with reduced seizure activity, while another (Harsono et al 2016) found that head cooling in a model of neonatal seizures prevented endothelial injury, and ameliorated postictal loss of cerebral vasodilation. These findings suggest that cooling can not only reduce the neuronal alterations seen in epilepsy, but may positively influence the haemodynamic responses, and potentially reduce the occurrence of postictal hypoxia, thereby improving outcomes for patients.

1.6.3 Difficulties with cooling for patients

The major drawback of generalised hypothermia as a treatment for epilepsy is the risk of severe adverse effects, such as tissue injury, and high rates of fatal arrhythmias and coagulation events (Polderman and Herold 2009, Rekha et al 2013). When utilising generalised hypothermia these risks are often outweighed by the potential benefits to a

patient, but in the case of epilepsy, focal cooling of the brain may present an alternative with many of the benefits, but without the risk to other bodily systems.

Historically, the difficulties with developing devices to deliver minimally invasive cooling have diminished its utility, and research into the potential for cooling as a therapeutic stalled due to the limitations of available technologies. Generalised hypothermia appeared effective in reducing seizures (Sourek and Travnicek 1970, Orlowski et al 1984, Niesvizky-Kogan et al 2022) but came with the risk of more generalised complications for other body systems. Meanwhile, many of the original focal cooling techniques (e.g. irrigation with cooled solutions) increased the risk of infection for patients, and were near impossible to utilise on a regular or permanent basis (Sartorius and Berger 1998, Csernyus et al 2021).

Developments in thermoelectric devices and the technologies that support them has now allowed cooling to be re-evaluated as a therapy, but there are further difficulties that must be addressed before moving to the clinic (Csernyus et al 2021).

Another major challenge for developing focal cooling as a therapeutic is establishing an appropriate temperature range to terminate seizure activity without causing damage to the cortex underlying the cooling device. The minimum level of cooling required to affect seizure activity has been highly studied but is still strongly debated. One study (Guilliams et al 2013) indicates that inducing mild hypothermia is effective in terminating seizure activity in children, supported by a rat study (D'Ambrosio et al 2013) suggesting that a drop of only a few degrees can have a profound effect on seizures. Other studies suggest cooling to anywhere between 25 and 15°C (Fujii et al 2010, Nomura et al 2014). This leads to further questions of safety. What is the maximal amount of cooling that can be applied in humans without causing damage to the brain?

1.6.4 Previous work on cooling in epilepsy

Many of the cooling methodologies employed in experimental settings would not be feasible for long-term implantation as a therapeutic strategy. One commonly used technique is to fill steel tubing with a cold solution (often chilled methanol or saline), with the change in temperature of the steel then cooling the surrounding tissue. This cryoloop system was first introduced by Horel et al (1984), and similar systems have since been used in the study of epilepsy, and many other neurological systems (Lomber et al 1999, Ponce et al 2008, Meredith et al 2011). This has proven to be very effective in producing temperature changes within the brain, and has the added benefit of providing cooling to deeper structures. However, these devices would prove difficult to chronically implant, and come with some significant safety risks. Some of the most significant difficulties come from the size and weight of the device, the metal used being incompatible with magnetic resonance imaging, lack of temperature feedback, and use of alcohols as the cooling solution. These difficulties were addressed by Cooke et al (2012) when they developed a lightweight chronically implantable version of the cryoloop, including a thermocouple for temperature measurement at the site of cooling. This device, while much lighter in weight, and potentially MRI compatible, still utilised ethanol as the cooling solution. While these systems were an effective way to provide cooling, they also came with many disadvantages. Primarily, any leak in the implanted system would result in the coolant directly contacting neural tissue, potentially causing permanent damage. Furthermore, the use of a chilled liquid coolant increases the time required to reach the lowest cooling temperatures, potentially prolonging the time before effective alteration of epileptiform activity.

The difficulties with producing a chronically implantable cooling device have meant that cooling was not a viable therapeutic option, however, developments in thermoelectric devices and the technologies that support them has now allowed cooling to be re-evaluated as a therapy.

1.6.5 Thermoelectric cooling devices

Thermoelectric cooling devices (Peltier chips) take advantage of the Peltier effect whereby a potential difference (a current) is capable of creating a temperature difference. Peltier chips are created from arrays of semiconductors which are connected electrically in series and contained between ceramic plates. Each individual semiconductor cube is 'doped' with impurities such that each cube contains either fewer (P-type conductor) or extra (N-type conductor) free electrons. These N and P type semiconductor cubes are then arranged such that they have a series electrical connection and parallel thermal connection. As current flows through the chip, a temperature difference is induced, causing one plate to rapidly cool, as the other heats. This cooling phenomenon has allowed the use of Peltier chips in the study of epilepsy (Rothman and Yang 2003). The first study utilising Peltier chips to study epilepsy was conducted by Hill et al (2000) and found that the cooling provided by the Peltier device was capable of terminating seizure activity induced by 4-AP injection. Since then, numerous studies have examined Peltier chips as conduits to deliver cooling in epilepsy models both to the cortical surface (Imoto et al 2006, Ren et al 2017) and to deep brain structures (Yang et al 2006, Tanaka et al 2008). Despite the success of these studies, demonstrating that Peltier devices are capable of significantly reducing seizure activity, there is still a lack of devices that are suitable for chronic implantation, and all of the devices described in these studies were controlled by an external operator. If cooling is to be

developed into a viable therapy it would require a self contained device, suitable for chronic implantation, and capable of operating without an external operator, thereby allowing patients the freedom to undertake daily activities without having to monitor potential seizure activity.

1.6.7 Conclusions/summary

Cooling provides a unique possibility for those patients who are not eligible for current surgical treatment options, with the potential to be used in areas of eloquent cortex not suitable for resection, and the possibility of deep brain cooling devices allowing for targeted treatment of deeper seizure foci.

However, despite the exciting possibilities cooling provides, there are still large advancements required to create a device that is suitable for use in patient populations. Permanent implantation requires all components be made from bio-safe materials, any coolant liquid must be non-toxic, and the system, including any power supply, should be self contained.

1.7 Alzheimer's disease

Alzheimer's disease is a neurodegenerative disease characterised by accumulation of Amyloid Beta plaques, and neurofibrillary tau tangles, thought to induce neuronal damage and dysfunction (Iadecola 2017). Alzheimer's is the most common cause of dementia, with around 50 million patients currently diagnosed worldwide, and this

number is expected to double every 5 years (Breijyeh and Karaman 2020). Alzheimer's causes memory loss, difficulty thinking, and trouble with language and problem solving skills.

1.7.1 Amyloid beta plaques and tau tangles

Alzheimer's pathology has been well studied, and the hallmark features associated with Alzheimer's disease are extracellular amyloid beta plaques, and intracellular neurofibrillary tangles, created by hyperphosphorylated tau (Armstrong 2009). Though both amyloid beta and tau occur in the healthy brain, during Alzheimer's pathogenesis a number of pathological processes occur in order to create the toxic variants seen in Alzheimer's disease.

For many years now Amyloid beta plaques have been considered the most important pathological feature of Alzheimer's disease, and the discovery of Amyloid beta within extracellular plaques in 1984 led to development of the amyloid cascade hypothesis of Alzheimer's pathogenesis (Hardy and Selkoe 2002).

Amyloid beta is formed from the amyloid precursor protein by cleavage of beta and gamma secretase (Selkoe et al 1996). The balance between continual formation of amyloid beta and sufficient clearance is vital for preventing toxic aggregation. Amyloid Precursor protein (APP) can be processed through both amyloidogenic and non-amyloidogenic pathways. The non-amyloidogenic pathway involves APP being first processed by alpha-secretase, and then gamma-secretase, to form soluble APPs-alpha fragments and a small p3 fragment. This pathway precludes the formation of Amyloid beta. The amyloidogenic pathway requires APP to first be cleaved by beta-secretase, forming APPs-beta and CFTβ. Gamma-secretase then cleaves CFTβ to form Amyloid beta (Chen et al 2017). Amyloid beta monomers can take many forms including oligomers, protofibrils and the more toxic fibrils that are larger, insoluble, and capable of forming amyloid plaques (Chen et al 2017). Forms of amyloid beta are denoted by the number of amino acids they contain, with this length being determined

by their cleavage by Gamma-secretase. The 42 amino acid form of amyloid beta (Aβ42) is more toxic than others, and more likely to seed plaques within the brain (Miller et al 1993, Armstrong 2009). Formation of amyloid beta 40 or lower occurs with much higher frequency than formation of amyloid beta 42 in a healthy patient, but in Alzheimer's disease this ratio is altered as levels of toxic Aβ42 increase within the brain, resulting in formation of extracellular plaques (Hardy and Selkoe 2002, Breijyeh and Karaman 2020).

Alongside amyloid plaques, neurofibrillary tangles consisting of hyperphosphorylated tau are a hallmark of AD (Naseri et al 2019). Tau is naturally present in developing and mature neurons, and plays a role in microtubule assembly and stability (Weingarten et al 1975). It exists normally in a 1:1 ratio of 4-repeat and 3-repeat tau, with 3-repeat tau being mainly produced during development, and 4-repeat tau being produced in adulthood. It has been suggested that disruption of this ratio may play a role in Alzheimer's disease, however no clear patterns have emerged (Goedert and Spillantini 2000). It is well known that hyperphosphorylation of tau is implicated in development of neurofibrillary tangles, as studies have shown that phosphorylation reduces tau's ability to bind microtubules, and induces self-assembly into tangles and filaments (Naseri et al 2019). The evolution of hyperphosphorylated tau within the brain can be tracked through the different stages of NFT development. As tau is naturally present within neuronal cells, the pre-tangle phase sees phosphorylated tau proteins accumulating within the somatodendritic compartment, but not forming paired helical filaments (Naseri et al 2019). Mature neurofibrillary tangles are characterised by filament aggregation alongside displacement of the nucleus, and extracellular tangles are the final stage, resulting from neuronal loss due to extreme levels of tau filaments.

1.7.2 Risk factors

It has been found that the strongest risk factors for developing Alzheimer's disease can be attributed to heritable factors, with risk being 60-80% dependent on genetics (Tanzi 2012). Early onset AD (also referred to as familial AD) occurs as a direct result of heritable factors, and accounts for <1% of AD cases. Familial AD can be attributed to mutations in the APP, PSEN1, and PSEN2 genes, these mutations are fully penetrant and causal of AD. Mutations in the APP gene account for ~15% of early onset AD cases, with PSEN1 mutations accounting for a much larger proportion (~80%), and PSEN2 mutations only accounting for 5% of cases (TCW and Goate 2017). In contrast, genetic impact on development of late onset AD is less direct, with multiple different genetic mutations passing on risk or protection (Andrews et al 2019). Determining risk for late onset AD involves polygenic risk scores, calculated thanks to large genome-wide association studies. GWAS has found that there are over 40 different AD associated risk alleles. However, APOE4 has the strongest association, with one APOE4 allele increasing the likelihood of disease 3-4 times, and homozygous APOE4 alleles increasing risk 10-fold while other risk alleles provide an odds ratio of only 1.05-1.2 (de Rojas et al 2021).

Alongside genetic risk factors, there are many modifiable and acquired risk factors that contribute to an individual’s likelihood of developing AD. The strongest risk factor for Alzheimer’s disease besides genetic factors is increased age (generally considered over 65), with evidence that the cellular and molecular consequences of ageing such as telomere shortening, increased DNA damage, and epigenetic changes all play a role in increasing risk of developing AD (Lopez-Otin et al 2013, Herrmann et al 2018, Hou et al 2019)

The other most commonly reported risk factors for AD are cerebrovascular diseases, with diabetes, hypertension, obesity and dyslipidemia all serving to increase the risk of AD development (Love and Miners 2016).

1.7.3 Prevention and protective factors

As with risk, protective factors will accumulate over a lifetime, and though it is impossible to state that a specific preventive or protective measure will eradicate a patient's risk of developing AD, research has found a number of factors that are protective against AD.

Firstly, as the APOE4 allele has been found to convey risk, the APOE2 allele has been demonstrated to confer protection. Those expressing the APOE2 allele have been found to have a slightly reduced risk, and increased mean age of onset, while those who are homozygous for the APOE2 allele have a greatly reduced risk of developing AD (Farrer et al 1997, Genin et al 2011).

Recent research has also identified a number of other potentially protective genes (Andrews et al 2019), however, there has so far been very little research completed investigating the mechanisms behind their protective effects.

Alongside genetic protection, lifestyle factors can play a large role in decreasing an individual's risk.

Cognitive reserve has been identified as a potential protective factor in Alzheimer's disease (Stern 2002, 2009). It has been observed in a number of cases that the histopathological findings post-mortem did not match the level of cognitive decline observed clinically (Neuropathology Group 2001). This led to the theory of cognitive reserve, relating to the brain's ability to use the existing healthy network, and the ability to recruit other neural

resources to support functioning in the presence of damage. Cognitive reserve is a theoretical construct, and as such is often measured through proxy variables such as: education level, occupational attainment, engagement in socially and cognitively engaging leisure activities (Nogueira et al 2022). Studies have shown that individuals with lower levels of schooling and professional achievement (indicating lower cognitive reserve) have a near 2-fold higher risk of developing dementia (Stern et al 1994). In addition, those who partake in more leisure activities (increasing cognitive reserve) have a lower risk of developing dementia (Scarmeas et al 2001).

Furthermore, recent meta-analysis has indicated that exercise can reduce the risk of Alzheimer's by roughly 45%, likely due to a network of factors such as reduced blood pressure, improvement in lipid profiles, and improved endothelial function (Hamer and Chida 2009). Exercise can also cause adaptations that lead to improved CBF, higher oxygenation of key cognitive areas, increase in hippocampal volume, and increased levels of brain derived neurotrophic factor which is associated with development and survival of neurons and synapses (Hamer and Chida 2009, Huang and Reichardt 2009, Paillard et al 2015).

1.7.4 Blood flow alterations in AD - The Vascular Hypothesis

Alongside the amyloid cascade hypothesis, there is a developing interest in the role of altered cerebral blood flow in the development of AD. The vascular hypothesis postulates that the combination of reduced CBF and increased BBB permeability lead to accumulation of neurotoxic macromolecules, causing neuronal dysfunction and neurodegenerative alterations independently of Aβ deposition (de la Torre and Mussivand 1993).

Recent studies have shown that vascular changes can be found in over 50% of clinically diagnosed AD cases (Cortes-Canteli and Iadecola 2020, Sweeney et al 2019). Decreases in cerebral blood flow have been found in areas such as the hippocampus, entorhinal cortex, amygdala, and anterior cingulum (Iadecola 2004, Hays et al 2016). These are all areas strongly associated with cognition, and impacted in AD pathology, suggesting that changes in blood flow may play a prominent role in the development of the disease process.

Analysis of images taken from the Alzheimer's Disease Neuroimaging Initiative and modelling of Late-onset AD suggests that this vascular dysfunction and dysregulation is actually an early event, and potentially contributes to initial pathology (Iturria-Medina et al 2016).

A number of studies have suggested that changes in the cerebrovascular system lead to decreased clearance of Aβ and elevated expression of APP, thereby exacerbating the problem of Aβ deposition (Weller et al 2008, Sagare et al 2012, Hughes et al 2014, 2018).

It has also been found that amyloid beta can have strong vasoactive effects, with one study demonstrating that the presence of amyloid beta reduced the increase in blood flow caused by acetylcholine in AD mice, even before formation of plaques or significant cognitive decline (Zhang et al 1997). Finally, amyloid beta is capable of inducing contraction in pericytes and vascular SMCs, thereby worsening hypoperfusion and BBB dysfunction (Deane et al 2003, Nortley et al 2019).

There have also been numerous reports of a relationship between vascular dysfunction and accumulation of phospho-tau. Chronic hypoperfusion as a result of left common carotid artery occlusion was found to increase levels of phospho-tau in the hippocampus of 3-month old AD mice, and in the hippocampus and cortex of 16-month old AD and WT mice (Qiu et al

2016). These findings were backed by similar findings in other animal models (Zhang et al 20120, Raz et al 2019), as well as in studies of AD patients (Rubinski et al 2021, Swinford et al 2023) where it was found that tau pathology was negatively correlated with CBF.

Finally, it has been found that reductions in cerebral blood flow can increase neuronal levels of amyloid beta and tau phosphorylation, while also impairing ATP synthesis, and decreasing neuron's abilities to fire action potentials (Kitaguchi et al 2009, Kelleher and Soiza 2013). These increases in levels of amyloid beta and phosphorylated tau could be attributed to decreased levels of glymphatic clearance in AD. It has been established that the glymphatic system plays an important role in the removal of proteins and metabolites from the brain (Jessen et al 2015), and that this waste removal system is impaired in AD (Peng et al 2016, Nedergaard and Goldman 2020). Researchers have found that the decrease in glymphatic drainage is associated with a decline in arterial pulsatility (Kress et al 2014), and as such, can be ameliorated by gamma stimulation (Murdock et al 2024), promoting arterial pulsatility and glymphatic drainage, and thereby decreasing amyloid burden.

These alterations in blood flow and subsequent decreases in glymphatic drainage can lead to worsening accumulation of toxins within the brain. As such, increasing cerebral blood flow is a potential therapeutic target to decrease cognitive deficits by increasing both clearance and neuronal functionality.

1.7.5 Current treatments

Current treatments for AD are primarily targeted towards reducing symptoms, rather than altering disease course, and as a result a significant portion of research has now turned to protection and risk reduction.

Pharmacological therapies for AD in the UK consist of a choice between 3 drugs: donepezil, galantamine, and rivastigmine (Anand and Singh 2013, Sharma 2019, Breijyeh and Karaman 2020). These drugs are either anticholinesterase inhibitors, or anti-glutaminergics, meaning they act either to increase acetylcholine levels within the brain, or to regulate glutamate levels. Acetylcholine is a vital component of the memory system, and enhancing its availability can partially correct the deficit found in the brains of those with AD (Bartus et al 1982, Tabet 2006). Glutamate also has important roles in learning and memory, but if levels are too high it can cause neuronal cell death, and this has been shown to occur in AD patients (Wang and Reddy 2017). These drug treatments can delay the progression of disease, as well as contributing to stabilisation or temporary improvement for patients (Breijyeh and Karaman 2020). However, these treatments are most effective in the earliest stages of disease, at a point that many people may not have been diagnosed. They are also unable to affect the course of the disease, meaning that even if someone receives treatment as soon as they are diagnosed, they will still progress through the disease course, and eventually reach a point where the current treatments are unable to help (Breijyeh and Karaman 2020).

The newest advancements in treatment for AD are immunotherapies, donanemab and lecanemab. These treatments have recently been approved for use in the UK, though will not be available for treatment on the NHS. Both donanemab and lecanemab have been shown to reduce levels of amyloid within the brain, as well as slowing the progression of cognitive decline in AD patients (van Dyck et al 2023, Sims et al 2023). While these drugs are a promising step, they are still only effective for those early in the course of the disease, and even for those patients, the decline associated with Alzheimer's disease is still only slightly slowed. As such further research is still needed to help a wider range of patients.

1.7.6 Future treatments

Despite ongoing research there are still very limited options for those living with AD, and the drugs that are currently available come with a number of side effects, such as loss of appetite, headaches, feeling tired or dizzy, and difficulty sleeping (Breijyeh and Karaman 2020). A number of these side effects are also symptoms that patients can already be suffering from, or can lead to greater problems further on. The most recently developed treatments for AD are focussed on reducing levels of Aβ42 through immunotherapies. This approach has shown some promise, however, as we broaden our view from the amyloid cascade hypothesis to looking at other factors such as blood flow, we also need to develop novel therapies targeting the dysfunction in these areas. If we can take a holistic approach to AD, taking into consideration genetics, age, cognitive reserves, vascular health, and all the other factors that contribute to disease development, we may finally move closer to developing a cure.

1.7.7 Treatments targeting cerebral blood flow

The necessity for novel treatments for AD is well known, and due to the difficulties being faced when designing treatments to target amyloid plaque formation, novel therapies are likely to come from targeting other systems such as cerebral blood flow.

One emerging research area is the impact of gamma oscillations (synchronous activity with a frequency of 20-50Hz) on plaque load in AD. Previous work has established that gamma oscillations are associated with increased CBF and arterial pulsatility (Balbi et al 2021, Murdock et al 2024), and induced gamma oscillations in AD mice have been shown to decrease amyloid load (Iaccarino et al 2016) and increase glymphatic clearance of amyloid (Murdock et al 2024).

Additionally, work to repurpose previously approved drugs to treat AD has found that sildenafil (viagra) could benefit AD patients. One study of both real world patient data and found that use of sildenafil was associated with a 54% reduced incidence of AD (Gohel et al 2024), while a recent study found that use of sildenafil increased cerebrovascular pulsatility and perfusion (Webb et al 2024).

Studies investigating the impact of gas treatments on neurovascular function in AD models have found that breathing 100% oxygen significantly enhanced baseline blood flow in AD mice (Shabir et al 2020), and hyperbaric oxygen therapy (HBOT) was able to reduce amyloid burden and tau phosphorylation, as well as improving behavioural deficits (Shapira et al 2018). One case study of HBOT in an AD patient found that an 8-week course of HBOT was able to reverse symptomatic decline, and created a 6.5-38% increase in brain metabolism (Harch and Fogarty 2018). A later study found that 20 days of 40 minute HBOT was able to improve cognitive function in patients with amnestic MCI and AD at 1, 3, and 6 month follow-up (Chen et al 2020).

Carbon dioxide has also long been known to have potent vasodilatory effects on the cerebral vasculature, with studies demonstrating that cerebral blood volume, cerebral blood flow, and mean blood velocity in the cerebral vasculature are all increased by hypercapnic conditions (Ito et al 2003, Moriyama et al 2022).

Carbogen gas is a combination of CO_2 and oxygen, and has been used in treatment of sudden hearing loss, central retinal artery occlusion, and is being studied as a potential therapeutic for epilepsy (Fowler 2012, Lee et al 2012, Forsyth et al 2024).

The theory behind carbogen as a treatment for AD relies on simultaneous dilation of cerebral blood vessels, increase in cerebral blood flow to improve clearance, and increasing

the levels of tissue oxygenation, preventing hypoxic stress and damage. This represents a therapy that could potentially reduce neuropathology and improve cognitive performance, as well as being delivered in the patient's own home.

1.8 Aims

This thesis aims to investigate novel neurovascular therapies for both epilepsy and AD. First the impact of cooling will be examined, specifically looking at its impact on neural and haemodynamic activity during chemically induced seizures in the rat 4-AP model (chapter 3) using novel chamber-based technology recently developed in the laboratory (Boorman et al 2023). A novel cooling implant will also be investigated, elucidating its potential utility as a translational therapy for drug resistant epilepsy (chapter 4). Finally, the use of Carbogen gas as a potential AD therapy will be examined in a pilot study looking at its impact on plaque load in the APP/PSEN1 mouse model of AD (chapter 5).

1.8.1 List of Aims

- To investigate the impact of cortical cooling on 4-AP induced seizure activity and the consequent haemodynamic response (chapter 3). Hypothesis: Cortical cooling will reduce neural activity in a temperature dependent manner, and the haemodynamic profile will show a subsequent reduction in HbO in the area of seizure focus.
- To examine the utility of a novel cooling implant, investigating the impact of cooling on 4-AP induced seizure activity, and the ability of onboard electrodes to detect the same (chapter 4).

- To investigate the effect of Carbogen gas treatment on plaque load in the APP/PSEN1 mouse model of AD (chapter 5). Hypothesis: Carbogen treatment will reduce plaque load, specifically reducing amyloid surrounding prominent cortical vessels.

Chapter 2

Methods

2.1 Statement of Ethics

All rat and mouse procedures outlined below were developed and performed in accordance with the Animals (Scientific Procedures) Act 1986, under approval of the UK Home Office, and with approval from the University of Sheffield licensing committee and ethical review board.

2.2 Surgical Procedures

2.2.1 Pre-Surgical Preparation

Studies 1 and 2 were conducted using male and female Lister Hooded rats weighing between 300-600g (sourced from Charles River Ltd). Prior to experimentation all animals were housed in a 12-hr light/dark cycle, with an average room temperature of 22℃, with food and water available ad libitum.

Experiments were conducted under terminal anaesthesia due to the invasive nature of the temperature modulation and seizure induction. Animals were anaesthetised with urethane at a concentration of 20% in sterile H_2O, and a dose of 0.5ml/100g (injected intraperitoneally). Urethane has been shown to preserve both excitatory (glutamatergic) and inhibitory ($GABA_A$ and $GABA_B$ mediated) synaptic transmission (Maggi and Meli 1986, Boorman et al 2023), allowing seizure activity to be studied with minimal anaesthetic interference.

Anaesthetic depth was monitored throughout the surgical and experimental procedures through monitoring of breathing state and absence of pedal reflex in response to toe pinch stimulation. In a subset of animals, blood gas measurements were obtained through cannulation of the femoral artery. In study 1 animals were tracheotomised to allow

controlled ventilation and monitoring of end-tidal CO_2 (CapStar-100, CWE Systems, USA), and atropine was administered at 0.4 mg/kg s.c. to lessen mucous secretions.

Body temperature was maintained between 36-37°C throughout all procedures with use of a homeothermic blanket with rectal temperature measurement (Harvard Apparatus, UK).

2.2.2 Cannulation Surgery

Cannulation of the femoral artery allows blood pressure and blood gas concentration to be monitored throughout the duration of the experiment (as described below), and cannulation of the femoral vein in study 1 allowed infusion of phenylephrine (0.13–0.26 mg/h) so that MABP could be maintained between 100 and 110 mmHg.

Once animals were anaesthetised, and pedal withdrawal reflex had been lost, an incision was made into the left hind limb, and blunt dissection of fatty tissue exposed the left femoral nerve bundle. The artery and vein were gently separated from the nerve before being cannulated as follows. A suture was tied at the base of the exposed vessel, with a vessel clamp placed at the top. A small incision was made into the vessel between the suture and clamp using micro-scissors, and the cannula was inserted before the clamp was removed, and a suture was used in its place to secure the cannula within the vessel. Once both vessels were cannulated the incision was sutured, and the animal was positioned within the stereotaxic frame.

2.2.3 Surgical Preparation

In preparation for all surgeries described below the hair on the top of the head was shaved from behind the eyes to the beginning of the scruff. The rat was then placed in a stereotaxic

frame to secure the head. Prior to surgical incision, rats were injected with bupivacaine (0.5%) subdermally at the incision site.

2.2.4 Thinned Cranial Window

A thinned cranial window is an area of the skull thinned to translucency, allowing optical techniques to be performed over the cerebral cortex.

An incision was made at the midline to allow removal of surface tissue. The skull was exposed, and the region of skull overlying the right hemisphere (bordered by bregma, lambda, and midline) was thinned to form a thinned cranial optical window (bone approximately 100-200μm thick) using a dental drill (BienAir Prolab basic, BienAir, UK) with a steel ball drill-bit (HP4, Dentsply, Ash Instruments, UK). Sterile saline was used to cool the skull during drilling, reduce bruising, and increase depth visibility. Once the desired level of translucency was achieved, a circular plastic chamber with internal stainless-steel coil, described below, was then secured to the skull using dental cement.

2.2.5 Craniectomy

In contrast to a thinned cranial window, craniectomy involves removal of a section of skull to completely expose the underlying dura and cortex.

Incision at the midline allowed removal of surface tissue and retraction of the skin, enabling visualisation of the skull overlying the right hemisphere, and exposing the temporalis muscle. The right temporalis muscle was separated from the skull and retracted. With the skull fully exposed, the region of skull overlying the right hemisphere (bordered by bregma, lambda, and midline, and extending down the temporal bone) was removed. A dental drill (BienAir Prolab basic, BienAir, UK) with a steel ball drill-bit (HP4, Dentsply, Ash Instruments,

UK) was used to drill a perimeter around the section, with sterile saline used to cool the skull during drilling to minimise thermal injury. Once the perimeter was thinned enough that the area of skull to be removed could be depressed with light pressure, it was carefully removed, avoiding damage to the dura.

With the cortex fully exposed, gauze soaked in sterile saline was applied to the dura to prevent drying and maintain light pressure until the electrode and implant were placed in position.

2.3 Experimental Imaging

2.3.1 Two-Dimensional Optical Imaging Spectroscopy (2D-OIS)

2D-OIS is an imaging technique that enables spatiotemporal measurements of changes in total haemoglobin (HbT), oxyhaemoglobin (HbO) and deoxyhaemoglobin (HbR) concentrations.

The 2D-OIS methodology has been widely used within the Sheffield Neurovascular lab and has previously been described in detail (Berwick et al 2008, Boorman et al 2023).

This method of imaging relies on the differing absorption spectra of oxygenated and deoxygenated haemoglobin. These differences are maximised at specific wavelengths, as such, the wavelengths utilised during the experiments in this thesis were 494 ± 20nm, 560 ± 5nm, 575 ± 14nm, and 595 ± 5nm.

2D-OIS relies on the absorption and remission of light from a surface. While it is relatively simple to calculate the absorption of light by a surface, this calculation becomes more complicated when light is scattered - as occurs when imaging the cortex. When light is shone

onto the cortex, the different tissues within the brain cause light to scatter, and as such it is not possible to measure a single continuous path of photons within the brain tissue.

To overcome this, a Monte Carlo simulation is applied to estimate the pathlength of photons, considering different absorption angles and the scattering angles of photons. These estimated path lengths can then be used in a modified Beer Lambert Law allowing computed absorption to be converted to 2D Spatiotemporal images of the micromolar changes in HbO, HbT, and HbR (Berwick et al 2005).

Over the course of these experiments, control of illumination and wavelength switching was provided by a Lambda DG-4 high-speed galvanometer, with a Dalsa 1M60 CCD camera being used to record remitted light from the cortical surface.

2.4 Blood Gas Measurements

2.4.1 Study 1

Blood gas measurements were acquired from the ABL80 FLEX Blood Gas Analyser (Radiometer Ltd), and are reported in chapter 3.

2.4.2 Study 2

Blood gas measurements were taken from blood samples obtained from the femoral artery cannulation. Blood was analysed using the VetScan i-STAT 1 system, and CG8+ cartridges (Abaxis inc. USA), and all measurements are reported in chapter 4.

2.5 Multi-channel electrophysiology

Measures of neural activity were taken using a 16-channel microelectrode (177μm^2 site area, 100μm spacing, Neuronexus Technologies, USA). The electrode was connected to a

pre-amplifier (Medusa Bioamp, Tucker-Davis-Technologies, USA) optically linked to a data acquisition system (RZ5, Tucker-Davis-Technologies, USA). Data was acquired from all 16 channels at 16bit with temporal resolution of 24.4KHz. The electrode also contained a drug infusion port, allowing injection of 4-AP for seizure induction.

2.5.1 Electrode insertion

2.5.1.1 Study 1

In this study a multiprobe (NX-BF/OT/E pO2 and temperature sensor, Oxford Optronix UK) was inserted alongside the electrode. The monitoring system was connected to a data acquisition system (CED1401, Cambridge electronic design, UK), which continuously recorded pO2 and temperature throughout experiments. To determine best placement of the electrode and multiprobe 2s whisker stimulation was used to localise the active region of the whisker barrel cortex. Stimulation was provided by inserting two stainless-steel stimulation electrodes subcutaneously into the left (contralateral) whisker pad. 30 trials were conducted, consisting of a 5s baseline and 2s stimulation at 5Hz, and totalling 25 seconds per trial. 2D-OIS was used to collect optical data throughout the stimulation experiment, and all trials were then averaged and subjected to spectroscopy analysis to reveal the micromolar changes in HbT elicited by stimulation.

Images from the stimulation period were compared to the pre-stimulation baseline, and any pixels showing activation 1.5 standard deviations above the pre-stimulus baseline were determined to be activated above threshold, and a region was drawn around these activated pixels.

This region was overlaid onto a reference image of the exposed cortical region showing the vasculature. Areas central to the activated region, and containing minimal surface vasculature, were selected for probe placement to prevent bleeding during implantation (figure 2.1). The location of the electrode was prioritised over that of the multiprobe.

A small burr-hole was drilled through the remaining skull overlying the selected region, and the 16-channel linear array electrode was attached to a stereotaxic arm and inserted to a depth of approximately 1500μm. The multiprobe was attached to a secondary stereotaxic arm and inserted to a depth of 500μm.

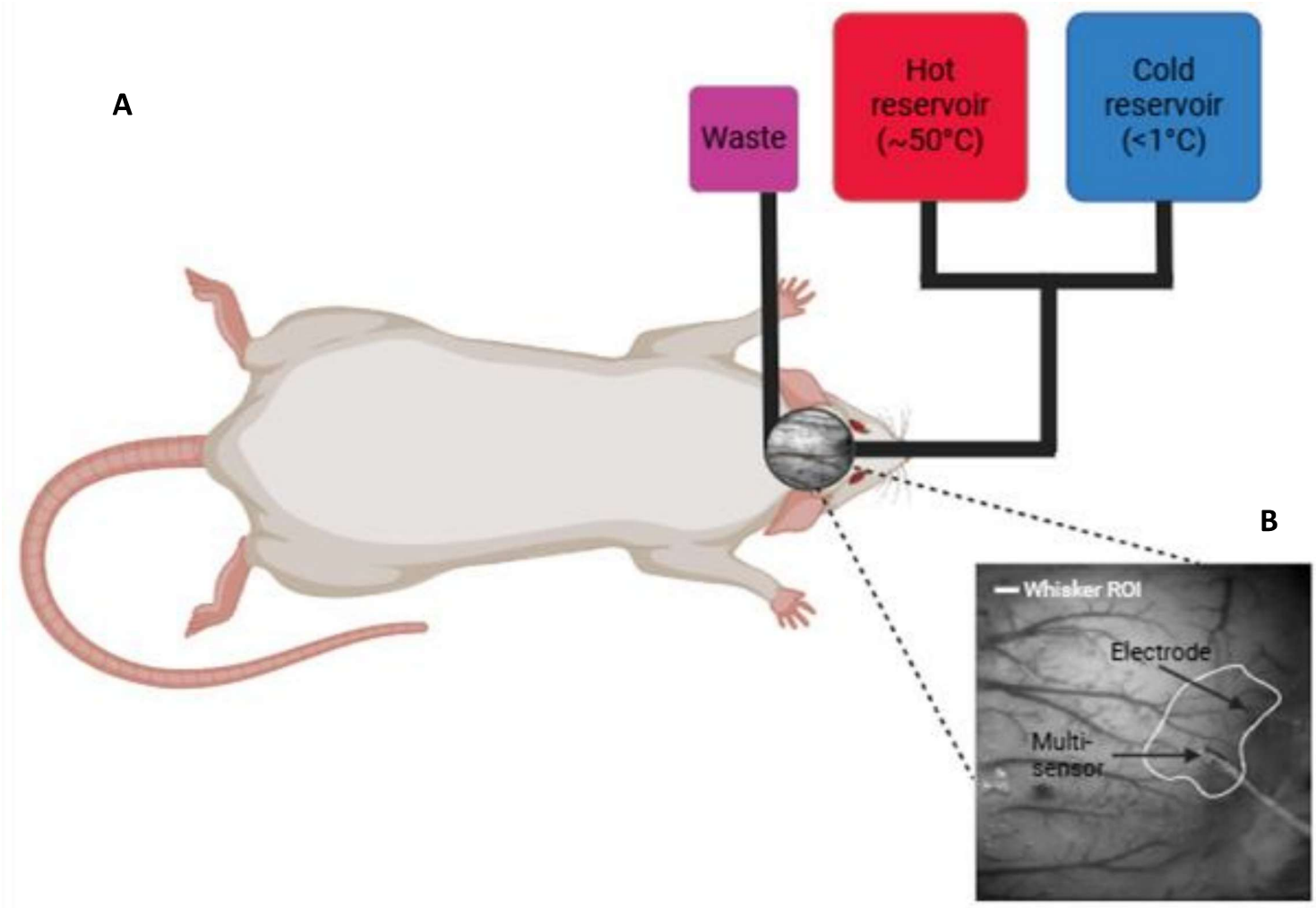

Figure 2.1 – Cooling chamber schematic and sensor placement

(A) *Schematic of the cortical cooling approach, with water reservoirs used to alter chamber temperature.* ***(B)*** *Image of the cortical surface taken through the thinned cranial window, showing the established whisker region and subsequent placement of the electrode and multi-*

2.5.1.2 Study 2

Prior to electrode insertion a model implant was placed over the brain surface, allowing visualisation of the intended position of the peltier chip and electrodes (figure 2.2). Positioning of the drug-infusion electrode was determined by the location of the peltier chip, while also avoiding surface vasculature to minimise potential bleeding during implantation. The model implant was then removed and the electrode implanted, from the direction of the midline, within the cortical tissue such that it lay laterally to the surface of the brain.

Following electrode insertion a small amount of sterile saline was placed on the surface of the brain to prevent drying and allow a better recording from the implants onboard electrodes. The implant was placed such that it filled the craniectomy area, with the peltier chip centred over the electrode tip, and the onboard electrodes in contact with the dura. The recording from the onboard electrodes was inspected to ensure that they were in full contact with the dura, and the implant was then held in place using the stereotactic arm.

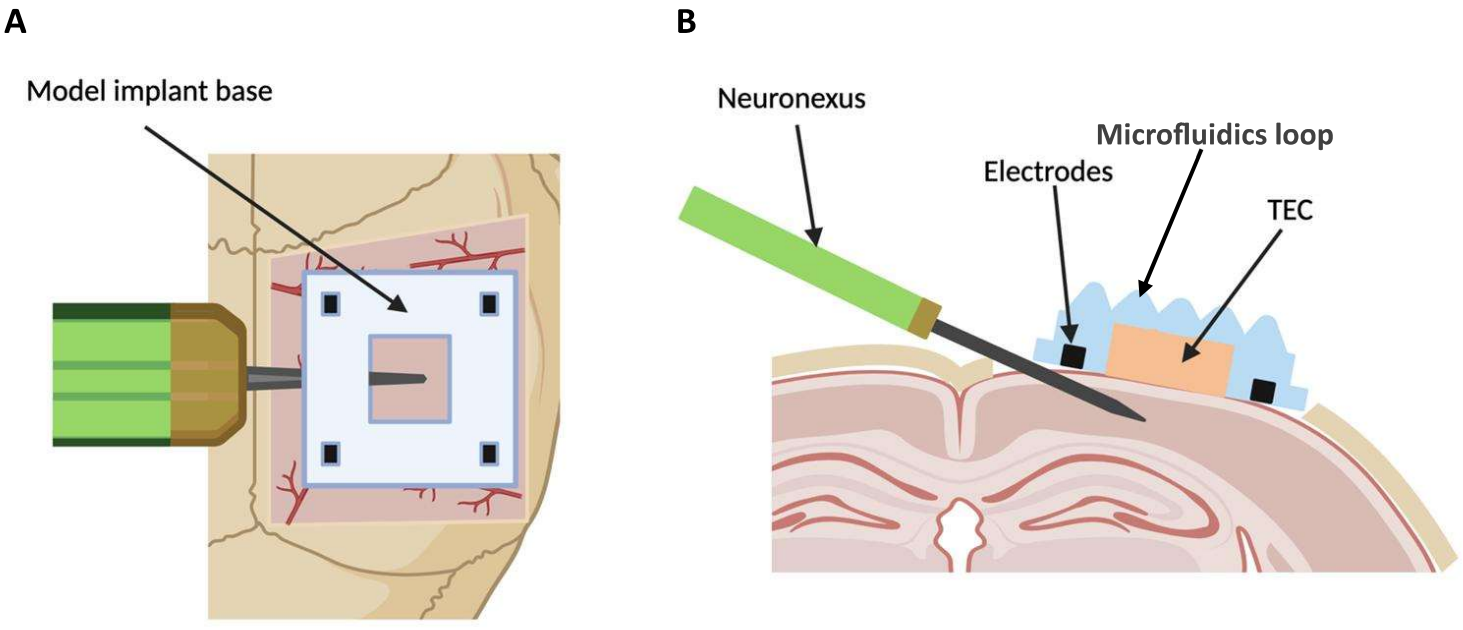

Figure 2.2 – Electrode and implant positioning

The neuronexus was positioned using a model implant base ***(A)*** *to ensure the tip of the probe was centred under*

2.6 Seizure induction

The potassium channel blocker 4-aminopyridine (4-AP, Sigma, 15 mM, 1 µl) was injected through the fluidic port of the drug infusion electrode using a 10μl hamilton syringe and syringe pump delivering 1μl over the course of 5 minutes (200nl/minute) (Harris et al 2014).

Electrophysiology recordings were observed throughout the injection course, and if no seizure activity was identified on the recording within ~5 minutes of injection completion, another injection was performed. Injection was repeated until seizure activity was established, and once seizure activity was present and sustained (figure 4.1), the implant cooling protocol commenced.

2.7 Cortical temperature alteration

2.7.1 Study 1 - Skull-attached Chamber

The skull-attached chamber and controller system described below were designed and created by Dr Luke Boorman and have previously been described in detail in a recent paper from Boorman et al (2023).

The chamber attached to the skull was formed of an internal circumference of a stainless steel tube formed into a coil, and an external plastic circumference. The reservoir formed by this chamber was filled with sterile saline.

Two external reservoirs were filled with either heated (50^{o}C) or cooled (<1^{o}C) distilled water, and contained submerged thermocouples to monitor temperature. They were topped up with small volumes of distilled water as required, and their temperatures remained stable throughout the course of the experiment. Micropumps (M100S-SUB, TCS Micropumps, Kent UK) within each reservoir were attached to silicone tubing, which connected to a T-piece,

followed by PVC tubing, and then to the inflow to the steel coil. The steel coil outflow ran through PVC tubing to a wastewater collection vessel (figure 2.1). This system allowed either hot or cold water to run through the steel tubing, thereby heating or cooling the saline within the reservoir. A separate thermocouple within the saline reservoir monitored the performance of the temperature modulation system.

2.7.1.1 Controller system

The control software and user interface was written in LabVIEW (National Instruments, Texas USA) allowing bidirectional communication between the controller PC and the temperature sensing and pump controller. The submerged thermocouples were connected to a data logger (TC-08, 8 Channel data logger, Pico Technologies, Cambridgeshire), sampling up to 1 kHz and connected to the PC via USB. A software development kit (SDK) was used to interface the data logger with LabVIEW (PicoSDK 10.6.12, Pico Technology).

2.7.2 Study 2 - Novel Implant

The implant and control systems below were designed and built by Dr Spencer Moore.

The novel implant consisted of a thermoelectric cooler (1TC17-16178-1617.H, company), with a thermocouple (company info) attached to both the hot and cold side, and a stainless steel square (0.2mm thick, 6.3mmx6.3mm) attached to the hot side.

This system was contained within base layers of SE1700 silicone. 4 surface electrodes were printed with a graphite solution within the base layer, and connected to gold wires.

A liquid loop system was printed on the top surface of the silicone implant, and connected to silicone tubing (0.4 mm I/D x 0.3 mm wall) leading to an integrated pump system.

2.7.2.1 Control System

The control hardware was built on a custom PCB, with an ARM Cortex-M microcontroller to manage the implant's thermoelectric cooler, thermocouple-based temperature feedback, and microfluidic functionality. Neural activity was recorded using a 16-bit Intan RHD2216 electrophysiology interface chip, and coolant flow was controlled using an I2C-controlled piezoelectric air pump (UXPB5401200A, The Lee Company) and a flow sensor (SLF3S-1300B, Sensirion). The control system was housed within a custom 3D-printed unit.

Control software was developed in C (ISO/IEC 9899:1999) and compiled using the ARM Keil µVision IDE for deployment on STM32 series microcontrollers, with a LabVIEW (2022 Q3) user interface allowing visualisation of data in real time, and easy control of implant functionality.

2.8 Statistical analysis

Statistical tests are applied throughout the experimental chapters (chapter 3, 4 & 5). All statistical tests were conducted in SPSS and R, with figures created in MATLAB. Outliers were assessed using box plots, with values greater than 1.5 box lengths from the edge of the box classified as outliers. Normality was assessed using the Shapiro Wilk test. Specifics of statistical tests are described in the appropriate experimental chapter.

2.9 Carbogen Treatment

Nine APP/PSEN1 mice (5 male, 4 female) were utilised for this pilot study. Four mice (2 male, 2 female) were treated using Carbogen gas, and the remaining mice acted as non-treated controls.

All mice were perfused, and staining was performed to enable visualisation of amyloid plaques in tissue, and surrounding blood vessels.

2.9.1 Carbogen Treatment Protocol

Carbogen treatment was performed using a custom built biospherics chamber, and mice were treated for 1 hour every weekday, for a total of 42 treatment hours (roughly 2 months). Mice remained in their home cages, which were placed within the chamber. Carbogen gas (a combination of 5% CO_2 and 95% O2) was fed into the chamber for between 4 and 5 minutes until the internal carbon dioxide concentration reached 4%. Carbon dioxide concentration was then maintained between 3.9 - 4.3% for 1 hour, with the concentration kept as stable as possible, and slight variation occurring as a result of leakage from the chamber.

2.9.2 Methoxy-X04 injections

Methoxy-X04 is a fluorescent amyloid-β probe that stains amyloid-beta plaques, tangles, and cerebrovascular amyloid.

After 2 months of Carbogen treatment (or at the equivalent age for untreated controls) mice were injected intraperitoneally with methoxy-X04 (concentration and supplier) and left for 24 hours to allow penetration of the blood brain barrier and staining of amyloid to develop.

2.9.3 Perfusion

24 hours post methoxy injection, mice were euthanised with pentobarbital (100 mg/kg, Euthatal, Merial Animal Health Ltd). Following loss of pedal withdrawal reflex, cardiac perfusions were performed using saline, and formalin. In brief, the rib cage was cut and retracted to expose the thoracic cavity. A butterfly-clip needle was attached to a syringe of warm saline solution (5ml of 0.9% saline) and inserted into the bottom of the heart's left ventricle. The right atrium/vena cava was then cut to allow expulsion of blood from the body. Saline was perfused through the body, followed by formalin (5ml at 4%v/v) and once

this was completed mice were decapitated and brains were manually dissected from the skull.

Once isolated, brains were placed in formalin for fixation. Images of methoxy staining were then taken and analysed as described in chapter 6.

Chapter 3

The Effect of Cortical Cooling on 4-AP Induced Synaptic and Haemodynamic Activity

3.1 Abstract

Drug resistant epilepsy affects roughly 30% of epilepsy patients, and can lead to an increased risk of injury and even death. Creating novel therapies could potentially help these patients, and reduce the risks and quality of life difficulties associated with uncontrolled seizures.

The impact of cooling on seizure activity has been widely studied, and it is now well established that cooling can reduce neuronal seizure activity. The impact of seizure activity on blood flow has also been well documented. However, there is a lack of research surrounding the impact of focal cooling on localised blood flow responses to seizure activity. This chapter presents the results of experiments investigating the impact of cortical cooling on both neural and haemodynamic activity. Recordings were conducted in the rat 4-AP model of epilepsy, utilising a novel cortical cooling chamber designed to enable 2D-OIS imaging of the cortex during seizure activity and cooling. The study found that cooling to 10°C was sufficient to reduce neuronal seizure activity and reduce HbT levels within the seizure (whisker) region. Cooling to 20°C was not sufficient to reduce neuronal seizure activity, and caused an increase in levels of HbO in both the overall whisker region and the MCA region.

This study shows that cooling could potentially help patients with drug resistant epilepsy, but that further research is required into methods for cortical cooling that are suitable for translation to patient populations.

3.2 Introduction

Epilepsy is one of the most common neurological diseases. Resulting from disruptions in network activity within the brain that manifests as seizures, epilepsy affects roughly 50

million people worldwide (WHO epilepsy, 2019). Despite numerous developments in anti epileptic drugs (AEDs) seizures remain uncontrolled in roughly 30% of patients (Kanner and Bicchi 2022), and current non-pharmacological options are limited in who may benefit from them. As such, there is a great need for novel therapies.

Cooling has long been posited as a potential therapy for those with drug resistant epilepsy. Its neuroprotective effects have been successfully deployed in the treatment of a number of neurological conditions, with therapeutic hypothermia reducing neuronal damage and improving occupational outcomes for patients following traumatic brain injury and asphyxia (Azzopardi et al 2000, Inder et al 2004, Shankaran et al 2005). It has been shown previously that seizure activity can induce increases in cortical temperature in both epilepsy models and patients (Harris et al 2018, Wakuya et al 2022). Increases in brain temperature are known to have a profound effect on both neural activity and blood flow (Boorman et al 2022, Tan et al 2024), and this increase in temperature could play a role in continuing epileptogenesis, as is seen resulting from febrile seizures in childhood (Pollandt and Bleck 2018). As such, cortical cooling presents a critical opportunity to not only reduce neural activity but also potentially alter blood flow and ongoing epileptogenesis.

The benefit of cooling to epilepsy patients has been shown, with application of chilled saline to patients during epilepsy resection surgeries resulting in significant long-term reduction of seizure events, and cessation of status epilepticus during the course of the surgery (Ommaya and Baldwin 1963). Despite the increasing volume of research into the effect of cooling on neuronal seizure activity (as explored in chapter 1 of this thesis), there is a lack of research showing the impact of cooling on haemodynamic responses to this seizure activity. Sustained seizure activity has been found to result in significant alterations in cerebral

oxygenation (Fong et al 2000, Farrell et al 2016, Wolff et al 2020, Prager et al 2019) with these changes being hypothesised to contribute to damage resulting from seizure activity through both hypoxic damage and increases in reactive oxygen species (Prager et al 2019). As such, it is important to understand the impact on seizure haemodynamics if we are to produce a potential therapy.

This study aimed to investigate the impact of cortical cooling (to both 10°C and 20°C) on seizure-like neuronal activity resulting from 4-AP injection, as well as the resulting haemodynamic response.

The 4-AP model of epilepsy is well established and has been found to successfully demonstrate the efficacy of standard epileptic drugs (Heuzeroth et al 2019). It is also an established model within the Sheffield Neurovascular Lab (Harris et al 2014, 2018). 4-AP is a potassium channel blocker that, following focal cortical injection, results in the occurrence of seizure-like discharges, allowing for prolonged study of cooling therapies on a stable seizure state.

A fluid-filled skull-attached chamber was utilised to control cortical temperature. The chamber was placed over a thinned cranial window, allowing for 2D-OIS usage to elucidate the levels of HbO, HbT, and HbR, in the region of cortex affected by the seizure activity.

3.2.2 Aims

This chapter aimed to investigate the impact of cortical cooling on the neural and haemodynamic response to 4-AP seizure induction, with the hypothesis that both LFP and haemodynamic activity will be reduced by cortical cooling.

3.3 Methods

Surgical methods and an overview of the cooling chamber can be found in the methods section of this thesis. The methods highlighted in this chapter refer to the specifics of the temperature control, the experimental protocols employed in this study, and the specific analysis that was performed.

7 female hooded lister rats were utilised in this study. All animals underwent thinned cranial window surgery, chamber implantation, electrode and multi-probe insertion, seizure induction, and 2D-OIS imaging as described in chapter 2.

3.3.1 Experimental protocol

Once the surgery and chamber implantation had been completed, animals were allowed to stabilise for 30 minutes before the 2D-OIS protocol commenced.

A whisker stimulation experiment was performed to determine the area for electrode and multiprobe insertion before the main experiment. Following seizure induction, one of two cooling protocols was employed. In the first protocol the chamber was cooled to 20°C, then down to 10°C, before being rewarmed to 20°C, and finally rewarmed to baseline temperature. In the second protocol the chamber was cooled to 10°C, rewarmed to 20°C, cooled again to 10°C and then returned to baseline (figure 3.1). Throughout these experiments neuronexus and 2D-OIS recordings were taken to enable visualisation of both the synaptic and haemodynamic response to the seizure-like activity, and to the cooling. The multiprobe also reported the cortical temperature during all cooling periods.

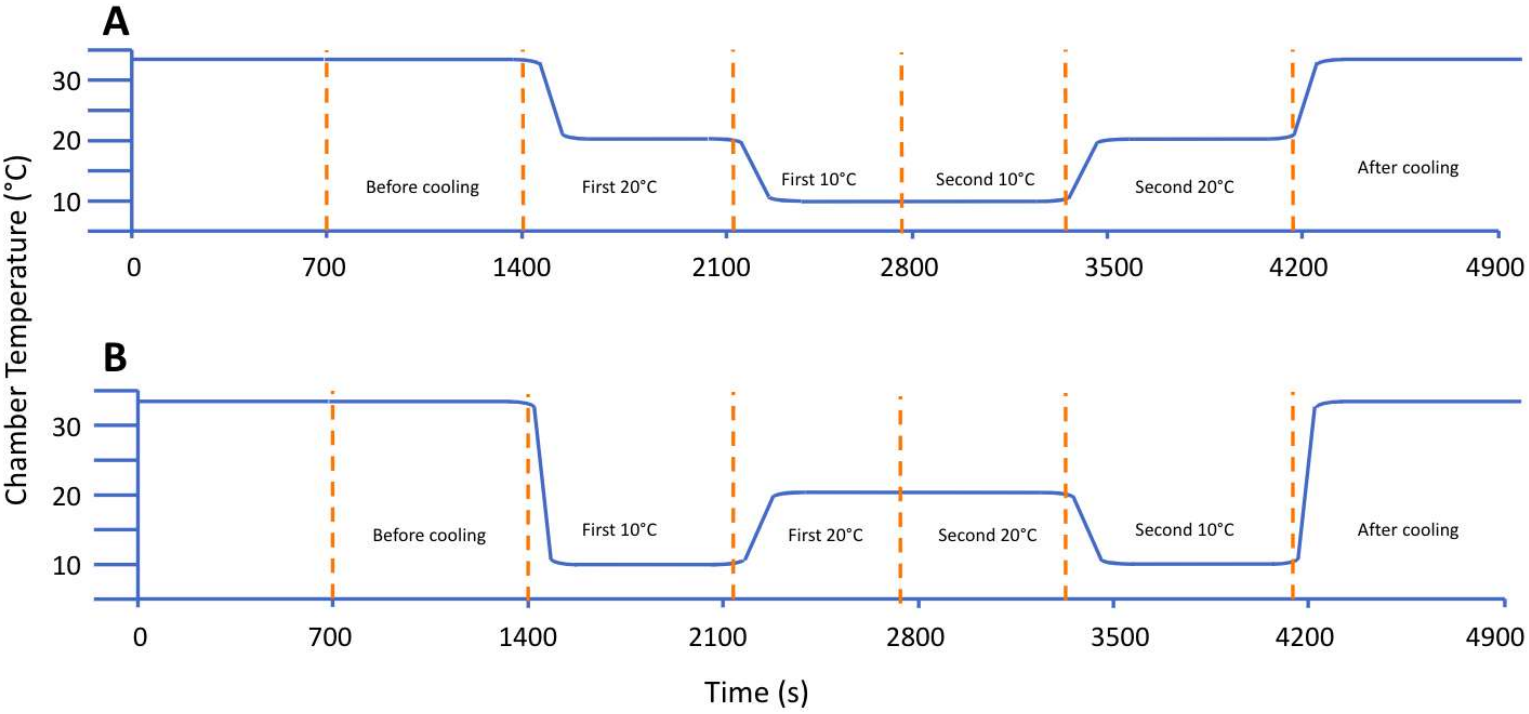

Figure 3.1 - Experimental protocols for investigating cooling

Cooling was investigated using two experimental protocols. ***A.*** *Cooling gradually to 20°C, then to 10°C, followed by rewarming gradually to 20°C and finally baseline temperature.* ***B.*** *Cooling sharply to 10°C, rewarming to 20°C, cooling to 10°C and rewarming to baseline temperature. Orange lines indicate separation of cooling periods.*

3.3.2 Data extraction

Neural and haemodynamic data were split into 6 time periods, and a 200s section from the middle of each period was sampled for analysis. Cortical temperature information was averaged across the entirety of each cooling period. The time periods are illustrated in figure 3.1.

3.3.3 Local Field potential (LFP) analysis

Periods of 200s were taken from each experimental period for averaging and comparison between temperature conditions. LFP data representing synaptic activity was displayed across all electrode channels, and for purposes of analysis we separated the LFP data into 4 channel blocks; channels 1-4, 5-8, 9-12, and 13-16. The number of LFP spikes within each 200s data period across each electrode channel was calculated and averaged within the channel blocks.

Due to the positioning of the electrode perpendicular to the cortical surface (figure 2.1), the locations of maximal seizure initiation and maximal cooling effect were directly opposed (figure 3.2). Separating the LFP data into channel blocks allowed investigation of the cooling effect on synaptic activity across four different depths. We hypothesised that this opposition of maximal cooling and maximal seizure will result in the greatest cooling effect in the top channels (1-8), with increased seizure power and lesser cooling effect reducing the efficacy of cooling in the lower channels (9-16).

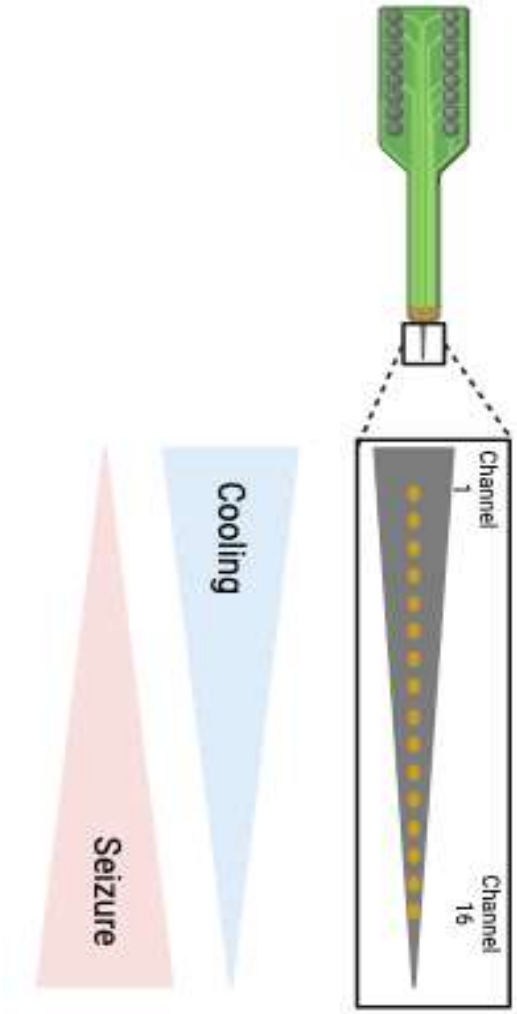

Figure 3.2 – Differing intensities of cooling and seizure activity

Injection of 4-AP occurs at the tip of the drug-infusion electrode, with seizure activity being most intense at channel 16. The electrode is inserted perpendicular to the cooling chamber, with cooling having the greatest effect at channel 1.

3.3.4 Haemodynamic data analysis

Haemodynamic data were collected using 2D-OIS, as described in chapter 2. Data were then outputted as a time-series across the entire experimental time-course. Haemodynamic data was separated into the same 200s periods as the LFP data, and the average HbT, HbO, and HbR values were calculated across each time period. Haemodynamic values were taken from a region of interest overlying a branch of the middle cerebral artery, and a large region of interest encompassing the entire active region (as defined in the 2D-OIS methods section 2.3.1).

3.3.5 Statistical analysis

LFP data were statistically analysed using Mixed 2-way ANOVA with Bonferroni correction for multiple comparisons. This examined the effect of the group factor (order of temperature presentation), and the impact of cooling temperature (10°C, 20°C, no cooling) on neural activity (measured by the sum of LFP spikes within each time period). Animals were assigned to either group A or B depending on the order of temperature presentation (figure 3.1) and group differences were assessed. As no group differences were found, data were assigned to cooling periods for analysis based on whether it was the first or second presentation of that temperature (figure 3.1). The cooling periods were assigned as; 1-before cooling, 2-first 10°C, 3-first 20°C, 4-second 10°C, 5-second 20°C, 6-post cooling (see figure 3.1).

Data from each channel block was analysed, and is presented, separately, to examine the effect of depth from the cooling apparatus.

Haemodynamic data was separated into the same cooling periods, and HbT, HbR, HbO were all analysed separately using a Mixed 2-way ANOVA with Bonferroni correction for multiple

comparisons. This examined the effect of the group factor (order of temperature presentation), and the impact of cooling temperature (10°C, 20°C, no cooling) on haemodynamic activity (measured by the mean HbT, HbO, and HbR across each time period). Animals were assigned to groups as in the neural analysis, and where group differences were found, post hoc or simple effects tests (univariate analysis of variance) were applied as appropriate to interrogate those differences.

Cortical temperature data was separated into the same cooling periods as above and periods where the same temperature were presented were averaged together, with the addition of a period before seizure induction (for a total of 5 time points). One sample t-tests were applied to the 10°C and 20°C cooling period data to determine whether cortical temperature was significantly different to the expected temperatures of 10°C or 20°C, and a Friedman test was employed to identify differences across temperatures.

3.4 Results

Inspection of box-plots revealed no outliers in the neural or haemodynamic data, and all data was found to be normally distributed using the Shapiro Wilk's test ($p>0.05$). One outlier was identified in the cortical temperature data, with one animal in group B showing a cortical temperature greater than 1.5x the IQR from quartile 3. As this animal is still included in the neural and haemodynamic data, it was kept in the temperature data for analysis.

Both neural seizure activity and haemodynamic activity are visually altered during the course of cooling application (figure 3.3). Cooling to 10°C appears to cause a reduction in neural activity, this is followed by a gradual decrease in HbO, HbT, and HbR. Cooling to 20°C appears to slightly reduce neural activity, however it appears to have a lesser effect than cooling to 10°C, flattening the epileptiform spike profile rather than reducing the number of LFP spikes

to the same extent as cooling to 10°C. Similarly, cooling to 20°C appears to alter the haemodynamic profile (reducing oscillations) without altering the volume of HbO, HbT, and HbR.

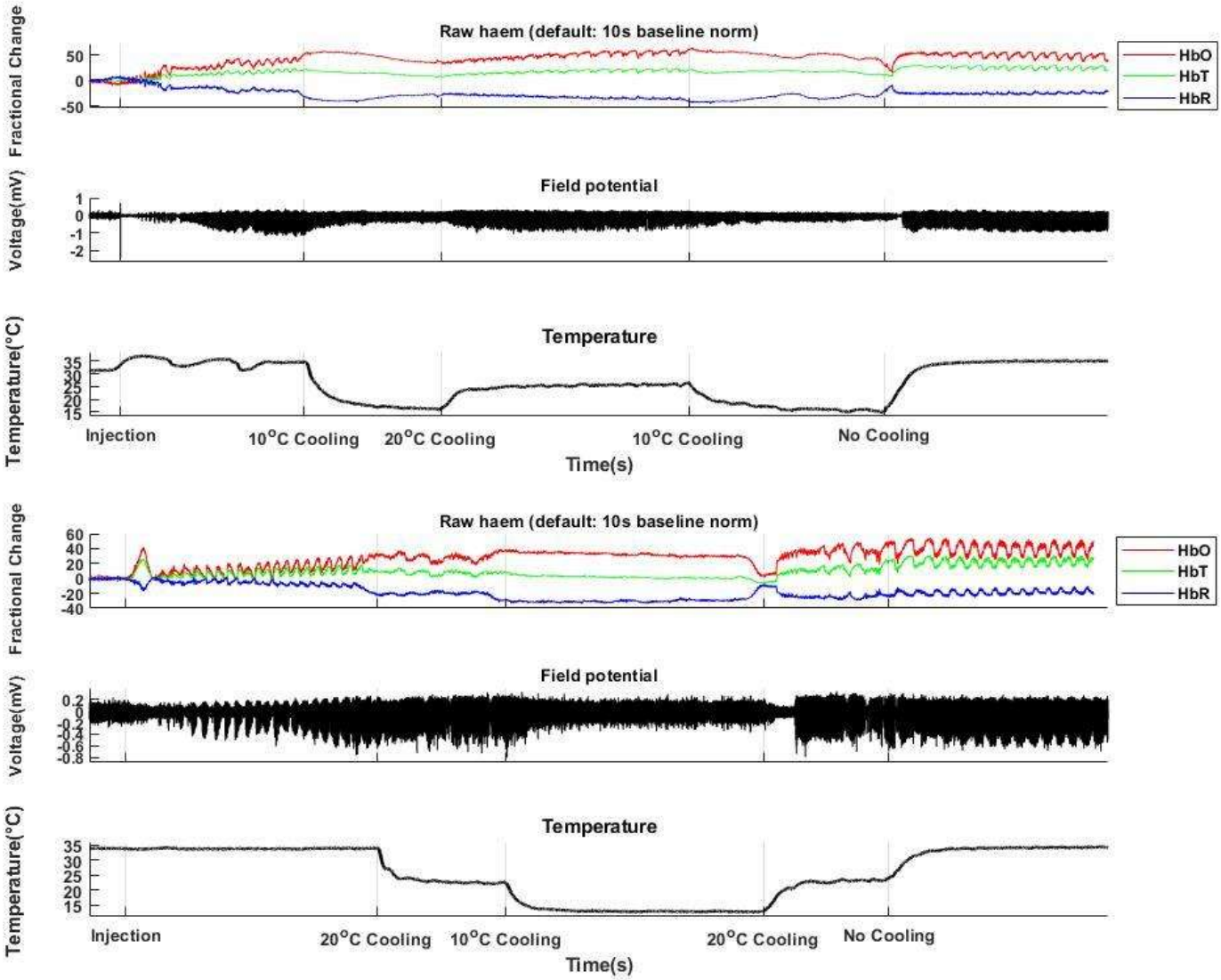

Figure 3.3 – Time series showing haemodynamic, neural, and temperature data

4-AP was injected early in the experimental time-course. Once seizure activity was established the cooling chamber was cooled according to the assigned cooling paradigm. Haemodynamic and neural data was collected throughout the time-course, with visual inspection showing a profound effect of cooling on each.

3.4.2 Effect of chamber temperature on cortical temperature

Chamber temp vs cortical temp	Baseline	Seizure, no cooling (before)	10°C chamber temp	20°C chamber temp	After cooling
Cortical Temp (°C)	33.616 ± 0.436	34.075 ± 0.444	16.619 ± 3.289	24.781 ± 2.169	34.372 ± 0.690

Table 3.1 - Cortical temperature during cooling

The mean cortical temperature during each cooling period (n=7). Error shown is STD.

Cortical temperature was significantly different between cooling periods $X^2(2)=25.943$, $p<0.001$. Pairwise comparisons were performed with Bonferroni correction for multiple comparisons.

3.4.2.2 10°C Chamber temperature

Cooling to 10°C produced a significant reduction in cortical temperature compared to temperature before and after cooling.

One sample t-tests established that the temperature reached during 10°C cooling was significantly greater than 10°C $t(6)=5.32$, $p=0.002$.

3.4.2.3 20°C Chamber temperature

Cooling to 20°C produced a significant reduction in cortical temperature compared to after cooling.

The temperature reached during 20°C cooling was significantly greater than 20°C $t(6)=5.83$, $p=0.001$.

3.4.2.4 Summary

Cortical temperature did not reach the same levels as the chamber temperature during either cooling to 20°C or 10°C, but significant reductions in cortical temperature were seen at both temperatures when compared to the temperature after cooling had ceased.

3.4.3 Focal cortical cooling reduces synaptic activity during induced seizures

Sum of LFP spikes	Before Cooling (1)	First 10°C (2)	First 20°C (3)	Second 10°C (4)	Second 20°C (5)	After Cooling (6)
Channels 1-4 group A	34.436 ± 15.313	7.553 ± 2.893	17.965 ± 5.923	8.215 ± 3.104	18.718 ± 5.996	36.501 ± 16.363
Channels 1-4 group B	29.586 ± 9.342	5.622 ± 7.804	22.632 ± 8.022	9.381 ± 12.089	26.060 ± 11.458	59.223 ± 25.561
Channels 5-8 group A	52.019 ± 21.401	14.906 ± 9.001	32.710 ± 10.606	15.782 ± 9.980	31.576 ± 9.509	54.578 ± 17.004
Channels 5-8 group B	43.765 ± 9.278	16.030 ± 10.344	35.769 ± 7.546	20.520 ± 12.539	42.054 ± 14.143	87.445 ± 34.818
Channels 9-12 group A	42.518 ± 20.529	14.101 ± 6.360	29.954 ± 9.440	15.182 ± 7.584	27.181 ± 8.568	44.653 ± 8.782
Channels 9-12 group B	40.154 ± 11.303	16.993 ± 11.729	32.996 ± 6.121	20.993 ± 11.237	38.109 ± 9.772	79.926 ± 30.808
Channels 13-16 group A	34.957 ± 20.416	12.612 ± 6.372	26.187 ± 10.398	13.473 ± 6.584	23.102 ± 9.936	34.852 ± 8.659
Channels 13-16 group B	37.609 ± 11.351	18.230 ± 11.746	31.348 ± 5.794	21.020 ± 9.310	34.996 ± 7.086	71.066 ± 28.189

Table 3.2 - Sum of LFP spikes during cooling

The mean sum of LFP spikes for each cooling period, separated into channel blocks. Mean is calculated across the four channels and across all animals ((A)n=3, (B)n=4). Error shown is STD.

3.4.3.1 Channels 1-4

Mauchly's test of sphericity indicated sphericity was met for the two-way interaction, $X^2(2)=24.219$, $p=0.096$. There was no significant interaction between group and cooling intervention on LFP spikes, $F(5,25)=2.309$, $p=0.074$, partial $\eta^2=0.316$.

No main effect of group was found $F(1,5)=0.428$, $p=0.542$, partial $\eta^2=0.079$, indicating that the order of temperature presentation had no effect.

The main effect of cooling showed a statistically significant difference in LFP spikes during the different periods, $F(5,25)=22.697$, $p<0.001$, partial $\eta^2=0.819$.

Pairwise comparison showed that the first 10°C cooling period significantly reduced the number of LFP spikes by 25.423 (95% CI, 5.525 to 45.321) compared to the period before cooling, $p=0.017$. A similar effect was seen for the second instance of 10°C cooling - a reduction in spike number (compared to before cooling) of 23.213 (95% CI, 0.483 to 45.943), $p=0.046$.

Synaptic activity during both instances of cooling to 10 degrees was also significantly reduced compared to both instances of cooling to 20 degrees. First 10°C cooling showed a reduction of 13.711 (95% CI, 3.295 to 24.126), $p=0.015$ to the first 20°C cooling, and a reduction of 15.801 (95% CI, 1.775 to 29.827), $p=0.030$ to the second 20°C cooling. Second 10°C cooling showed a reduction of 11.501 (95% CI, 0.032 to 22.969), $p=0.049$ compared to the first 20°C cooling, and a reduction of 13.591 (95% CI, 1.915 to 25.267), $p=0.026$ compared to the second 20°C cooling.

Finally, the period following the cooling protocol showed significantly increased synaptic activity compared to the first 10°C cooling, an increase of 41.274 (95% CI, 7.665 to 74.883),

p=0.02, as well as to the second 10°C cooling, an increase of 39.064 (95% CI, 7.951 to 70.176), *p*=0.018.

3.4.3.2 Channels 5-8

Mauchly's test of sphericity indicated sphericity was met for the two-way interaction, X2(2)=25.722, p=0.068.

There was no significant interaction between group and cooling intervention on LFP spikes, F(5,25)=1.797, p=0.150, partial ɳ2=0.264.

No main effect of group was found F(1,5)=0.892, p=0.388, partial ɳ2=0.151.

The main effect of cooling showed a statistically significant difference in LFP spikes during the different periods, F(5,25)=15.600, p<0.001, partial ɳ2=0.757.

In channels 5-8 the most effective cooling period was the first instance of 10°C cooling, showing significantly decreased synaptic activity (difference of 32.424 (95% CI, 3.480 to 61.368) compared to before cooling, p=0.030, and the first instance of cooling to 20 degrees (reduction of 18.771 (95% CI, 6.167 to 31.376), p=0.008. The second 10°C cooling period also displayed a reduction compared to the first instance of cooling to 20 degrees (reduction of 16.088 (95% CI, 3.741 to 28.436), p=0.015).

3.4.3.3 Channels 9-12

Mauchly's test of sphericity indicated sphericity was met for the two-way interaction, X2(2)=26.307, p=0.059.

There was no significant interaction between group and cooling intervention on LFP spikes, F(5,25)=1.683, p=0.175, partial ɳ2=0.252.

No main effect of group was found $F(1,5)=3.324$, $p=0.128$, partial $\eta 2=0.399$.

The main effect of cooling showed a statistically significant difference in LFP spikes during the different periods, $F(5,25)=10.817$, $p<0.001$, partial $\eta 2=0.684$.

The only significant difference to occur in synaptic activity in channels 9-12 was between the first instances of 10°C cooling and 20°C cooling, with 10°C cooling causing a reduction of 15.928 (95% CI, 1.987 to 29.870), $p=0.028$ compared to the first instance of 20°C cooling.

3.4.3.4 Channels 13-16

Mauchly's test of sphericity indicated sphericity was met for the two-way interaction, $X2(2)=18.620$, $p=0.299$.

There was no significant interaction between group and cooling intervention on LFP spikes, $F(5,25)=1.647$, $p=0.184$, partial $\eta 2=0.248$.

No main effect of group was found $F(1,5)=5.665$, $p=0.063$, partial $\eta 2=0.531$.

The main effect of cooling showed a statistically significant difference in LFP spikes during the different periods, $F(5,25)=7.979$, $p<0.001$, partial $\eta 2=0.615$. Despite this, pairwise comparisons revealed no significant alterations in synaptic activity between different cooling periods.

3.4.3.5 Summary

Cooling the cortex to 10 degrees was sufficient to significantly reduce the neuronal activity occurring as a result of 4-AP injection. This effect is seen in the upper channels of the multi-channel electrode (channels 1-8), but the same effect is not found in the lowest channels

(13-16). Cooling the cortex to 20 degrees is not sufficient to significantly reduce neuronal activity, though a trend towards reduction is seen at this temperature.

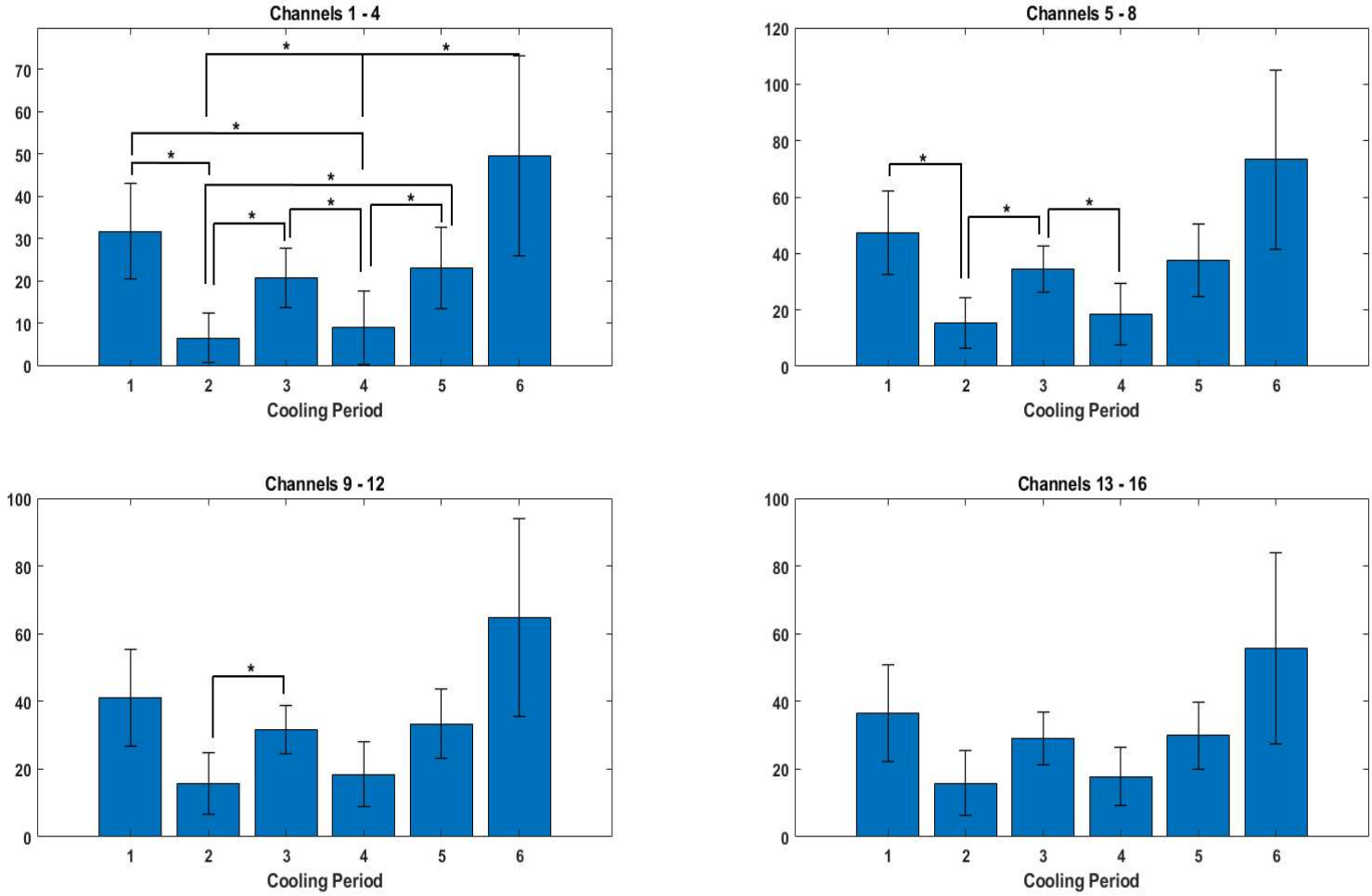

Figure 3.5 – The effect of cortical cooling on seizure induced LFP activity

*Changes in LFP spike activity in response to cooling to 10°C or 20°C (n=7). Bars represent mean sum of LFP spikes occurring across each channel block within the cooling periods (defined above). Error bars represent STD, * represents p<0.05.*

3.4.4 Impact of cortical cooling on haemodynamic activity

Mean Fractional Change in haemodynamics	Before Cooling (1)	First 10°C (2)	First 20°C (3)	Second 10°C (4)	Second 20°C (5)	After Cooling (6)
Whisker HbT Group A	13.345 ± 5.903	-0.647 ± 7.263	10.792 ± 6.287	-10.046 ± 19.1	15.730 ± 6.570	22.747 ± 3.977
Whisker HbT Group B	26.183 ± 18.347	18.596 ± 15.379	25.052 ± 14.162	20.656 ± 11.406	28.016 ± 13.175	33.830 ± 15.086
Whisker HbO Group A	27.587 ± 11.590	29.185 ± 14.527	33.284 ± 11.563	16.819 ± 26.906	44.218 ± 11.092	43.745 ± 7.707
Whisker HbO Group B	42.672 ± 13.595	46.665 ± 20.746	47.568 ± 15.326	47.719 ± 15.803	53.308 ± 15.539	52.887 ± 15.136
Whisker HbR Group A	-14.243 ± 5.694	-29.831 ± 7.287	-22.492 ± 5.438	-26.865 ± 8.132	-28.488 ± 5.361	-20.998 ± 4.050
Whisker HbR Group B	-16.489 ± 6.575	-28.069 ± 8.649	-22.516 ± 8.493	-27.063 ± 6.008	-25.292 ± 9.727	-19.058 ± 6.492
Artery HbT Group A	15.939 ± 11.548	-4.826 ± 3.571	8.743 ± 4.662	-11.500 ± 8.059	16.232 ± 6.972	23.100 ± 6.835
Artery HbT Group B	24.447 ± 16.762	14.033 ± 14.765	20.603 ± 9.910	13.488 ± 18.772	21.611 ± 10.883	22.462 ± 14.800
Artery HbO Group A	29.351 ± 19.618	21.961 ± 10.180	30.045 ± 11.739	9.506 ± 20.554	41.385 ± 10.019	41.325 ± 13.400
Artery HbO Group B	38.480 ± 19.990	39.476 ± 24.374	38.238 ± 19.501	37.528 ± 22.843	40.392 ± 20.179	36.056 ± 18.971
Artery HbR Group A	-13.412 ± 8.146	-26.787 ± 10.198	-21.302 ± 7.891	-21.006 ± 14.099	-25.152 ± 7.788	-18.226 ± 6.975
Artery HbR Group B	-14.033 ± 5.503	-25.443 ± 9.933	-17.635 ± 10.949	-24.040 ± 5.864	-18.781 ± 10.811	-13.594 ± 6.985

Table 3.3 - Mean of haemodynamic activity during cooling

The mean haemodynamic change for each cooling period. Mean is calculated across all animals ((A)n=3, (B)n=4). Error shown is STD.

3.4.4.1 Whisker Region - HbT

Mauchly's test of sphericity indicated sphericity was not met for the two-way interaction, $X^2(2)=28.873$, $p=0.031$. As such, for all interaction tests the Greenhouse-Geisser estimate was used for correction.

There was no significant interaction between group and cooling intervention on HbT levels, $F(1.4,6.8)=2.404$, $p=0.166$, partial $\eta^2=0.325$.

The main effect of cooling showed a statistically significant difference in HbT levels during the different periods, $F(1.4,6.8)=12.642$, $p=0.007$, partial $\eta^2=0.717$.

No main effect of group was found $F(1,5)=3.567$, $p=0.118$, partial $\eta^2=0.416$.

Pairwise comparisons found that HbT values over the whisker region decreased compared to the period prior to cooling upon the first 10°C cooling, with a decrease of 10.789 (95% CI, 1.264 to 20.314), $p=0.029$. There was no significant difference found between periods of 10°C cooling and 20°C cooling.

After cooling cessation there was a significant increase in HbT levels compared to the first 10°C cooling (19.314 (95% CI, 5.196 to 33.431), $p=0.021$), the first 20°C cooling (10.366 (95% CI, 5.097 to 15.635), $p=0.002$), and the second 20°C cooling (6.415 (95% CI, 1.668 to 11.162), $p=0.013$).

The lack of significance during the second 10°C cooling period is possibly due to high variability within this data set (mean=7.50, std=21.35).

3.4.4.2 Whisker Region - HbO

Mauchly's test of sphericity indicated sphericity was not met for the two-way interaction, $X^2(2)=26.943$, $p=0.05$. As such, for all interaction tests the Greenhouse-Geisser estimate was used for correction.

There was no significant interaction between group and cooling intervention on HbO levels, $F(1.3,6.6)=1.611$, $p=0.258$, partial $\eta^2=0.244$.

The main effect of cooling showed no statistically significant difference in HbO levels during the different periods, $F(1.3,6.6)=4.643$, $p=0.065$, partial $\eta^2=0.481$.

No main effect of group was found $F(1,5)=2.283$, $p=0.191$, partial $\eta^2=0.313$.

3.4.4.3 Whisker Region - HbR

Mauchly's test of sphericity indicated sphericity was not met for the two-way interaction, $X^2(2)=36.421$, $p=0.004$. As such, for all interaction tests the Greenhouse-Geisser estimate was used for correction.

There was no significant interaction between group and cooling intervention on HbR levels, $F(1.8,9)=0.462$, $p=0.626$, partial $\eta^2=0.085$.

The main effect of cooling showed a statistically significant difference in HbR levels during the different periods, $F(1.8,9)=12.936$, $p=0.003$, partial $\eta^2=0.721$.

No main effect of group was found $F(1,5)=0.024$, $p=0.884$, partial $\eta^2=0.005$.

Pairwise comparisons found a significant difference in the HbR levels during the second instance of 20°C cooling. This period showed significantly decreased HbR levels compared to the first 20°C cooling period (4.386 (95% CI, 2.102 to 6.670), $p=0.002$), and the period after cooling cessation (6.862 (95% CI, 0.791 to 12.932), $p=0.029$).

3.4.4.4 Artery - HbT

Mauchly's test of sphericity indicated sphericity was met for the two-way interaction, X2(2)=24.728, p=0.086.

There was a significant interaction between group and cooling intervention on HbT levels, F(5,25)=2.912, p=0.033, partial η2=0.368. Due to this, post hoc comparisons for main effects could not be run in the same manner. As such, univariate analysis of variance tests were conducted to identify the simple main effects.

Univariate analysis of variance testing found a singular significant result. When examining group A cooling significantly altered HbT levels, $F(5,10)=10.223$, $p=0.001$.

The main effect of cooling showed a statistically significant difference in HbT levels during the different cooling periods, $F(5,25)=10.758$, $p<0.001$, partial $\eta 2=0.683$.

No main effect of group was found $F(1,5)=2.089$, $p=0.208$, partial $\eta 2=0.295$.

3.4.2.5 Artery - HbO

Mauchly's test of sphericity indicated sphericity was not met for the two-way interaction, $X2(2)=52.700$, $p<0.001$. As such, for all interaction tests the Greenhouse-Geisser estimate was used for correction.

There was no significant interaction between group and cooling intervention on HbO levels, $F(1.5,7.7)=4.578$, $p=0.056$, partial $\eta 2=0.478$.

The main effect of cooling showed no statistically significant difference in HbO levels during the different periods, $F(1.5,7.7)=4.704$, $p=0.053$, partial $\eta 2=0.485$.

No main effect of group was found $F(1,5)=0.494$, $p=0.514$, partial $\eta 2=0.090$.

3.4.2.6 Artery - HbR

Mauchly's test of sphericity indicated sphericity was met for the two-way interaction, $X2(2)=23.607$, $p=0.110$.

There was no significant interaction between group and cooling intervention on HbR levels, $F(5,25)=1.245$, $p=0.318$, partial $\eta 2=0.199$.

The main effect of cooling showed a statistically significant difference in HbO levels during the different periods, $F(5,25)=8.431$, $p<0.001$, partial $\eta 2=0.628$.

No main effect of group was found F(1,5)=0.109, p=0.755, partial η2=0.021.

Pairwise comparisons found no significant difference in HbR levels between the different cooling periods.

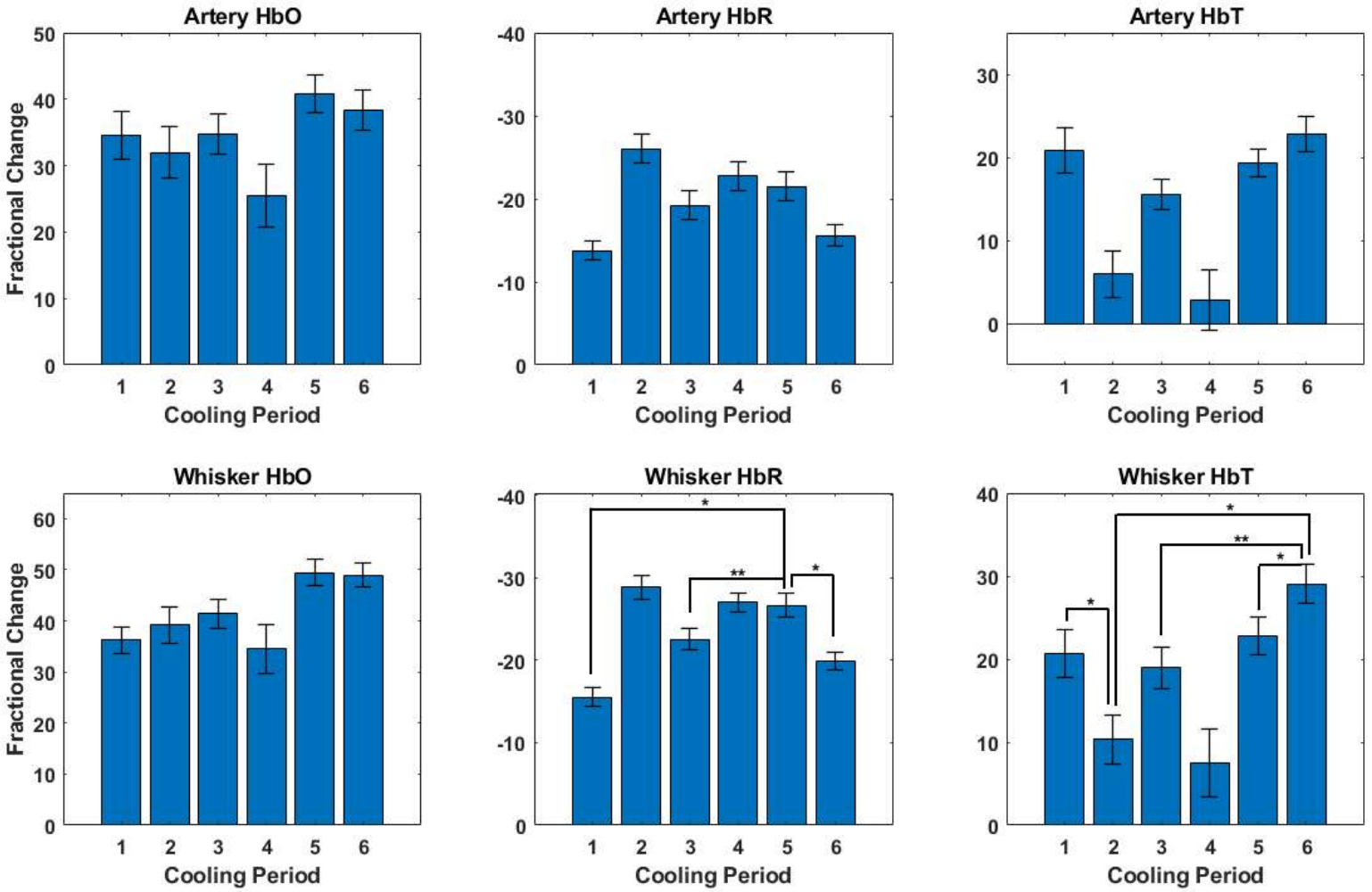

Figure 3.5 – The effect of cortical cooling on seizure induced haemodynamic activity
*Fractional change in HbO, HbR and HbT in the whisker region and MCA region (n=7). Bars represent mean fractional change over each cooling period, error bars represent SEM, * represents p<0.05, ** represents p<0.01.*

3.5 Discussion

3.5.1 Results Summary

Cooling the cortex to 10 degrees was sufficient to significantly reduce the neuronal activity occurring as a result of 4-AP injection. This effect is seen in the upper channels of the multi-channel electrode (channels 1-8), but the same effect is not found in the lowest channels (13-16) (table 3.1, figure 3.4). Cooling the cortex to 20 degrees is not sufficient to significantly reduce neuronal activity.

When examining the HbT levels within the whisker region, cooling to 10°C was sufficient to decrease HbT levels compared to the periods before and after cooling. Cooling to 20°C was also sufficient to reduce HbT levels compared to the period after cooling. HbR levels were reduced during the second instance of cooling to 20°C. HbT levels within the artery showed a significant interaction with the effect of cooling being dependent on the order of temperature presentation. No significant changes were observed in the artery HbR levels.

3.5.2 Neural response to cortical cooling during induced seizure activity

In agreement with previous research indicating the efficacy of cooling in reducing epileptiform activity in both primate and rat models (Tanaka et al 2008, Ren et al 2017, Niesvizky-Kogan et al 2022), the neural seizure activity induced by 4-AP was significantly reduced by cortical cooling to 10°C. This reduction reinforces the potential for cortical cooling as a therapeutic approach for refractory epilepsy. However, there are concerns that cooling the cortex to 10°C may induce damage, with early research in peripheral nerves finding that cooling induced significant damage and changes in schwann cells (Schaumburg et al 1967), and more recent CNS study finding that cooling to 0°C induced reversible

damage (Bakken et al 2003). Although other studies have found no long lasting damage from cooling to this temperature, the potential for risk is one that must be strongly considered when testing new therapies. As such, the future of focal cortical cooling as a therapeutic may be based in less severe cooling.

No statistically significant difference was found to occur in the LFP spike activity as a result of cooling to 20°C. There are a number of possible explanations for this. The recorded temperature within the cooling chamber was found to not be representative of the true cortical temperature in some cases. This is possibly due to heat exchange occurring thanks to cerebral blood flow, and the separation of the chamber from the cortical surface by the thinned cranial window. This may reduce the efficacy of cooling to 20°C, as the temperature at the cortical surface may not reduce a sufficient cooling level to impact the neural activity.

Finally, the rate of cortical cooling in this experiment is limited by the use of a liquid coolant, with the high specific heat capacity of water increasing the time to maximal cooling. As such, it is possible that cooling the cortical surface to a true 20 degrees, or simply reducing the time to maximal cooling, may be sufficient to reduce seizure activity. This would require further research with new cooling technologies that remove the liquid coolant element, more directly reduce cortical temperature, and provide greater control over the rate of cooling, as performed in chapter 4.

3.5.3 Haemodynamic changes due to cortical cooling

The haemodynamic changes observed show a high variability in haemoglobin changes between the artery specific measurements, and measurements taken from the whole cooled area (whisker region).

One significant finding is the interaction effect seen in the artery HbT data. This showed a significant effect of temperature in group A, but no similar effect in group B. Having inspected the cortical temperature data, one animal in group B was identified as an outlier, with the periods of 10°C cooling only reaching cortical temperatures of 22.8°C and 24°C. This limited cooling may have limited the effects that could be seen in the group, with potentially outlying haemodynamic data not being recognised due to the small sample size in this group.

It is possible that a feature of the blood vessel physiology is responsible for this variability in the haemodynamic response. The cold sensing calcium channel TRPM8 is known to be expressed by the smooth muscle cell layer of blood vessels (Fedinec et al 2021), and is sensitive to temperatures below ~28°C. One recent study in rats (Sokolov, Mengal, and Berkovich 2023) found that application of menthol (a TRPM8 agonist) to meningeal arteries expressing TRPM8 resulted in dilation of these vessels. Interestingly, another study conducted in pigs (Fedinec et al 2021) found that activation of the TRPM8 channel expressed in pial arterioles resulted in attenuation of the dilatory response invoked by various neurotransmitters. During cooling we expect that the reduction in neural seizure activity would result in attenuation of the large dilatory response caused by the seizure activity, thereby causing a reduction in HbT levels. It is possible that this response is seen in the whisker region as a result of both the reduced neural activity, and the effect of TRPM8 activation on the arterioles - reducing the effect of dilatory signals. In contrast, the impact of TRPM8 activation on the artery would be to produce the opposite effect, increasing dilatory signals rather than attenuating them. This may explain the seeming lack of significance in the artery haemodynamic measurements compared to those seen in the whisker region.

Finally, the interaction effect found in the artery region in group A could be explained by a similar mechanism. The cold reactive calcium channel TRPA1 is also expressed in cerebral blood vessels, but is sensitive to lower temperatures than TRPM8, activating at temperatures <18°C. A study examining the effect of TRPA1 activation on vessel tone (Thakore, Ali, and Earley 2020) found that activation of TRPA1 results in a vasodilatory response in cerebral arteries. With the limitations of the skull attached cooling chamber, it is possible that a step-down cooling approach (as in group A) allowed the cortical surface to reach a lower temperature during the 10°C cooling runs. This may have allowed activation of TRPA1 to occur primarily in group A, rather than group B, providing a possible explanation for both the differences in haemodynamics between the whisker and the artery regions, and for the interaction seen in group A in the artery region.

3.5.4 Future Directions

This study has demonstrated the impact of cortical cooling on drug induced synaptic and haemodynamic activity. The reduction in LFP spikes found when cooling to 10°C reinforces the previous research in the field, suggesting that cooling could be a useful therapeutic approach for those with drug resistant epilepsy (Nomura et al 2014, Harsono et al 2016, Wakuya et al 2022). Though limited by a small sample size, HbT levels within the seizure (whisker) region were shown to be reduced when cooling to both 10°C and 20°C, strengthening the argument for the utility of cooling in epilepsy treatment, with the added potential for reducing the impact of seizures on cerebral blood flow.

In order to develop cooling as a therapeutic strategy, further work needs to be conducted, creating methods for cooling that can be permanently implanted for patients.

3.6 Conclusions

The skull attached chamber utilised in this study is a useful tool for studying both neural and haemodynamic alterations during cortical cooling. While the chamber allowed concurrent neural and haemodynamic recordings providing a vital insight into their interplay during cortical cooling, the cooling provided had a number of limitations, and this method for cortical cooling is not suitable for transition to treating patient populations.

This chapter demonstrates the ability of cortical cooling to reduce synaptic activity during induced seizures, and shows that reducing this synaptic activity can alter the subsequent haemodynamic responses. However, the ultimate goal for focal cooling research is to develop a potential therapy for those with drug resistant epilepsy. The cooling technique utilised within this chapter is not suitable for translation into a therapeutic approach. There is a need for further development of translational cooling techniques, allowing for rapid direct cortical cooling, with efficient and easily controlled temperature alteration. This possibility will be explored in the next chapter (chapter 4), with the testing of a novel cooling implant.

Chapter 4

Testing a Novel Implant to Provide Therapeutic Cooling

4.1 Abstract

The potential for cooling as a therapeutic approach to epilepsy has been well established, but there are numerous complications that make developing implantable cooling devices difficult. This chapter shows the results of experiments testing a novel cooling implant with translational potential. Electrophysiological recordings were conducted in the rat 4-AP model of epilepsy, and the ability of the implant to detect seizure activity, cool the cortex, and reduce seizure activity was examined. This study demonstrated that cortical cooling, provided by the novel implant, was sufficient to reduce seizure activity at cooling temperatures between 25 and 15 degrees, with a linear relationship between the depth of cooling and reduction in neural seizure activity.

4.2 Introduction

While it has been demonstrated that cooling can effectively reduce neuronal activity during seizure-like events (Tanaka et al 2008, Ren et al 2017, Niesvizky-Kogan et al 2022), this knowledge has yet to be converted into an appropriate therapy for people suffering with intractable epilepsy. The majority of experimental cooling protocols require a chilled coolant being fed through pipes or tubing within the brain (Lomber et al 1999, Ponce et al 2008, Meredith et al 2011, Niesvizky-Kogan et al 2022). This comes with a number of drawbacks for translation into patient populations, presenting the possibility of coolant leaking, and liquid cooling systems providing a slow rate of cooling. As such, for many years there was a technological gap preventing cooling becoming a viable therapy (Cooke et al 2012). However, new technologies mean that advancements can be made towards potential therapeutic cooling devices.

Peltier devices present a novel opportunity for implantable cooling devices, as they are capable of cooling without the need for liquid coolants, can be connected to form cooling 'nets', and provide more precise and efficient cooling than liquid-based systems are capable of. Combining this new cooling potential with the ability to record neural activity could result in a closed loop system capable of detecting seizure activity and triggering an automatic cooling run to treat the seizure. This was the aim of the Integrabrain project - a novel multimodal cooling implant with the potential for translation into patient populations.

A number of pilot studies were conducted (described below) to establish an appropriate seizure model and test the limits of the implant prior to conducting rigorous cooling testing. The majority of this chapter focuses on the subsequent testing of the implants cooling capabilities, establishing whether this implant could provide sufficient cooling to effectively reduce the 4-AP induced seizure activity.

The study found that cooling to temperatures anywhere between 25-15°C was sufficient to reduce synaptic seizure activity, with cooling to 18°C providing the greatest potential for future translational work.

4.2.1 Aims

This study aimed to test a novel implant developed by Dr Spencer Moore. The implant was tested using the 4-AP model of focal epilepsy to interrogate its ability to: detect seizure activity using onboard electrodes, cool to a range of temperatures, and reduce seizure activity.

4.3 Pilot studies - Experimental Model and Implant Functionality

Prior to the systematic testing of the implant described below, 12 animals were used in pilot studies to establish the 4-AP model and confirm functionality of the implant within the experimental setting. For these studies all animals underwent the surgical protocol described in chapter 2 (section 2.2.5).

4.3.1 Electrode insertion

The method for electrode insertion had to be adapted from previous studies conducted within the lab. Previously, electrodes were inserted perpendicular to the cortical surface (as described in chapter 2 for study 1 of this thesis) however, the requirement for concurrent implant placement necessitated insertion of the electrode at a more acute angle (figure 2.2B). To facilitate the correct electrode placement, a model implant base was created (figure 2.2A). This could be placed over the craniectomy region, enabling visualisation of the intended position of the peltier chip and onboard electrodes. With the model base positioned over the cortex, the electrode was positioned stereotactically above the cortex, and optimal electrode placement was visualized - the tip of the electrode directly beneath the peltier chip, as close to parallel with the cortex as possible, and with the insertion point avoiding any major blood vessels. Once appropriate positioning had been found, stereotactic measurements were taken to ensure the electrode was inserted correctly, the model base was removed, and the dura pierced with a sharp needle before the electrode was slowly inserted to the calculated position.

4.3.2 Seizure Induction

The 4-AP model of seizure induction had been used previously in the lab (Harris et al 2014, 2018) but had not been used for >5 years. The first pilot studies conducted established the necessary volume of 4-AP required to induce sustained and consistent seizure activity. Using a hamilton syringe pump, increasing volumes of 4-AP were infused until sustained seizure activity was observed (figure 4.1). This served as a baseline for the future experiments, with 4-AP being infused at a rate of 1μl over the course of 5 minutes (200nl/minute). Two infusions were completed at this rate before sustained seizure activity could be observed, with the slow rate of infusion and small volume helping to reduce the risk of inducing damage through the infusion.

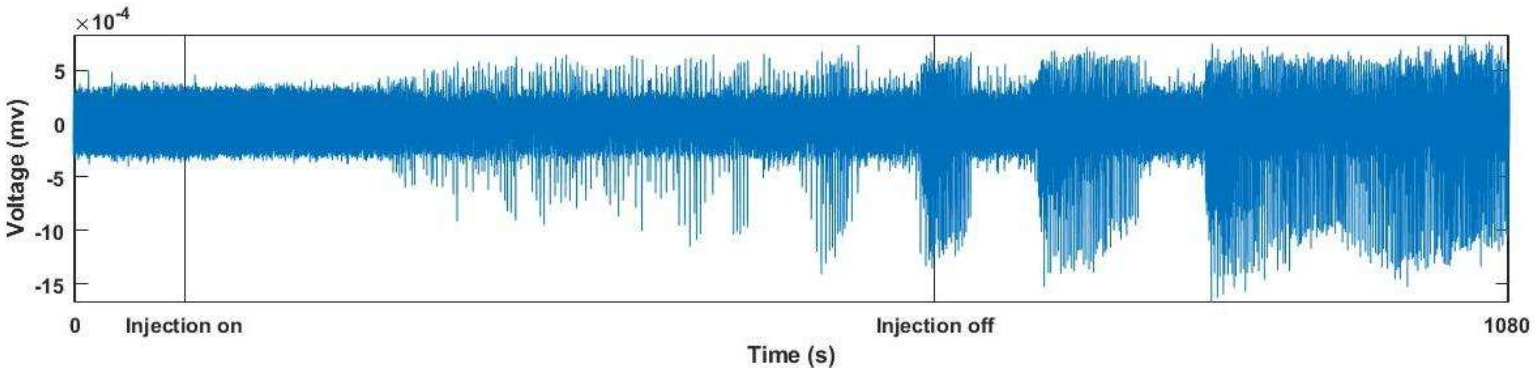

Figure 4.1 – Seizure Induction

An example snapshot of neuronexus recording showing the onset of seizure following a second injection of 4-AP. The snapshot displays data collected from channel 8 of the neuronexus electrode, showing the second injection of 4-AP performed, with subsequent seizure events developing into a sustained seizure.

4.3.3 Onboard electrodes

Neural data recorded from the onboard electrodes (built into the base of the novel implant) was compared to data collected over the same time period by the neuronexus electrode. The data were synchronized with a TTL pulse sent from the implant controller to the neuronexus data acquisition hardware. This pulse was sent at the beginning of each experiment and was then configured to send a pulse at specified points - the start of each cooling run, change of state of the thermoelectric cooler (TEC) (on/off), change of state of

the microfluidic pump (on/off). This allowed the onboard electrode data to be directly compared to the neuronexus data.

4.3.4 Cooling capabilities

Prior to moving to *In Vivo* testing, Dr Spencer Moore performed a number of cooling tests *In Vitro*. These tests demonstrated that the implant was capable of cooling to 15°C. The *In Vivo* cooling tests examined the ability of the implant to cool with the added strain of rewarming from cortical blood flow, and a warmer experimental environment.

The cortical temperature of the rats was ~33.5°C at the point of thermal equilibrium being reached by the implant. Once this equilibrium was reached, the cooling tests were started.

4.4 Methods

Surgical methods and an overview of the cooling implant can be found in the methods section of this thesis (chapter 2, sections 2.2 and 2.7.2). The methods highlighted in this chapter refer to the specifics of the novel device, and the experimental protocols employed in this study. A total of 19 animals were utilised following the pilot studies, with 5 experiments terminated due to technological failure, and 2 excluded from analysis due to electrical noise masking neural data.

4.4.1 Surgery overview

All animals underwent craniectomy surgery, electrode insertion, seizure induction and implant placement. In a subset of animals, cannulation of the femoral artery and vein was performed to allow measurement of blood gases over the course of the experiment (described in Chapter 2).

4.4.2 Experimental Protocol

The experimental cooling protocol was started once seizure activity was established. Cooling was applied at 4 different temperatures (25°C, 20°C, 18°C, 15°C) cooling from the baseline cortical temperature of ~33.5°C. Each temperature was applied as a set of 4 cooling periods, with cooling lasting 60s, followed by a rewarming period of 120s for a total run time of 180s per cooling period (figure 4.2). The 4 temperatures were applied in a randomly generated order in each animal.

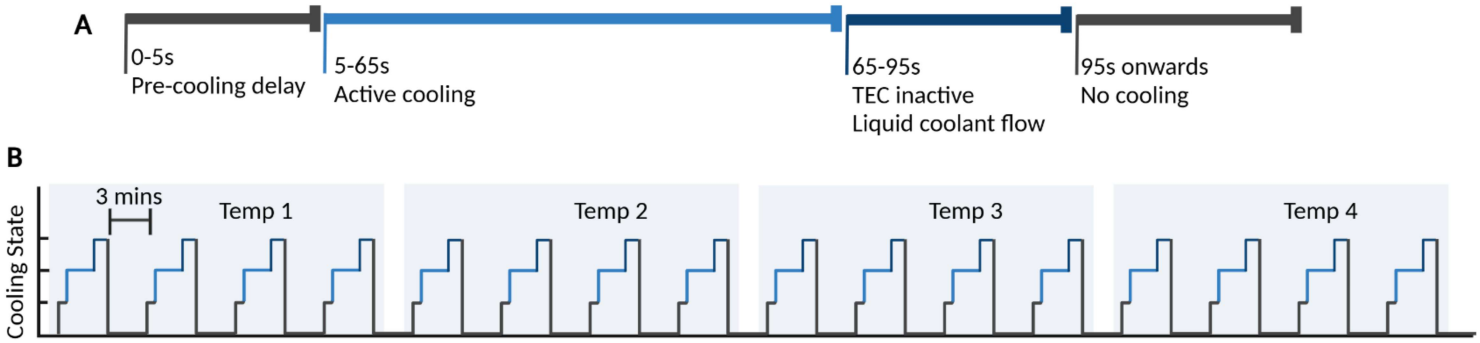

Figure 4.4 – Experimental Cooling Protocol

(A) *Timeseries of a single cooling period, showing the timing of each aspect of the cooling.* ***(B)*** *Overall experimental timeseries showing all cooling runs conducted following seizure induction. The 4 temperatures were randomised. There was a 3-minute delay between cessation of 1 cooling run and the start of the next.*

4.4.3 LFP Analysis

LFP data was extracted from the neuronexus data collected from a total of 12 animals, with some animals including multiple experimental runs for a total of 18 experimental sessions. LFP data was split into cooling periods totalling 160s each, with 50s of baseline activity, followed by the 65s cooling period, the 30s liquid flow period, and concluding with a final 15s rewarming period (figure 4.2).

Once the data was split into cooling periods, a contour trace was applied to each period, tracking the lowest point of the LFP spikes (figure 4.3). This contour was calculated from the

mean of the 4 electrode channels displaying the greatest effect of cooling. The contour value before cooling was defined as the contour value at 50s, with the contour value during cooling being the point of maximal change (contour peak) for each period. These values were then extracted for comparative analysis.

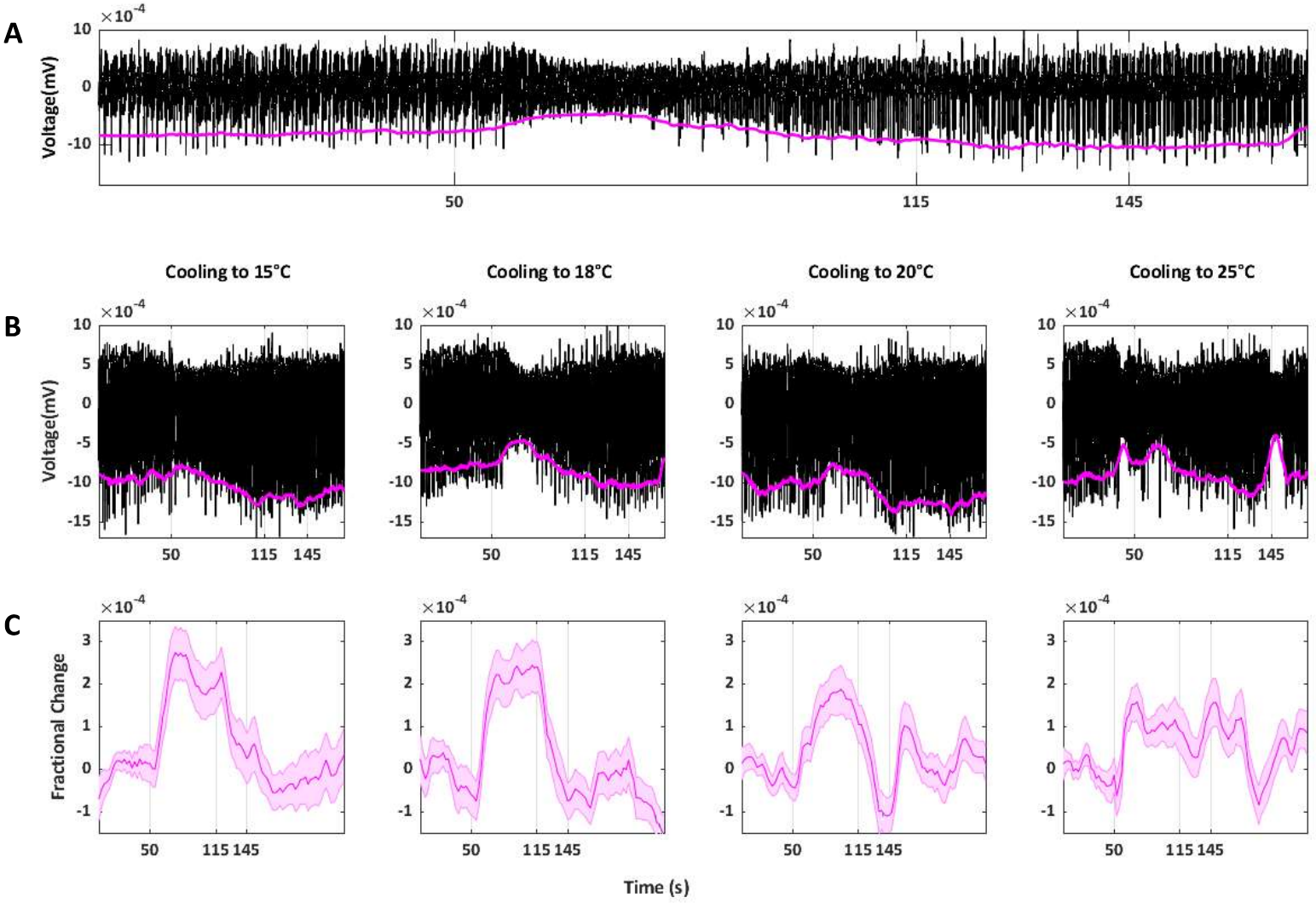

Figure 4.3 – LFP and contour traces

*A contour trace was applied to every cooling trial in each animal, and the change in contour magnitude was extracted for analysis. Figure shows **(A)** a single cooling period with contour tracing applied, **(B)** example electrode recording and contour trace from each temperature (contour applied to a single cooling trial at each temperature), **(C)** the fractional change in contour (averaged across 4 cooling trials) because of cooling to each temperature. Example data taken from animal with ID 241023.*

4.4.4 Statistical Analysis

Despite difficulties with cooling to 15°C, these cooling attempts were analysed alongside the trials cooling to 25°C, 20°C, and 18°C. The temperature range for these attempts was 15-18°C, and the data acquired during these lower temperature cooling runs is still able to provide valuable information about the impact of the implant's cooling on seizure activity.

Outliers were assessed through inspection of boxplots. A shapiro-wilks test established that all data were normally distributed ($p>0.05$). R was used to analyse the data using a linear mixed model, with the Animal ID as the random factor, comparing the contour peak across the cooling temperatures to the 34°C baseline with Tukey's correction for multiple comparisons. Outliers were identified in R, using the identify_outliers() function from the rstatix package. Data points falling outside 1.5 times the inter quartile range from the 1st or 3rd quartile were identified as outliers. A resulting 10 values were identified and removed from analysis after inspection of the raw data identified cessation of seizure activity unrelated to cooling, or excessive electrical noise.

4.5 Results

4.5.1 Onboard Electrodes

A visual snap-shot of the recorded data is shown in figure 4.4 demonstrating the ability of the onboard electrodes to record neural activity, despite the difference in location of the onboard electrodes compared to the neuronexus probe (figure 2.2), with the neuronexus performing intracerebral recording and the implants onboard electrodes performing electrocorticographic recording.

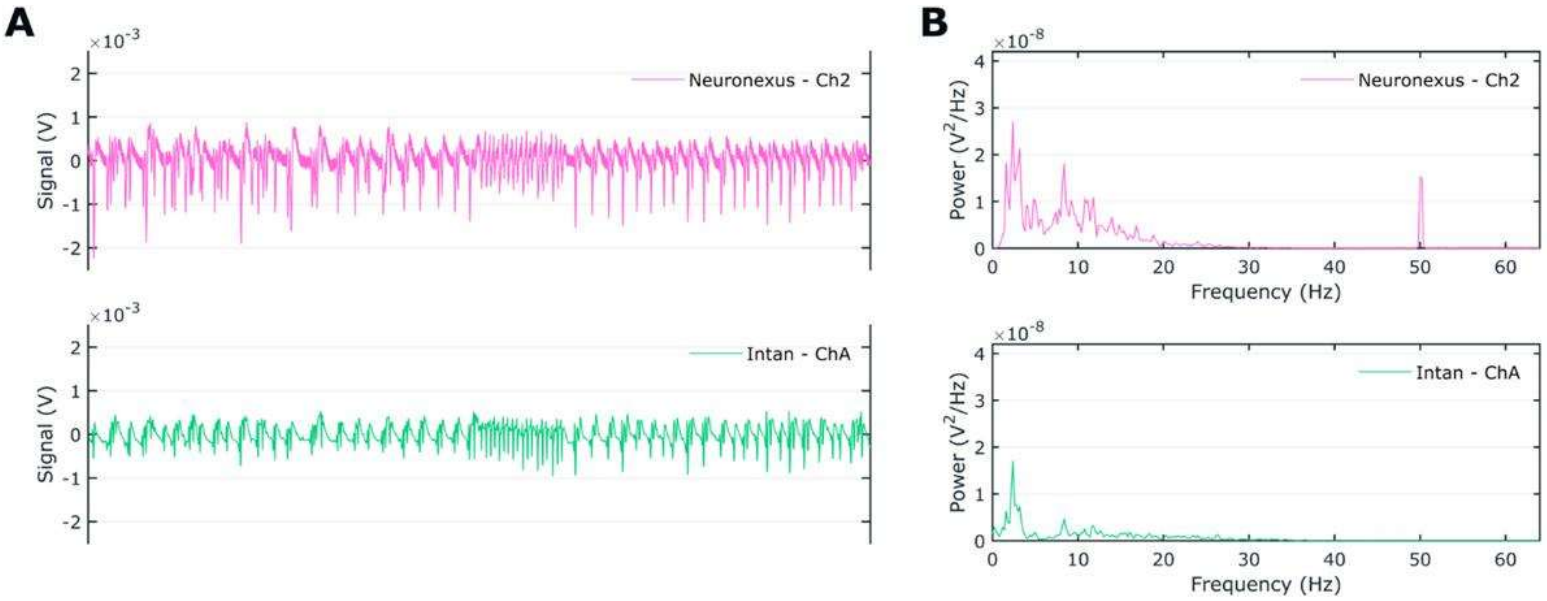

Figure 4.4 – Electrode comparison

(A) *A snapshot of neural recording from both the neuronexus and the onboard electrodes, showing comparable readouts from both systems.* ***(B)*** *Power spectral density of recordings from onboard electrodes and neuronexus, indicating similar profiles.*

4.5.2 Cooling Capabilities

The tests found that the implant was capable of cooling to 18°C without difficulty (figure 4.5). However, the implant was unable to consistently and reliably cool to 15°C, due to the liquid within the heat dissipation system warming up from the ~20°C it was kept at during *In Vitro* testing to between 25 to 27°C in the *In Vivo* experimental room.

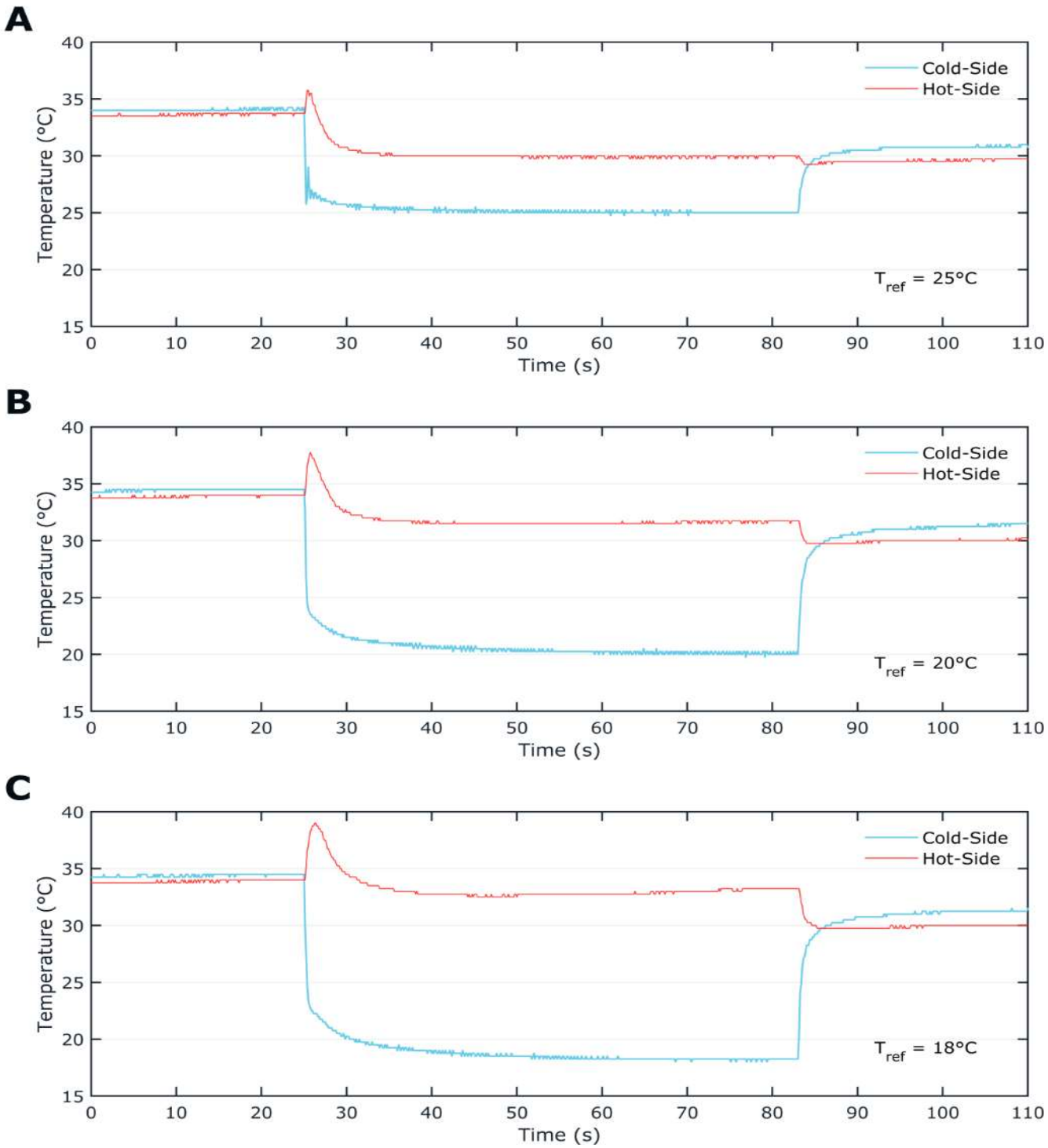

Figure 4.3 – Implant Cooling Ability

*Single run temperature recordings from both the hot and cold sides of the TEC when attempting cooling to **(A)** 25°C, **(B)** 20°C, **(C)** 18°C In Vivo. The TEC is capable of cooling to 18°C, with a consistent cooling profile observed across the 3 temperatures.*

Figure supplied by Dr Spencer Moore.

4.5.3 Impact of cooling on LFP amplitude

All data was normally distributed as assessed by Shapiro-Wilk's test ($p>0.05$).

Contour values (mV)	Before Cooling	During Cooling
25°C Cooling runs	-0.00138 ± 0.0000895	-0.000941 ± 0.0000636
20°C Cooling runs	-0.00168 ± 0.0000935	-0.00112 ± 0.0000573
18°C Cooling runs	-0.00163 ± 0.0000799	-0.00103 ± 0.0000476
15°C Cooling runs	-0.00164 ± 0.0000743	-0.000958 ± 0.0000490

Table 4.1 - Contour values

Mean contour values (mV) taken before and during cooling (values averaged across all trials at each temperature). Values extracted as described in section 4.4.3. Error shown is STD.

Significant differences were found between pre- and post-cooling contour magnitude at all cooling temperatures when cooling was applied.

Cooling successfully reduced the contour magnitude, during all cooling temperatures compared to their baselines (25°C cooling vs baseline: b=-0.000436, SE=0.0000860, t=5.068), (20°C cooling vs baseline: b=-0.000401, SE=0.0000649, t=6.182), (18°C cooling vs baseline: b=-0.000568, SE=0.0000649, t=8.746), (15°C cooling vs baseline: b=-0.000651, SE=0.0000692, t=9.409).

Linear mixed model analysis found no significant differences in the contour amplitudes between cooling runs of different temperatures.

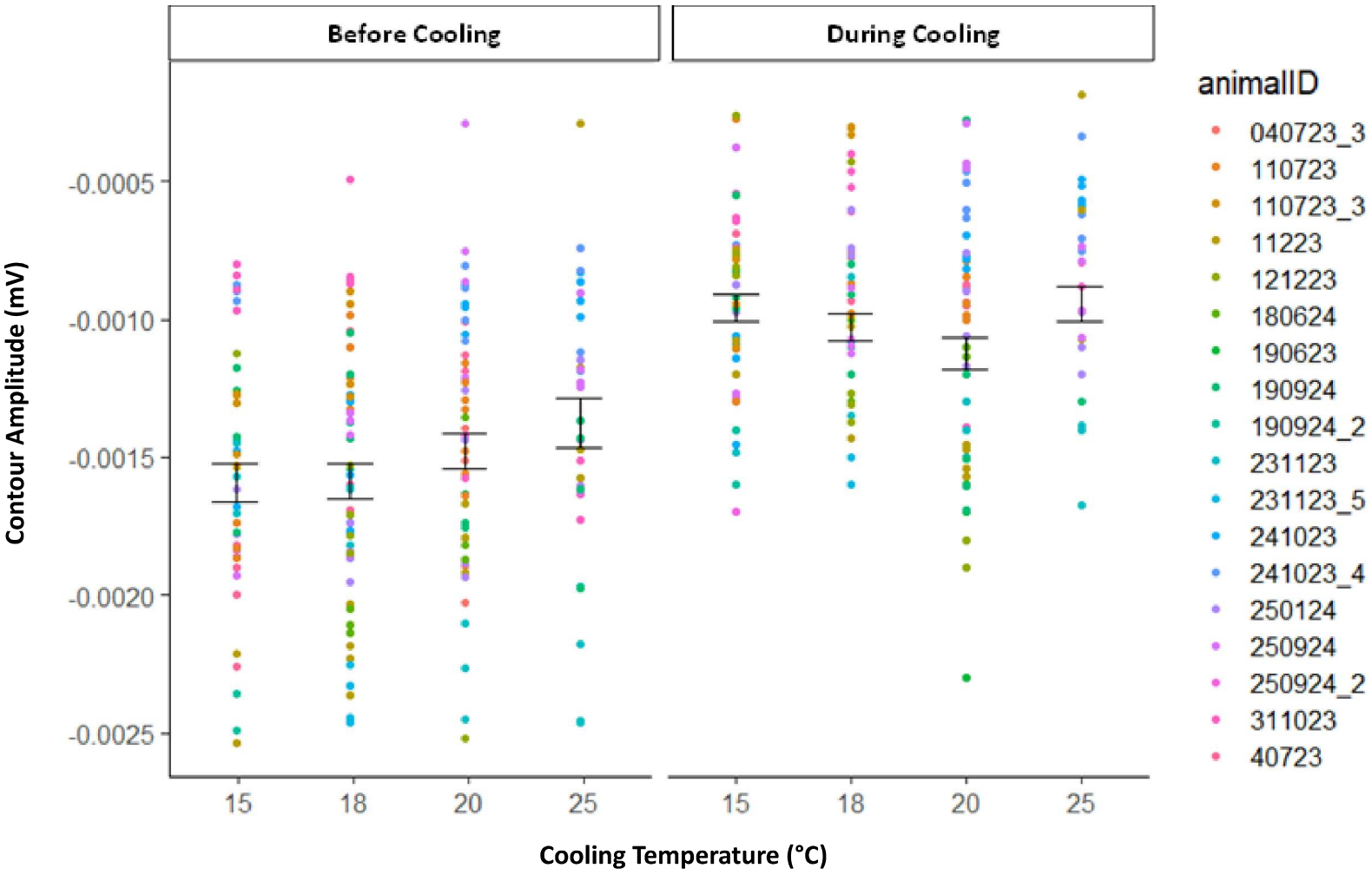

Figure 4.6 – Impact of Cooling on LFP Spike Value
Contour magnitude value (a measure of spike amplitude) taken before and during each cooling trial. Separated by temperature, with each colour representing 1 animal, and each dot representing 1 cooling trial.
Bars represent mean and SEM.

4.6 Discussion

4.6.1 Results Summary

The onboard electrodes within the implant were capable of recording neural activity, with near identical signal dynamics to the neuronexus electrode. The implant was also capable of cooling to between 25°C and 18°C with no significant strain on the system, though was unable to consistently reach 15°C during *In Vivo* experiments. Finally, the cooling delivered

by the TEC was sufficient to significantly reduce the amplitude of the 4-AP induced LFP spikes.

4.6.2 Cooling capabilities

The alteration in the implant's ability to cool to 15°C could result from a number of factors. Firstly, the *In Vivo* experimental room had an ambient temperature of between 25°C and 27°C, which likely resulted in the coolant liquid within the microfluidic loop having a higher baseline temperature than in the *In Vitro* testing. It is also possible that the microfluidics system was unable to compensate for the large initial temperature spike from the hot side of the TEC. As shown in figure 4.3 the initial temperature spike increases as the temperature commanded from the device decreases. It is possible that the larger increase in temperature caused by a 15°C cooling run resulted directly in system instability, or in a triggering of the safety shut-off built in to prevent the hot side of the TEC from overheating.

One potential solution to this may be to adjust the systems programming, starting the microfluidics system before turning on the TEC. Currently the systems start simultaneously, with a slight delay (~500ms) occurring before water starts moving in the microfluidics system. It is possible that with the water initially stationary within the liquid loop, there is not enough of a temperature differential to enable efficient heat transfer from the hot side of the TEC to the water. Starting the microfluidic system prior to attempting cooling may allow more efficient heat transfer and thereby allow the system to consistently cool to 15°C.

4.6.3 Impact of cooling on LFP spike amplitude

In support of a number of previous studies (Tanaka et al 2008, Ren et al 2017, Niesvizky-Kogan et al 2022), and the previous chapter (chapter 3) in this thesis, cooling was seen to

have a profound effect on LFP activity. The amplitude of LFP spiking was significantly reduced by all cooling temperatures, as demonstrated by the significant change in the LFP contour. The previous chapter in this thesis found that cooling to 20°C was not sufficient to reduce cortical seizure activity, this is in contrast to the current findings that cooling to even 25°C was sufficient to reduce synaptic seizure activity. It is likely that the cooling provided by the novel implant is more efficient than that provided by the previously described skull-attached chamber. Firstly, the implant is in direct contact with cortical tissue, cooling it directly, rather than through a layer of skull. It is therefore likely that the temperature recorded at the site of the implants TEC is the same as the temperature experienced by the cortical tissue, unlike the previous cooling setup where the temperature recorded in the chamber could be up to 10°C cooler than that within the cortex. Further, the implant is capable of delivering cooling at a rate of ~3°C per second, classifying it as a rapid focal cooling device. This rapid cooling rate could potentially be the reason for the improved impact of cooling seen in this chapter (with cooling to 25°C significantly reducing neural activity, in contrast to the 20°C results in chapter 3), as the skull-attached chamber delivered cooling at a rate of 0.12°C per second (3°C change in 25.5s). In support of the findings of this study and chapter 3, Motamedi et al (2006) demonstrated that rapid cooling rates caused even small temperature changes to effectively reduce neuronal activity, while slower cooling rates required greater temperature changes to achieve the same reduction.

The implant was not able to consistently reach 15°C *In Vivo*, however, a number of studies (D'Ambrosio et al 2013, Guilliams et al 2013) have demonstrated that a drop of only a few degrees in body temperature can have a profound effect on seizures. This is demonstrated above, as no significant difference was found between the different cooling conditions. Previous research has suggested cooling to anywhere from 25°C to 15°C (Fujii et al 2010,

Nomura et al 2014), but this study seems to suggest that a lower level of cooling can have the same impact as more severe changes in temperature. It is possible that this is again due to the rapid nature of the cooling provided by the implant.

4.6.4 Future Directions

This study has demonstrated the efficacy of a new implantable cooling device, capable of detecting neural activity, and providing cooling that is sufficient to reduce seizure activity. The next steps in this research would entail developing a neural classification algorithm capable of classifying the neural activity recorded by the onboard electrodes, and triggering cooling from the TEC in response to detected seizure activity. This would create a closed loop system, which could be combined with optogenetic techniques such as those utilised by Krook-Magnuson et al (2013), where they found that on-demand inhibition of excitatory neurons through halorhodopsin activation was capable of halting seizure activity. A multi-modal implant would allow for even more precise seizure control, and the potential to target deeper cortical structures. Precisely targeted seizure control (as provided by small peltier chips and optogenetic techniques) would reduce the likelihood of off-target effects resulting from treatment, thereby increasing quality of life for patients.

The model used in this study was also not a spontaneous seizure model, this would be a useful test to establish whether the cooling from the implant could halt seizure activity in the case of spontaneous rather than drug induced seizures. Finally, some aspects of the implant design would require adaptation if the implant is to move from an experimental to a clinical device. Many of those not eligible for surgical resection treatment may have deep seizure foci, or multiple foci. Addressing this would require the production of a heat pipe, to carry the cooling into deeper brain structures. Tanaka et al (2008) successfully suppressed

hippocampal seizure in rats through application of focal cooling using a copper needle attached to a TEC. This heat pipe allowed the tip of the needle to be cooled by a TEC on the cortical surface, with no histological damage observed as a result of the cooling intervention. Coupling of a similar heat pipe with the current design would allow for cooling of both cortical and deep brain structures.

Addressing multiple seizure foci may require the coupling of multiple TEC components and electrodes to create a 'cooling net' capable of detecting seizure activity and cooling in multiple cortical regions, or the combination of surface and deep structure cooling alongside other seizure suppression techniques such as optogenetics to target synaptic activity directly and prevent seizure spread.

4.7 Conclusions

The novel implant described above provides a real possibility for a future therapeutic cooling device. The ability to both detect neural activity and provide effective cooling combined into a single device is a leap forward in the development of cooling therapies. Further testing in spontaneous seizure models, and the development of the closed-loop system with seizure detection algorithm would push this implant to the forefront of novel therapies for epilepsy.

Chapter 5

Carbogen Gas as a Novel Treatment for Alzheimer's Disease

5.1 Abstract

There is a necessity for novel treatments for Alzheimer's disease, with the number of cases climbing, and current treatments only suitable for those early in the course of symptomatic AD. Current pharmacological treatments are targeted to either reduce levels of amyloid within the brain, or act to reduce symptoms of memory loss and cognitive difficulties without altering disease course. Research into hyperbaric oxygen treatment (Chen et al 2020) suggests the possibility that gas treatments could provide a novel therapeutic approach for AD. This pilot study investigated the impact of carbogen gas (95% O_2, 5% CO_2) treatment on cortical plaque load in the APP/PSEN1 model of AD. The study found no significant alteration in plaque load between the treated and untreated mice, however did reveal a novel finding of lower plaque burden in regions of cerebral cortex supplied by large branches of the MCA. Limitations of the short treatment period, and the current lack of further histological analysis mean that we cannot discount carbogen as a potential therapy, but should rather investigate further, with an increased treatment period, and further outcome measures.

5.2 Introduction

There are currently around 50 million patients diagnosed with Alzheimer's disease worldwide, with that number likely to double every 5 years (Breijyeh and Karaman 2020). AD is characterized by accumulation of Amyloid Beta plaques, and neurofibrillary tau tangles, and is often identified due to the associated memory loss, and cognitive impairment (Iadecola 2017).

The current pharmacological treatments for AD target acetylcholine and glutamate levels within the brain, in order to ameliorate memory difficulties, and slow down neuronal decline

(Anand and Singh 2013, Sharma 2019, Breijyeh and Karaman 2020). Newly developed treatments (donanemab and lecanemab) are immunotherapies, acting to reduce levels of amyloid within the brain. However, these therapies are only suitable for patients very early in the course of symptomatic AD and, due to high costs, are not available on the NHS (van Dyck et al 2023, Sims et al 2023).

New treatment methods should aim to alter disease course as well as reducing amyloid levels, and in order to do this we must move away from only targeting amyloid directly, to also targeting other potential disease mechanisms. research into hypercapnia (Moriyama et al 2022, Moris et al 2023) shows improvements in cognitive function and increased cerebral blood flow in healthy individuals. Atmospheric oxygen has been shown to cause a large change in baseline perfusion in young AD mice (Shabir et al 2020), and hyperbaric oxygen therapy (HBOT) has shown promising effects in animal models of AD, successfully reducing amyloid load (Shapira et al 2018). In addition, hyperbaric oxygen therapy has been found to reverse symptomatic decline in patients (Chen et al 2020). This approach is however still limited, requiring patients to attend clinics or hospitals for daily appointments. Carbogen therapy has the potential to become an in-home therapy, with the combination of oxygen and carbon dioxide's dilatory effects increasing cerebral vessel dilation, simultaneously increasing tissue oxygenation, and increasing clearance of amyloid. This chapter presents a pilot study investigating the efficacy of carbogen treatment at reducing amyloid plaque load in the APP/PSEN1 mouse model of AD.

5.2.2 Aims

This pilot study aimed to investigate the impact of carbogen treatment on amyloid plaque load in the APP/PSEN1 mouse model of AD.

5.3 Methods

Experiments were conducted in APP/PSEN1 mice, with treated mice receiving carbogen treatment for 1 hour a day over 2 months (not including weekends).

The methods used for carbogen treatment, methoxy staining, and tissue extraction can be found in the methods chapter of this thesis (chapter 2). The cortical tissue imaging and image analysis are described below.

5.3.1 Imaging

Following formalin fixation brains were imaged using a leica MZ205 fluorescence stereo microscope allowing visualisation of methoxy stained amyloid beta plaques. Images were taken of both the dorsal and ventral surfaces of the brain at 15.7x magnification, and images at 40x magnification were taken covering the somatosensory and posterior cortices of both hemispheres, the colliculi and cerebellum, and corresponding areas of the ventral surface.

Whole cortex images provide an overview of the amyloid deposits within the entire cortex, while images taken at 40x magnification allow identification of potential patterns in amyloid deposition. As treatment is focussed on increasing blood flow, images taken at a greater magnification allow for the areas surrounding major blood vessels to be compared to those without major vessels.

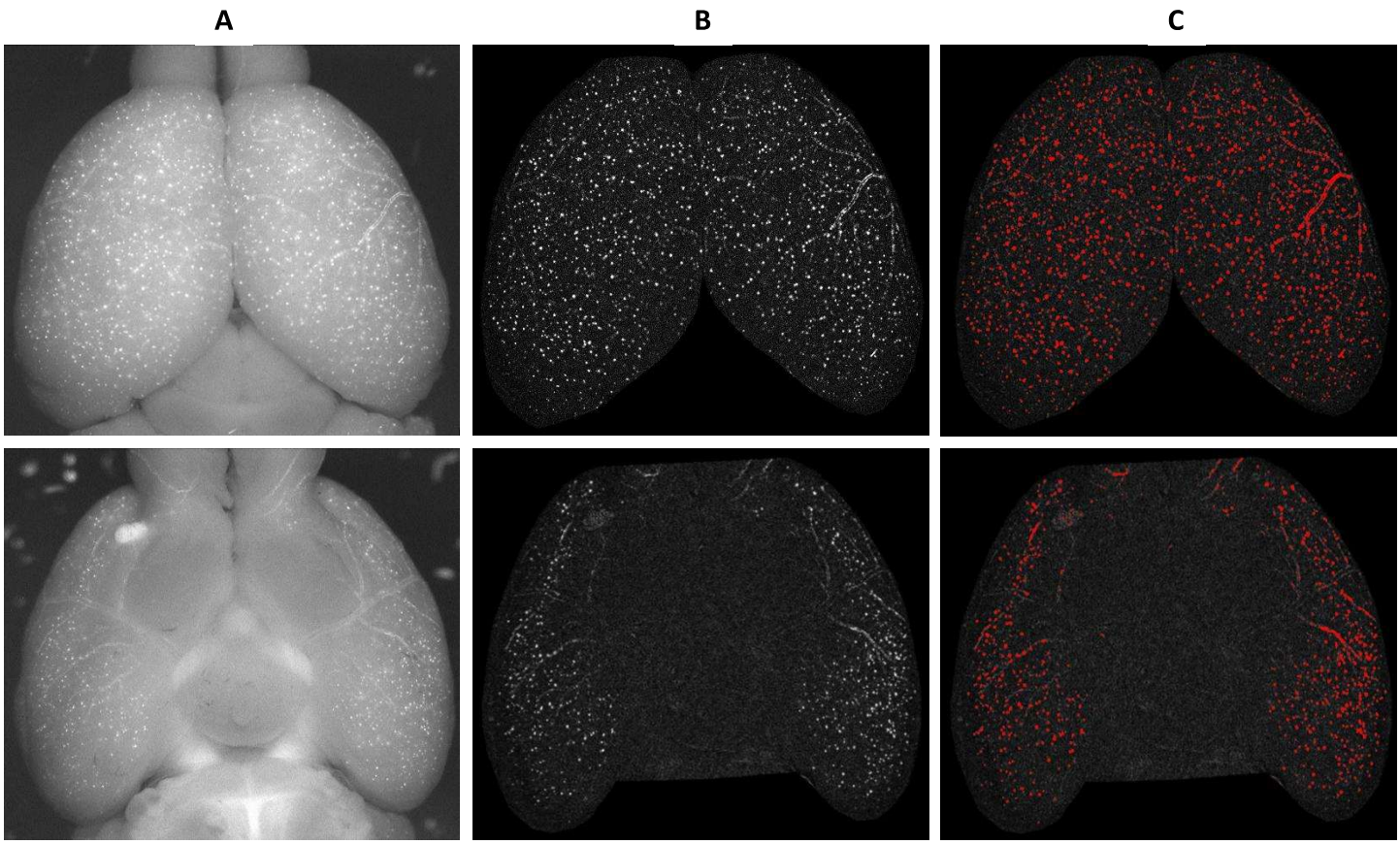

Figure 5.1 - 15.7x Magnification Image Analysis of Methoxy-XO4 Staining

(A) *Raw images of dorsal (top row) and ventral (bottom row) cortical surfaces taken at 15.7x magnification (with brightness enhanced), showing methoxy-XO4 labelling of amyloid.* ***(B)*** *Image showing selections of cortex taken for analysis, with image background removed* ***(C)*** *Threshold applied, identifying amyloid plaques for analysis.*

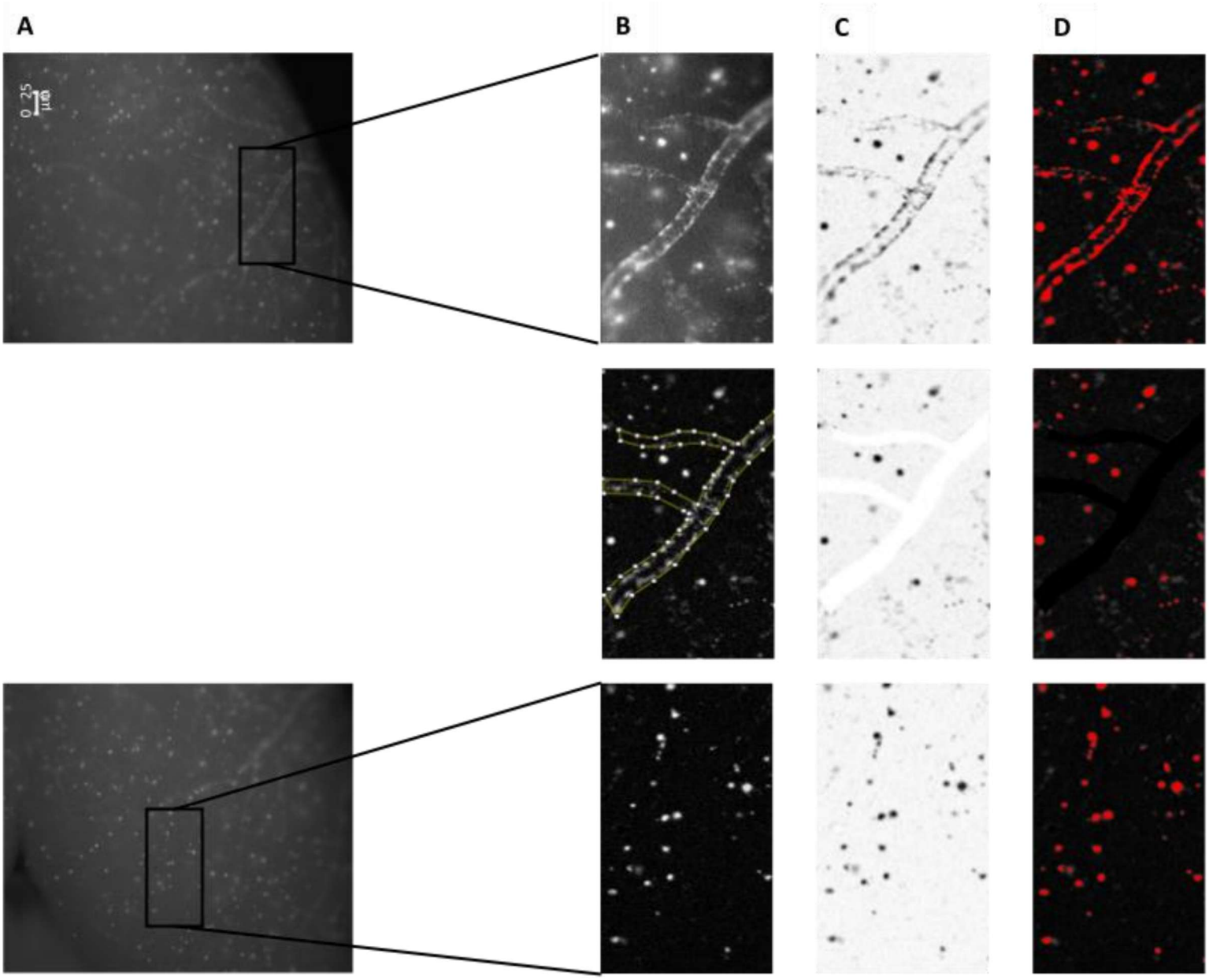

Figure 5.2 – 40x Magnification Image Analysis of Methoxy-XO4 Staining

(A) *Raw images of barrel (top and middle) and posterior (bottom row) cortex taken at 40x magnification, showing the barrel vessel and amyloid plaques.* ***(B)*** *Image sections of barrel and posterior cortex taken for analysis, showing the selection of the artery in the barrel cortex.* ***(C)*** *Smoothed inverted images, showing the vessel removed from the barrel cortex image.* ***(D)*** *Threshold applied, identifying amyloid plaques for analysis*

5.3.2 Image analysis

Image analysis was conducted using ImageJ (ImageJ, U. S. National Institutes of Health, USA). For analysis of the 15.7x magnification images, both the dorsal and ventral surfaces

were analysed in the same manner (figure 5.1). Firstly, a selection was made encompassing the entire cortical area, allowing the background of the image to be cleared, and a measure of the cortical area was taken. Any anomalous inclusions within the image (e.g. individual animal hairs) were selectively removed before the image was smoothed, reducing the impact of pixelation, and enabling clearer identification of plaques. The auto threshold feature was utilised to identify individual amyloid plaques, and these were counted using the 'Analyze particles' feature within ImageJ. The total number of plaques, average size of plaques, and area covered by plaques was extracted, and used to calculate the percentage of cortex covered by plaques (reported as area of plaques).

Analysis of the 40x magnification images included measures of the plaque load on the middle cerebral artery (MCA). Prior to analysis, 200x400µm sections of the 40x image were taken (figure 5.2). These sections covered the whisker barrel and posterior cortical areas, with the MCA included in the barrel cortex section. Firstly the background was cleared, the images smoothed, and plaques were counted as described above. A selection was then made of the MCA within the barrel cortex, and this MCA selection was removed before the image was processed and analysed as previously described. This accounted for variations in the size of vessels, and differences in levels of amyloid present in the vessels.

5.3.3 Statistics

Data from the 15.7x magnification images were analysed using an independent samples t-test, while data from the 40x magnification images were analysed using both independent and paired samples t-tests to examine differences between treated and control groups, as well as between cortical areas. During pre-testing of assumptions for the t-test outliers were identified through inspection of boxplots. Due to the small sample size in this pilot study all outliers were kept within the sample, but are identified below.

5.4 Results

5.4.1 Whole cortex image analysis

whole cortex Image analysis	Treated		Control	
	Dorsal	Ventral	Dorsal	Ventral
Plaque Count	2101.75 ± 160.866	1103.5 ± 130.712	2095.6 ± 271.180	909.8 ± 141.971
Plaque Size	974.196 ± 60.807	937.983 ± 45.685	993.506 ± 96.866	1065.552 ± 60.008
Area of Plaques (%)	6.2259 ± 0.594	3.1317 ± 0.377	6.3662 ± 0.494	3.1718 ± 0.497

Table 5.1 - Results of whole cortex image analysis
Mean results of plaque count, size, and area, averaged within treated (n=4) and control (n=5) groups. Error shown is STD.

5.4.1.1 Dorsal cortical surface

Outliers for all data were assessed by inspection of a boxplot. No outliers were identified in the dorsal plaque count data, 1 outlier was identified in the plaque size data for the control group, and 1 outlier was identified in the area of plaque data, also in the control group. Due to the small sample size outliers were kept in the data. Dorsal plaque count data was normally distributed as assessed by Shapiro-Wilk's test (p>0.05), and there was homogeneity of variances as assessed by Levene's test (p=0.072). Dorsal plaque count was not significantly different between the treated and control groups $t(7)=0.18$, $p=0.986$.
As assessed by Shapiro-Wilk's test, dorsal plaque size data was normally distributed in the treated group (p=0.631), however control group data was not normally distributed (p=0.036). No significant difference was found between treated and control groups as assessed by Mann-Whitney U test (U=9, z=9, p=0.806).

Dorsal area of plaque data in the treated group was normally distributed (p=0.537), while control data was not (p=0.045). No significant difference was found between treated and control groups as assessed by Mann-Whitney U test (U=12, z=12, p=0.624.

5.4.1.2 Ventral cortical surface

Inspection of a boxplot identified no outliers in the plaque count data, or the plaque area data, with 2 outliers identified in the plaque size data. A Shapiro-Wilk's test indicated that the treated animal plaque count data was not normally distributed (p=0.042), while the control data was normally distributed (p>0.05). Due to the robustness of the independent samples t-test, and the normal distribution of the control data, an independent samples t-test was still utilised to analyse the ventral data. Homogeneity of variances was confirmed by Levene's test (p=0.479).

Ventral plaque count was not significantly different between the treated and control groups (p=0.36).

Ventral plaque size data was normally distributed in both control (p=0.445) and treatment (p=0.931) groups, and no significant difference in plaque size was found between the two groups (p=0.797).

Ventral area of plaque data was normally distributed in both the treated group (p=0.960), and the control group (p=0.504), with no significant difference found between the treated and control groups (p=0.395).

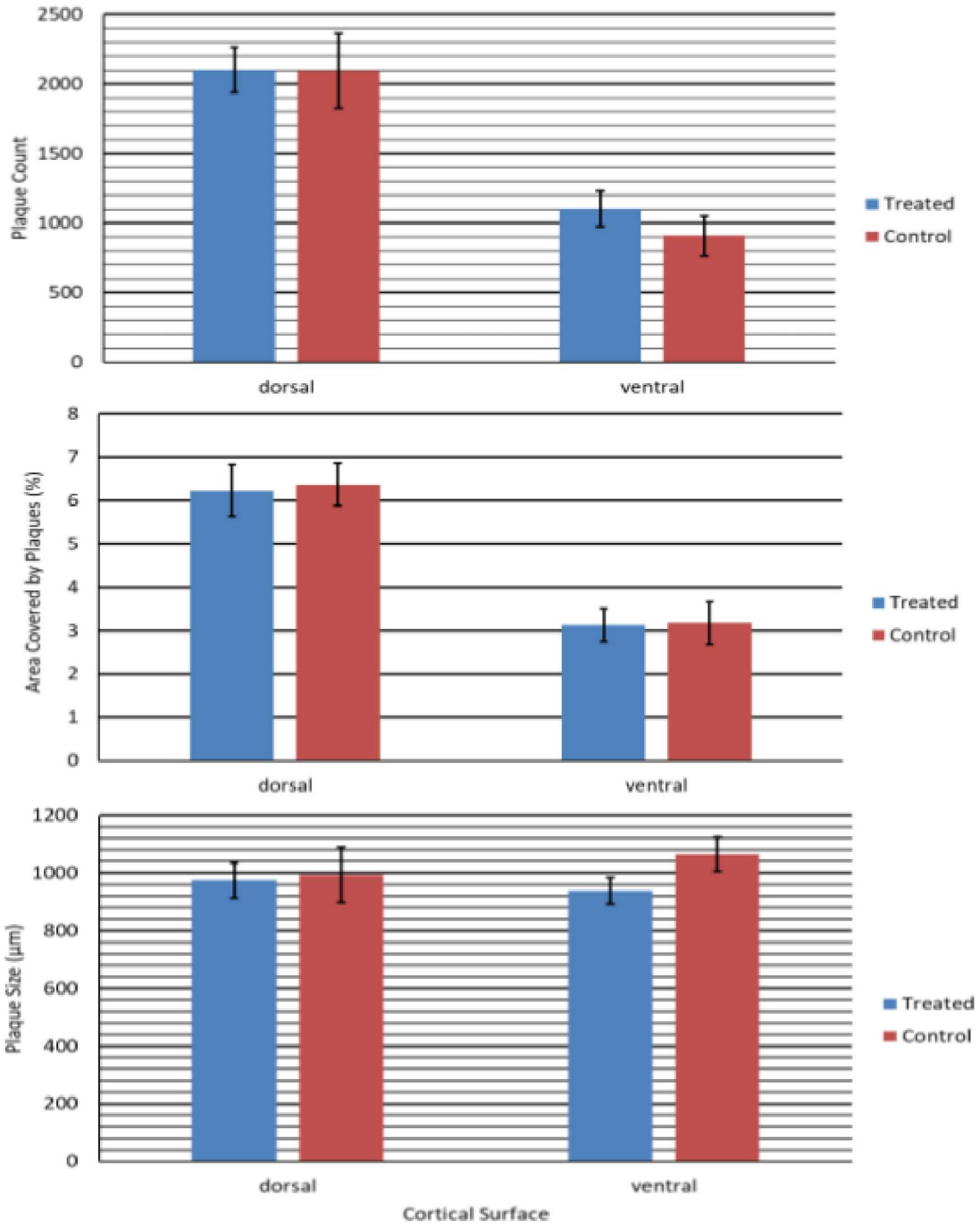

Figure 5.3 – 15.7x Results

Graphs showing the mean plaque count, area covered by plaques, and plaque size on both dorsal and ventral cortical surfaces from treated (n=4) and control (n=5) groups. Bars represent the mean, and error bars represent SEM.

5.4.2 40x image analysis

40x Image Analysis	Treated			Control		
	Barrel cortex	Posterior cortex	Barrel cortex minus vessel	Barrel cortex	Posterior cortex	Barrel cortex minus vessel
Plaque Count	97 ± 6.892	39.5 ± 5.362	24 ± 5.447	69.8 ± 6.960	35 ± 0.707	23.8 ± 3.137
Plaque Size	386.293 ± 43.829	307.146 ± 27.862	282.922 ± 36.161	371.705 ± 26.383	314.797 ± 28.440	283.169 ± 11.656
Area of Plaques (%)	6.733 ± 0.587	2.184 ± 0.318	1.443 ± 0.232	4.849 ± 0.789	2.000 ± 0.155	1.457 ± 0.174

Table 5.2 - Results of cortical sections image analysis

Mean results of plaque count, size, and area, averaged within treated (n=4) and control (n=5) groups. Error shown is STD.

5.4.2.1 Posterior cortex

An independent samples t-test was used to assess the plaque count, plaque size, and area of plaques data, with no outliers identified, and all data being normally distributed as assessed by Shapiro-Wilk's test (p>0.05). There was no significant difference in plaque count, plaque size, or area covered by plaques between treated and control groups.

5.4.2.2 Barrel cortex

An independent samples t-test was used to assess the plaque count data, with 1 outlier being identified in the data from the barrel cortex with the vessel removed in the control group, and all data being normally distributed as assessed by Shapiro-Wilk's test (p>0.05). There was a significant increase in the plaque count in the barrel cortex of treated mice

compared to control mice (27.2(95% CI 3.681 to 50.719), p=0.029). However, when the vessel was removed from this image, no significant difference was found between the number of plaques within the cortical tissue of the barrel cortex.

Plaque size data was mostly normally distributed as assessed by Shapiro-Wilk's test (p>0.05), with the only exception being the control group data from the barrel cortex with the vessel removed (p=0.033). No outliers were identified. No significant difference in plaque size was found between the treated and control groups.

Area of plaques data was all normally distributed as assessed by Shapiro-Wilk's test (p>0.05), with only 1 outlier identified in the control group in the data from the barrel cortex with the vessel removed. No significant differences in the area of plaque coverage were identified between the treated and control groups.

A further paired samples t-test was performed to assess the differences seen between the barrel cortex with the vessel removed, and the posterior cortex. No difference was found in the size of the plaques between these two cortical areas, nor in the plaque count. However, when interrogated there was a significantly greater area covered by plaques in the posterior cortex compared to the barrel cortex (0.631(95% CI 0.196 to 1.065), p=0.007).

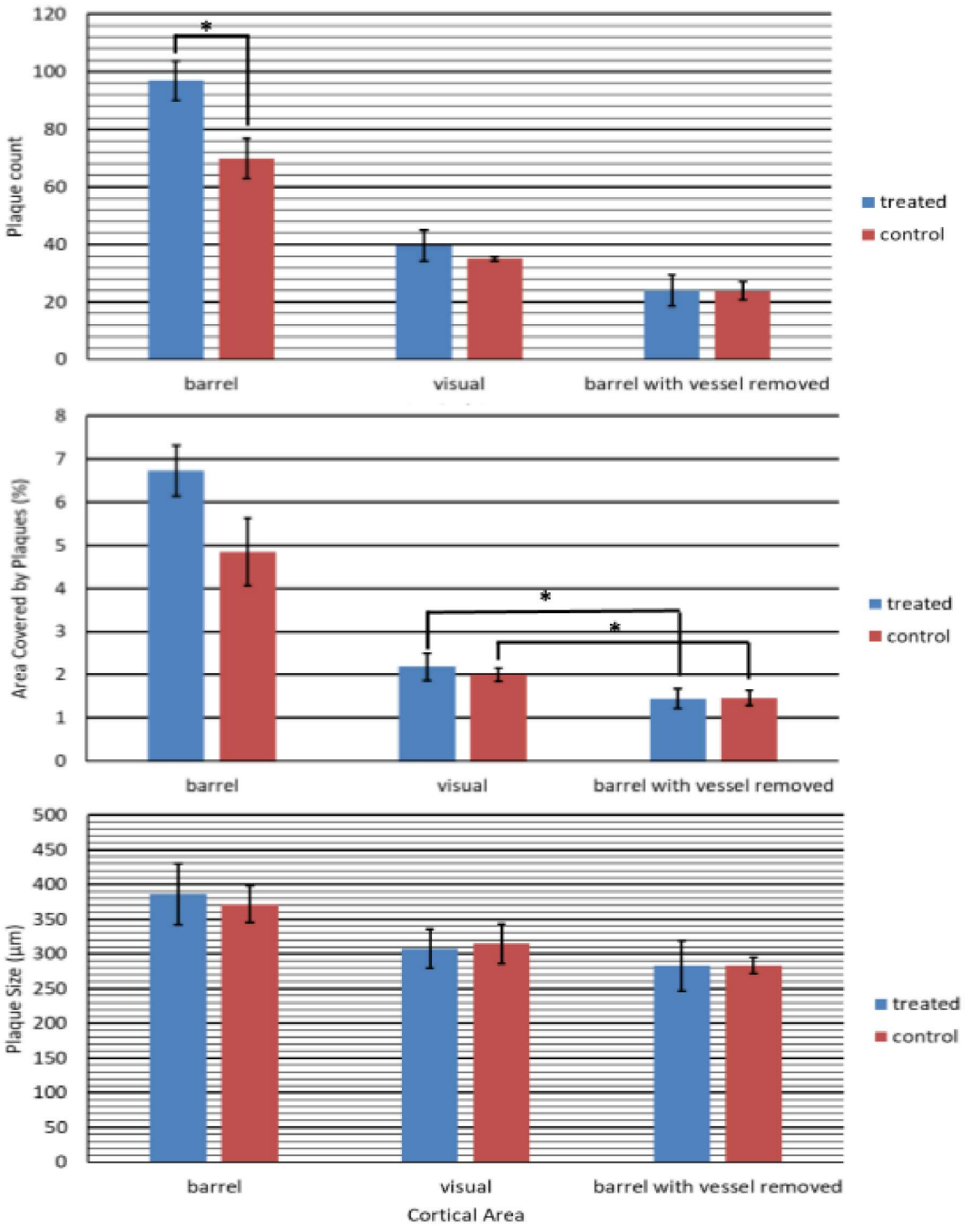

Figure 5.4 – 40x Results

Graphs showing the mean plaque count, area covered by plaques, and plaque size in barrel (with and without vessel) and visual cortex from treated and control groups. Bars represent the mean, and error bars represent SEM.

5.5 Discussion

5.5.1 Results Summary

This pilot study indicates that treatment with carbogen gas is not sufficient to reduce plaque load in the APP/PSEN1 model of Alzheimer's disease. When analysing the entire cortical area, no difference was found in the mice treated with carbogen gas for one hour a day over two months (excluding weekends).

This result is counter to the hypothesis that carbogen treatment may increase clearance of amyloid plaques through increasing cerebral blood flow. Previous research suggests that oxygen treatment in animal models can increase both cerebral blood flow and clearance of amyloid (Shabir et al 2020, Shapira et al 2018). Shapira et al examined the impact of HBOT in a triple-transgenic (3xTg) mouse model of AD, treating aged mice with HBOT for 1 hour a day for 14 consecutive days. They found that this HBOT treatment reduced both amyloid burden and tau phosphorylation in these animals, along with an elevation in cortical pO_2. Carbogen gas treatment has also been used in the treatment of sudden hearing loss (SHL). The pathogenesis of SHL is unclear, but vascular disorders are considered one of the main causes of SHL (Trune and Nguyen-Huynh 2012). A retrospective review study (Lee et al 2012) investigated the circulation-enhancing treatments carbogen gas inhalation and lipo-prostaglandin E1 (LPGE1) alongside standard prednisolone treatment (the usual treatment for SHL). The study found that treatment with carbogen gas raised overall recovery rates to 67.9% compared to 53.8% and 52.3% in the LPGE1 and prednisolone only groups. The researchers concluded that the increased recovery was due to a specific effect of carbogen increasing blood flow within the inner ear.

When analysing the barrel and posterior cortical sections, it was found that treated animals displayed significantly higher levels of amyloid within the barrel cortex (before removal of the vessel). This result has not been interrogated in the current pilot study, but could be investigated further to examine whether carbogen treatment is resulting in greater deposition within the vessel, or whether variations in vessel size between the groups could account for this difference.

One important result from the current pilot study is the finding that plaque load was lower in cortex supplied by large branches of the MCA. The posterior cortex region (lacking major blood vessels) had significantly higher plaque load than the barrel cortex region (supplied by large MCA branches), suggesting a significant role for blood flow in plaque load. The perivascular spaces surrounding blood vessels have been postulated to play a major role in the clearance of Aβ, with a recent review (Bonnar, Eyre, and van Veluw 2025) concluded that impaired perivascular clearance is strongly implicated in the pathophysiology of AD, and that increasing this clearance may improve disease outcomes. A number of studies have been conducted investigating techniques to increase perivascular and glymphatic clearance of proteins, with vasomotion, and gamma stimulation both successfully increasing glymphatic clearance of Aβ (Hauglund et al 2025, Murdock et al 2024). As such, this area should be further investigated, potentially combining carbogen gas treatments with interventions to increase perivascular clearance.

5.5.2 Limitations of the current study and potential future work

The potential impact of carbogen gas treatment on cognitive functioning has not been investigated in this pilot study, and thus it is not possible to conclude that carbogen gas has no potential as a therapeutic. It is possible that the increased oxygenation and blood flow to

cortical tissue would ameliorate cognitive symptoms as shown in previous work (Shapira et al 2018), and this should be assessed through a battery of behavioural tests. Investigation of cognitive abilities using behavioural tests such as Barnes Maze and Novel Object Recognition tests would allow examination of memory function (are animals able to recall a previously seen object, or navigate to a previously identified exit), and could elucidate the impact of carbogen treatment on cognitive abilities (Sharma, Rakoczy, and Brown-Borg 2010, Lang et al 2023).

Future work could also examine levels of amyloid using an enzyme-linked immunosorbent assay (ELISA). The ELISA is one of the most commonly used techniques to assess amyloid pathology, allowing for precise measurement of peptide levels, as well as differentiation between the Aβ40 and Aβ42 peptides (Schmidt et al 2012). This would also allow for analysis of plaque levels in deeper brain structures such as the hippocampus, which are affected earlier in the disease. Treatment may have differing effects across brain regions, which should be examined in both early and late stages of disease.

Further to this, there is a body of evidence suggesting that hypoxic conditions caused by AD pathology can increase levels of inflammation within the brain, leading to further reductions in blood flow, and increases in amyloid burden (Sun et al 2006, Iadecola 2013). Further histological analysis including staining of astrocytes and microglia would enable a visual inspection of the brain's inflammatory state. When stained for glial fibrillary astrocytic protein (GFAP) and ionized calcium-binding adapter molecule 1 (IBA1) respectively, the morphology of astrocytes and microglia can be examined. With inflammation both cell types will demonstrate an activated morphology, and increases in numbers of both astrocytes and microglia can be seen during neuroinflammation. Assessing the number of both activated

and non-activated cells would allow a measurement of inflammation levels within the brain, and this staining may find that while plaque load has not been reduced, there are alterations in the inflammatory response due to increased cerebral oxygenation. Shapira et al (2018) found that HBOT reduced both astrogliosis and microgliosis (abnormal increases in astrocyte and microglia numbers) in the 3xTg model of AD, with studies into other neuroinflammatory conditions finding similar results with HBOT (Lavrnja et al 2015, Xiu et al 2023).

It is possible that analysis of cerebral blood flow during carbogen treatment would reveal alterations that are not visible in this pilot study, with the combination of oxygen and vasodilatory carbon dioxide providing an increase in cerebral blood flow. A thinned cranial window surgery would allow chronic imaging of cerebral blood flow in a longitudinal study, providing the opportunity to compare cerebral perfusion across treated and untreated animals. Shabir et al (2020) used this technique to examine blood flow in the J20-hAPP mouse model, finding that hyperoxic conditions increased baseline blood volume and saturation.

It could also be suggested that the treatment period used in this pilot study is not sufficient to induce increases in clearance, and only treating for 5 days each week may reduce the efficacy of the treatment.

Other gas treatments (such as CO_2 and xenon gas) are gaining interest as potential therapies. A recent study looking at xenon gas in multiple AD mouse models (Brandao et al 2025) found that inhalation of the gas altered the state of microglia. The microglia entered what was described as an intermediate activation state, which enhanced compaction of amyloid plaques, and reduced neuritic dystrophy, as well as reducing brain atrophy and inflammation.

Finally, it is possible that while carbogen gas treatment increases blood flow, the importance of blood vessels indicated by the findings in the posterior and barrel cortices may lie in perivascular or glymphatic clearance. A recent paper (Hauglund et al 2025) found that slow vasomotion during sleep (mediated by norepinephrine) enhanced CSF flow and glymphatic clearance, concluding that vasomotion acts as a 'pump' driving flow of CSF and increasing clearance. This supports a previous paper (Murdock et al 2024) which found that regulation of arterial pulsatility by vasoactive interneurons facilitated glymphatic clearance. They also showed that multisensory gamma stimulations in 5xFAD mice promoted glymphatic clearance of amyloid through influx of CSF and efflux of interstitial fluid. Findings in patients (Manippa et al 2022) suggest that gamma stimulation has potential as a therapeutic approach. Combining techniques such as gamma stimulation with carbogen gas treatment could potentially simultaneously target amyloid clearance and increase blood flow, thereby increasing the impact of both treatments.

While the results of this pilot study suggest no effect of carbogen treatment, it would be prudent to undertake a larger scale study with a longer treatment period, with treatment occurring every day, before reaching a conclusion. With the strong potential of other related gas treatments, future work could also investigate combination gas treatments, or combining gas treatment with glymphatic stimulation, as well as drawing on the treatment and assessment methods employed in these studies.

5.6 Conclusions

Currently carbogen gas treatment cannot be considered as a potential therapeutic strategy, however, further testing of its behavioural effects could elucidate potential benefits. Additionally, this pilot study had a limited scope, with treatment only being applied on

weekdays, for 1 hour periods. Future studies could investigate the impact of more prolonged or consistent carbogen treatment on amyloid plaque load.

The use of gas treatment would allow patients to be treated within their own homes, with fewer side effects than current pharmacological treatment options. As such, despite the negative findings reported in this pilot study, further research is still needed to fully interrogate carbogen gas as a potential therapeutic.

Chapter 6

Discussion and Conclusions

6.1 Overview

The primary focus of this thesis was developing novel cerebrovascular therapeutic approaches for both epilepsy and Alzheimer's disease. I investigated cooling in the rat 4-AP model of epilepsy, its impact on neural activity and haemodynamics, its potential as a therapeutic approach for drug resistant epilepsy, and tested a novel implant that could be translated into a clinically effective treatment. I also studied the impact of treatment with carbogen gas on the mouse APP/PSEN1 model of AD.

This chapter will bring together the major findings of each chapter, discussing their importance for the research field, and their implications for future research.

6.2 Research Aims

The aims of the research outlined in this thesis were:

1. To investigate the impact of cortical cooling on 4-AP induced seizure activity and the subsequent haemodynamic response
2. To examine the utility of a novel cooling implant, investigating its impact on 4-AP induced seizure activity, the capability of onboard electrodes, and its potential therapeutic ability
3. To investigate the effect of carbogen gas treatment on plaque load in the APP/PSEN1 mouse model of AD.

6.3 Cortical cooling alters both synaptic activity and haemodynamics in the 4-AP seizure model

The work detailed in chapter 3 required analysis of a pre-existing dataset collected within the research group. The dataset consisted of neural and 2D-OIS haemodynamic recordings gathered from anaesthetised rats during 4-AP induced seizures. During the experimental time course, cortical cooling to 10°C and 20°C was applied to the animals by use of a skull-attached chamber filled with sterile saline. The aim of this study was to interrogate the impact of this cooling on the 4-AP induced neural activity and subsequent haemodynamic response. The impact of cooling on both neural and haemodynamic activity is an important factor in assessing the potential of cortical cooling as a therapeutic strategy. Both the excessive neural activity and large changes in blood flow that occur during seizures have been identified as potentially contributing to degenerative and damaging processes in epilepsy. In this study I found that cooling to 10°C is sufficient to reduce the magnitude of the LFP response occurring as a result of 4-AP injection. This conforms with the current literature, with multiple studies showing similar results in rat models, primates, and human trials (Ommaya and Baldwin 1963, Niesvizky-Kogan et al 2022). I found that cooling to 20°C did not significantly alter neuronal activity, in contrast with previous studies (Volgushev et al 2004, Yang et al 2005) which found significant alterations in neurotransmitter release and firing patterns when cooling to 20°C. It is possible that the saline temperature recorded within the skull-attached chamber was not accurate to the temperature experienced at the cortical surface, thereby reducing the efficacy of the applied cooling. In addition, previous cooling work (Boorman et al 2023) found that neural response to whisker stimulation was increased at 20°C compared to ambient temperature. The authors suggested that a reduction in feed-forward inhibition may be responsible for this alteration in the neural

response, potentially providing an important research area when examining the potential for cooling as a therapeutic.

I also found interesting haemodynamic responses to cooling, with major differences occurring between data collected from the whisker region as a whole and data collected specifically from the arterial region. It is possible that unique biology of the artery impacts the response to cooling, reducing the expected constriction through the activation of dilatory temperature sensitive ion channels (Sokolov, Mengal, and Berkovich 2023, Thakore, Ali, and Earley 2020). The differences in haemodynamic response in these areas could impact the efficacy of cooling as a therapeutic approach to epilepsy.

Previously the main focus of cooling research has been the impact on neuronal activity, and how reducing the aberrant firing occurring during seizures could decrease symptoms and reduce neuronal damage. With greater understanding of the impact that both hyperoxia and hypoxia may play in continued seizure development and neuronal damage (Masterson et al 2009, Vezzani et al 2011, Seifart et al 2010, Dingledine et al 2014) including the role of oxidative damage in ongoing epileptogenesis (Farrell et al 2017), understanding the impact of cooling on blood flow during seizures could aid in developing more targeted blood flow based treatments.

Prior work has shown that cortical cooling can reduce neural activity (Ommaya and Baldwin 1963, Niesvizky-Kogan et al 2022) but the impact of cortical cooling on haemodynamics has not been previously reported. This study is the first to show the different effects of cooling on haemodynamics within the general seizure region and the middle cerebral artery.

6.3.2 Limitations, and future directions

One of the major limitations of this study lies in the small sample size obtained. Though numerous experiments were conducted, only 7 experiments were successful in collecting both neural data, and haemodynamic data, during stable seizure activity.

The seizure model utilised in this study allowed for examination of cooling's effects on sustained seizure activity. A spontaneous seizure model such as the kainic acid model, fluid percussion model, or genetic epilepsy models (Wang et al 2022) could allow for more in depth analysis of the effects of cooling on neural activity, determining whether it could be sufficient to halt seizure activity entirely. Previous work in the fluid percussion model of epilepsy in rats has found that mild passive cooling (of 0.5-2°C) inhibited the onset of spontaneous seizures (D'Ambrosio et al 2012) introducing the possibility that once spontaneous seizures have started, they could be halted by cooling. This would also allow for investigation of haemodynamics post-seizure, providing insight into the utility of cooling in preventing post-ictal hypoxia.

Previous work examined the impact of temperature alterations on both neural and haemodynamic activity (Boorman et al 2023) and found a non-linear relationship between temperature and neural activity, as well as between temperature and haemodynamics. With the knowledge that seizures increase cortical temperature (Harris et al 2018, Wakuya et al 2022) further research should be conducted into the impact that these temperature increases have on both seizure activity and resulting haemodynamics.

With the rising interest in cooling as a therapeutic tool, further research should be conducted investigating the impact on cortical haemodynamics, and elucidating its effect on neurovascular coupling not only in healthy brains, but also during pathological processes.

Future work should focus on the reactions of major cerebral vessels to cooling, and how this may impact the efficacy of cooling therapy.

6.4 Testing a novel cooling implant

Chapter 4 details the *in vivo* testing of a novel cooling implant developed by collaborators Dr Spencer Moore and Dr Ivan Minev.

A number of studies were conducted, establishing the 4-AP seizure model and experimental protocol, and validating the implant capabilities. The implant's onboard electrodes recorded comparable neural data to that collected by the intracortical neuronexus electrode. Four cooling temperatures were tested (25°C, 20°C, 18°C, and 15°C) and the implant was found to be capable of cooling to 18°C without difficulty at a rate of ~3°C per second.

To investigate the effect of implant delivered cortical cooling on seizure activity, data collected from the intracortical neuronexus electrode was split into trials based on the temperature the implant was programmed to cool to. This data was analysed, comparing the peak of the contour to the baseline activity before the cooling was activated. These results showed significant reductions in seizure activity in response to cortical cooling delivered by the implant's TEC.

No significant differences were found in the neural data when comparing across cooling conditions, in agreement with previous research suggesting cooling to any temperature between 25°C and 15°C (Fujii et al 2010, Nomura et al 2014) was sufficient to reduce seizure activity. The efficacy of cooling to 25°C contrasts with the findings from chapter 3 of this thesis where cooling to 20°C was not sufficient to reduce neural activity. However, the cooling system was greatly improved in this study, directly contacting the cortical surface

ensured that the programmed temperature was the same as that experienced by the cortex, and the rate of cooling was greatly increased, supporting previous work suggesting that cooling rate can have a profound impact on the efficacy of cortical cooling (Motamedi et al 2006).

6.4.2 Limitations, and future directions

The major limitation of this study is the use of an anaesthetised acute seizure model. The 4-AP model of epilepsy produces sustained status epilepticus, and though it has been used to validate a number of AEDs, it is difficult to fully assess the potential of cooling for patients in this model, as the seizure state is not induced by the same physiological processes as occur in patients. One major step in validating this novel cooling implant would be utilising a spontaneous seizure model in order to establish whether the cooling treatment is capable of halting a spontaneous seizure. Utilising a spontaneous model such as the kainic acid model, or genetic epilepsy models (Wang et al 2022) would allow for study of the effect of cooling on more physiological seizures. As such, the efficacy of the implant in halting a physiological seizure could be assessed, determining its suitability as a therapeutic device for patients. This would also allow development and testing of seizure detection algorithms to detect and classify seizure activity in order to create a fully closed-loop system.

A recent study (Khoo et al 2021) found that of 617 patients assessed for epilepsy surgery, 12% had multiple seizure foci and were deemed ineligible, while 5% declined surgery due to risk of significant deficits as seizure foci were located in eloquent cortex. While the current device design would be beneficial for those with seizure foci in eloquent cortex, treating those with multiple foci would require design alterations. Similarly, hippocampal or parahippocampal seizures can be common manifestations of temporal lobe epilepsy

(Chatzikonstantinou 2014), and targeting these structures is not possible with the current device. As such, the current implant design is limited in scope for treating these patients. Developing a heat pipe TEC system to allow cooling of deep brain structures (Tanaka et al 2008) and integrating it into a closed-loop system would increase the number of patients that could benefit from cooling therapy. Further to this, combining multiple electrodes and TECs, or adding optogenetic capabilities (Krook-Magnuson et al 2013) could allow for treatment of multiple seizure foci simultaneously, with optogenetics allowing for inhibition or activation of excitatory or inhibitory neurons, taking advantage of the natural synaptic connections within the brain to target multiple areas simultaneously.

6.5 Carbogen gas as a potential treatment for Alzheimer's Disease

The pilot study detailed in chapter 5 involved treatment of 4 APP/PSEN1 mice with carbogen gas, for 1 hour/day over 2 months (excluding weekends), and the analysis of cortical plaques in comparison to untreated APP/PSEN1 mice. Analysis of methoxy stained amyloid plaques showed no significant effect of treatment on plaque load or plaque size, other than a greater number of plaques being present in the barrel cortex of treated mice (potentially due to differences in vessel size, or amyloid deposition within vessels).

A novel finding was identified when comparing the area surrounding the MCA in the barrel cortex with the visual cortex. The area covered by plaques when the MCA was removed from barrel cortex analysis was significantly lower than the area covered in the visual cortex. It is possible that the presence of a large vessel increases clearance or decreases development of amyloid plaques in its surrounding area. Therefore, although no effect of treatment was found in this study, this finding suggests that other treatments focussed on cortical blood flow may be able to affect plaque load.

6.5.2 Limitations, and future directions

As a pilot study, the sample size for this study is limited, and the number of measures taken was reduced. Previous studies have identified the impact of gas treatments on behavioural measures of cognitive performance, and carbogen treatment should not be ruled out until its impact on cognitive performance has been assessed. A battery of behavioural tests (Barnes maze, Novel object recognition) would allow assessment of memory function in treated vs untreated APP/PSEN1 mice, potentially finding improvements in memory thanks to blood flow alterations in treated mice (Sharma, Rakoczy, and Brown-Borg 2010, Lang et al 2023). Also, previous work has identified alterations in inflammatory processes in response to gas treatments (Lavrnja et al 2015, Shapira et al 2018, Xiu et al 2023). Staining for GFAP and IBA1 would allow visualisation of astrocytes and microglia, analysis of number and activation state of the cells providing a measure of inflammation.

Use of ELISA to assess amyloid pathology would provide measurements of Aβ40 and Aβ42 levels, as well as providing precise measures of peptide levels (Schmidt et al 2012). Altering the staining technique would also allow for assessment of hippocampal amyloid levels, providing insight into how different brain regions may be impacted by carbogen treatment.

Finally, combining carbogen gas treatment with interventions to drive glymphatic clearance would provide the double benefit of increasing tissue oxygenation and increasing amyloid clearance. Gamma stimulation has been shown to promote glymphatic amyloid clearance in the 5xFAD mouse model (Murdock et al 2024), and has been validated as a potential therapeutic approach in patients (Manippa et al 2022), and vasomotion has been shown to increase glymphatic clearance of amyloid (Hauglund et al 2025). It is possible that while carbogen could increase global cerebral blood flow, it is important to instead increase

oscillations in cerebral blood flow (such as vasomotion) that would massage the blood vessels, increasing glymphatic clearance of amyloid. This could be done by combining carbogen treatment with approaches such as gamma stimulation, or providing carbogen in an oscillating manner in order to induce blood flow oscillations without further interventions.

Though this pilot study suggests no impact of carbogen treatment, this methodology should not be ruled out without further investigation into its impact on inflammation, cognitive function, and deep brain structures. Future work should also focus on combining treatments to drive both cerebral blood flow and glymphatic clearance simultaneously.

6.6 Conclusions

In summary, the work completed over the course of this PhD has produced a number of original contributions and steps forward in the field of neurovascular therapies. Chapter 3 details a novel finding, with cooling having differing effects on haemodynamics in the artery compared to the overall seizure region. The extension of this cooling work (chapter 4) has validated a novel implant capable of recording neural activity and producing cooling that is sufficient to reduce seizure activity. This implant can now be taken forward and developed into a fully translatable therapeutic device. Finally, chapter 5 details a pilot study investigating carbogen as an Alzheimer's Disease therapy for the first time, with a novel finding of reduced plaque burden in cortex surrounding major branches of the MCA. The findings of this pilot study can help us move the field of Alzheimer's research forward, allowing further development of therapies targeting cerebral blood flow.

Bibliography

1. AHMAD, A., DEMPSEY, S. K., DANEVA, Z., AZAM, M., LI, N., LI, P. L. & RITTER, J. K. 2018. Role of Nitric Oxide in the Cardiovascular and Renal Systems. *Int J Mol Sci,* 19.

2. AHMAD, S., KHANNA, R. & SANI, S. 2020. Surgical Treatments of Epilepsy. *Semin Neurol,* 40**,** 696-707.

3. ALOMAR, S. A., MOSHREF, R. H., MOSHREF, L. H. & SABBAGH, A. J. 2023. Outcomes after laser interstitial thermal ablation for temporal lobe epilepsy: a systematic review and meta-analysis. *Neurosurgical Review,* 46**,** 261.

4. ANAND, P. & SINGH, B. 2013. A review on cholinesterase inhibitors for Alzheimer's disease. *Archives of Pharmacal Research,* 36**,** 375-399.

5. ANDRESEN, J., SHAFI, N. I. & BRYAN, R. M., JR. 2006. Endothelial influences on cerebrovascular tone. *J Appl Physiol (1985),* 100**,** 318-27.

6. ANDREWS, S. J., FULTON-HOWARD, B. & GOATE, A. 2019. Protective Variants in Alzheimer's Disease. *Curr Genet Med Rep,* 7**,** 1-12.

7. ANNEGERS, J. F., HAUSER, W. A. & ELVEBACK, L. R. 1979. Remission of seizures and relapse in patients with epilepsy. *Epilepsia,* 20**,** 729-37.

8. ARMSTRONG, R. A. 2009. The molecular biology of senile plaques and neurofibrillary tangles in Alzheimer's disease. *Folia Neuropathol,* 47**,** 289-99.

9. ASIRI, S., AL-OTAIBI, A., AL HAMEED, M., HAMHOM, A., ALENIZI, A., ESKANDRANI, A., ALKHRISI, M. & ALDOSARI, M. M. 2022. Seizure-related injuries in people with epilepsy: A cohort study from Saudi Arabia. *Epilepsia Open,* 7**,** 422-430.

10. ATTWELL, D., BUCHAN, A. M., CHARPAK, S., LAURITZEN, M., MACVICAR, B. A. & NEWMAN, E. A. 2010. Glial and neuronal control of brain blood flow. *Nature,* 468**,** 232-43.

11. BAKKEN, H. E., KAWASAKI, H., OYA, H., GREENLEE, J. D. & HOWARD, M. A., 3RD 2003. A device for cooling localized regions of human cerebral cortex. Technical note. *J Neurosurg,* 99**,** 604-8.

12. BALBI, M., XIAO, D., JATIVA VEGA, M., HU, H., VANNI, M. P., BERNIER, L.-P., LEDUE, J., MACVICAR, B. & MURPHY, T. H. 2021. Gamma frequency activation of inhibitory neurons in the acute phase after stroke attenuates vascular and behavioral dysfunction. *Cell Reports,* 34**,** 108696.

13. BALDWIN, M., FROST, L. L., WOOD, C. D. & LEWIS, S. A. 1956. Effect of Hypothermia on Epileptiform Activity in the Primate Temporal Lobe. *Science,* 124**,** 931-932.

14. BARTUS, R. T., DEAN, R. L., 3RD, BEER, B. & LIPPA, A. S. 1982. The cholinergic hypothesis of geriatric memory dysfunction. *Science,* 217**,** 408-14.

15. BARZEGAR, M., AFGHAN, M., TARMAHI, V., BEHTARI, M., RAHIMI KHAMANEH, S. & RAEISI, S. 2021. Ketogenic diet: overview, types, and possible anti-seizure mechanisms. *Nutritional Neuroscience,* 24**,** 307-316.

16. BEGHI, E. 2020. The Epidemiology of Epilepsy. *Neuroepidemiology,* 54**,** 185-191.

17. BEGHI, E., GIUSSANI, G., NICHOLS, E., ABD-ALLAH, F., ABDELA, J., ABDELALIM, A., ABRAHA, H. N., ADIB, M. G., AGRAWAL, S., ALAHDAB, F., AWASTHI, A., AYELE, Y., BARBOZA, M. A., BELACHEW, A. B., BIADGO, B., BIJANI, A., BITEW, H., CARVALHO, F., CHAIAH, Y., DARYANI, A., DO, H. P., DUBEY, M., ENDRIES, A. Y. Y., ESKANDARIEH, S.,

FARO, A., FARZADFAR, F., FERESHTEHNEJAD, S.-M., FERNANDES, E., FIJABI, D. O., FILIP, I., FISCHER, F., GEBRE, A. K., TSADIK, A. G., GEBREMICHAEL, T. G., GEZAE, K. E., GHASEMI-KASMAN, M., WELDEGWERGS, K. G., DEGEFA, M. G., GNEDOVSKAYA, E. V., HAGOS, T. B., HAJ-MIRZAIAN, A., HAJ-MIRZAIAN, A., HASSEN, H. Y., HAY, S. I., JAKOVLJEVIC, M., KASAEIAN, A., KASSA, T. D., KHADER, Y. S., KHALIL, I., KHAN, E. A., KHUBCHANDANI, J., KISA, A., KROHN, K. J., KULKARNI, C., NIRAYO, Y. L., MACKAY, M. T., MAJDAN, M., MAJEED, A., MANHERTZ, T., MEHNDIRATTA, M. M., MEKONEN, T., MELES, H. G., MENGISTU, G., MOHAMMED, S., NAGHAVI, M., MOKDAD, A. H., MUSTAFA, G., IRVANI, S. S. N., NGUYEN, L. H., NIXON, M. R., OGBO, F. A., OLAGUNJU, A. T., OLAGUNJU, T. O., OWOLABI, M. O., PHILLIPS, M. R., PINILLA-MONSALVE, G. D., QORBANI, M., RADFAR, A., RAFAY, A., RAHIMI-MOVAGHAR, V., REINIG, N., SACHDEV, P. S., SAFARI, H., SAFARI, S., SAFIRI, S., SAHRAIAN, M. A., SAMY, A. M., SARVI, S., SAWHNEY, M., SHAIKH, M. A., SHARIF, M., SINGH, G., SMITH, M., SZOEKE, C. E. I., TABARÉS-SEISDEDOS, R., TEMSAH, M.-H., TEMSAH, O., TORTAJADA-GIRBÉS, M., TRAN, B. X., TSEGAY, A. A. T., et al. 2019. Global, regional, and national burden of epilepsy, 1990–2016: a systematic analysis for the Global Burden of Disease Study 2016. *The Lancet Neurology,* 18**,** 357-375.

18. BEGHI, E., GIUSSANI, G. & SANDER, J. W. 2015. The natural history and prognosis of epilepsy. *Epileptic Disorders,* 17**,** 243-253.

19. BEN-MENACHEM, E. 2012. Neurostimulation-past, present, and beyond. *Epilepsy Curr,* 12**,** 188-91.

20. BERGQVIST, A. G. C., SCHALL, J. I., GALLAGHER, P. R., CNAAN, A. & STALLINGS, V. A. 2005. Fasting versus Gradual Initiation of the Ketogenic Diet: A Prospective, Randomized Clinical Trial of Efficacy. *Epilepsia,* 46**,** 1810-1819.

21. BERWICK, J., JOHNSTON, D., JONES, M., MARTINDALE, J., MARTIN, C., KENNERLEY, A. J., REDGRAVE, P. & MAYHEW, J. E. W. 2008. Fine Detail of Neurovascular Coupling Revealed by Spatiotemporal Analysis of the Hemodynamic Response to Single Whisker Stimulation in Rat Barrel Cortex. *Journal of Neurophysiology,* 99**,** 787-798.

22. BERWICK, J., JOHNSTON, D., JONES, M., MARTINDALE, J., REDGRAVE, P., MCLOUGHLIN, N., SCHIESSL, I. & MAYHEW, J. E. 2005. Neurovascular coupling investigated with two-dimensional optical imaging spectroscopy in rat whisker barrel cortex. *Eur J Neurosci,* 22**,** 1655-66.

23. BONNAR, O., EYRE, B. & VAN VELUW, S. J. Perivascular brain clearance as a therapeutic target in cerebral amyloid angiopathy and Alzheimer's disease. *Neurotherapeutics*.

24. BOORMAN, L. W., HARRIS, S. S., SHABIR, O., LEE, L., EYRE, B., HOWARTH, C. & BERWICK, J. 2023. Bidirectional alterations in brain temperature profoundly modulate spatiotemporal neurovascular responses in-vivo. *Communications Biology,* 6**,** 185.

25. BRANDAO, W., JAIN, N., YIN, Z., KLEEMANN, K. L., CARPENTER, M., BAO, X., SERRANO, J. R., TYCKSEN, E., DURAO, A., BARRY, J.-L., BAUFELD, C., GUNEYKAYA, D., ZHANG, X., LITVINCHUK, A., JIANG, H., ROSENZWEIG, N., PITTS, K. M., ARONCHIK, M., YAHYA, T., CAO, T., TAKAHASHI, M. K., KRISHNAN, R., DAVTYAN, H., ULRICH, J. D., BLURTON-

JONES, M., ILIN, I., WEINER, H. L., HOLTZMAN, D. M. & BUTOVSKY, O. 2025. Inhaled xenon modulates microglia and ameliorates disease in mouse models of amyloidosis and tauopathy. *Science Translational Medicine,* 17**,** eadk3690.

26. BREIJYEH, Z. & KARAMAN, R. 2020. Comprehensive Review on Alzheimer's Disease: Causes and Treatment. *Molecules,* 25.

27. CHAN, A. Y., ROLSTON, J. D., LEE, B., VADERA, S. & ENGLOT, D. J. 2018. Rates and predictors of seizure outcome after corpus callosotomy for drug-resistant epilepsy: a meta-analysis. *J Neurosurg,* 130**,** 1193-1202.

28. CHEN, B. R., KOZBERG, M. G., BOUCHARD, M. B., SHAIK, M. A. & HILLMAN, E. M. 2014. A critical role for the vascular endothelium in functional neurovascular coupling in the brain. *J Am Heart Assoc,* 3**,** e000787.

29. CHEN, G.-F., XU, T.-H., YAN, Y., ZHOU, Y.-R., JIANG, Y., MELCHER, K. & XU, H. E. 2017. Amyloid beta: structure, biology and structure-based therapeutic development. *Acta Pharmacologica Sinica,* 38**,** 1205-1235.

30. CHEN, J., ZHANG, F., ZHAO, L., CHENG, C., ZHONG, R., DONG, C. & LE, W. 2020. Hyperbaric oxygen ameliorates cognitive impairment in patients with Alzheimer's disease and amnestic mild cognitive impairment. *Alzheimers Dement (N Y),* 6**,** e12030.

31. COOKE, D. F., GOLDRING, A. B., YAMAYOSHI, I., TSOURKAS, P., RECANZONE, G. H., TIRIAC, A., PAN, T., SIMON, S. I. & KRUBITZER, L. 2012. Fabrication of an inexpensive, implantable cooling device for reversible brain deactivation in animals ranging from rodents to primates. *J Neurophysiol,* 107**,** 3543-58.

32. CORTES-CANTELI, M. & IADECOLA, C. 2020. Alzheimer's Disease and Vascular Aging: JACC Focus Seminar. *J Am Coll Cardiol,* 75**,** 942-951.

33. CSERNYUS, B., SZABÓ, Á., FIÁTH, R., ZÁTONYI, A., LÁZÁR, C., PONGRÁCZ, A. & FEKETE, Z. 2021. A multimodal, implantable sensor array and measurement system to investigate the suppression of focal epileptic seizure using hypothermia. *Journal of Neural Engineering,* 18**,** 0460c3.

34. D'AMBROSIO, R., EASTMAN, C. L., DARVAS, F., FENDER, J. S., VERLEY, D. R., FARIN, F. M., WILKERSON, H. W., TEMKIN, N. R., MILLER, J. W., OJEMANN, J., ROTHMAN, S. M. & SMYTH, M. D. 2013a. Mild passive focal cooling prevents epileptic seizures after head injury in rats. *Ann Neurol,* 73**,** 199-209.

35. D'AMBROSIO, R., EASTMAN, C. L., DARVAS, F., FENDER, J. S., VERLEY, D. R., FARIN, F. M., WILKERSON, H. W., TEMKIN, N. R., MILLER, J. W., OJEMANN, J., ROTHMAN, S. M. & SMYTH, M. D. 2013b. Mild passive focal cooling prevents epileptic seizures after head injury in rats. *Annals of Neurology,* 73**,** 199-209.

36. DE ROJAS, I., MORENO-GRAU, S., TESI, N., GRENIER-BOLEY, B., ANDRADE, V., JANSEN, I. E., PEDERSEN, N. L., STRINGA, N., ZETTERGREN, A., HERNÁNDEZ, I., MONTRREAL, L., ANTÚNEZ, C., ANTONELL, A., TANKARD, R. M., BIS, J. C., SIMS, R., BELLENGUEZ, C., QUINTELA, I., GONZÁLEZ-PEREZ, A., CALERO, M., FRANCO-MACÍAS, E., MACÍAS, J., BLESA, R., CERVERA-CARLES, L., MENÉNDEZ-GONZÁLEZ, M., FRANK-GARCÍA, A., ROYO, J. L., MORENO, F., HUERTO VILAS, R., BAQUERO, M., DIEZ-FAIREN, M., LAGE, C., GARCÍA-MADRONA, S., GARCÍA-GONZÁLEZ, P., ALARCÓN-MARTÍN, E., VALERO, S., SOTOLONGO-GRAU, O., ULLGREN, A., NAJ, A. C., LEMSTRA, A. W., BENAQUE, A., PÉREZ-CORDÓN, A., BENUSSI, A., RÁBANO, A., PADOVANI, A., SQUASSINA, A., DE

MENDONÇA, A., ARIAS PASTOR, A., KOK, A. A. L., MEGGY, A., PASTOR, A. B., ESPINOSA, A., CORMA-GÓMEZ, A., MARTÍN MONTES, A., SANABRIA, Á., DESTEFANO, A. L., SCHNEIDER, A., HAAPASALO, A., KINHULT STÅHLBOM, A., TYBJÆRG-HANSEN, A., HARTMANN, A. M., SPOTTKE, A., CORBATÓN-ANCHUELO, A., RONGVE, A., BORRONI, B., AROSIO, B., NACMIAS, B., NORDESTGAARD, B. G., KUNKLE, B. W., CHARBONNIER, C., ABDELNOUR, C., MASULLO, C., MARTÍNEZ RODRÍGUEZ, C., MUÑOZ-FERNANDEZ, C., DUFOUIL, C., GRAFF, C., FERREIRA, C. B., CHILLOTTI, C., REYNOLDS, C. A., FENOGLIO, C., VAN BROECKHOVEN, C., CLARK, C., PISANU, C., SATIZABAL, C. L., HOLMES, C., BUIZA-RUEDA, D., AARSLAND, D., RUJESCU, D., ALCOLEA, D., GALIMBERTI, D., WALLON, D., SERIPA, D., GRÜNBLATT, E., DARDIOTIS, E., DÜZEL, E., SCARPINI, E., CONTI, E., RUBINO, E., GELPI, E., RODRIGUEZ-RODRIGUEZ, E., et al. 2021. Common variants in Alzheimer's disease and risk stratification by polygenic risk scores. *Nature Communications,* 12**,** 3417.

37. DEANE, R., DU YAN, S., SUBMAMARYAN, R. K., LARUE, B., JOVANOVIC, S., HOGG, E., WELCH, D., MANNESS, L., LIN, C., YU, J., ZHU, H., GHISO, J., FRANGIONE, B., STERN, A., SCHMIDT, A. M., ARMSTRONG, D. L., ARNOLD, B., LILIENSIEK, B., NAWROTH, P., HOFMAN, F., KINDY, M., STERN, D. & ZLOKOVIC, B. 2003. RAGE mediates amyloid-β peptide transport across the blood-brain barrier and accumulation in brain. *Nature Medicine,* 9**,** 907-913.

38. DINGLEDINE, R., VARVEL, N. H. & DUDEK, F. E. 2014. When and how do seizures kill neurons, and is cell death relevant to epileptogenesis? *Adv Exp Med Biol,* 813**,** 109-22.

39. DYCK, C. H. V., SWANSON, C. J., AISEN, P., BATEMAN, R. J., CHEN, C., GEE, M., KANEKIYO, M., LI, D., REYDERMAN, L., COHEN, S., FROELICH, L., KATAYAMA, S., SABBAGH, M., VELLAS, B., WATSON, D., DHADDA, S., IRIZARRY, M., KRAMER, L. D. & IWATSUBO, T. 2023. Lecanemab in Early Alzheimer's Disease. *New England Journal of Medicine,* 388**,** 9-21.

40. ENGEL, J., JR., MCDERMOTT, M. P., WIEBE, S., LANGFITT, J. T., STERN, J. M., DEWAR, S., SPERLING, M. R., GARDINER, I., ERBA, G., FRIED, I., JACOBS, M., VINTERS, H. V., MINTZER, S. & KIEBURTZ, K. 2012. Early surgical therapy for drug-resistant temporal lobe epilepsy: a randomized trial. *Jama,* 307**,** 922-30.

41. ENGEL JR, J., VAN NESS, P., RASMUSSEN, T. & OJEMANN, L. 1993. Outcome with respect to epileptic seizures. Engel J Jr: Surgical Treatment of the Epilepsies ed 2 New York. Raven Press.

42. ENGLOT, D. J., ROLSTON, J. D., WRIGHT, C. W., HASSNAIN, K. H. & CHANG, E. F. 2016. Rates and Predictors of Seizure Freedom With Vagus Nerve Stimulation for Intractable Epilepsy. *Neurosurgery,* 79**,** 345-353.

43. ENGLOT, D. J., WANG, D. D., ROLSTON, J. D., SHIH, T. T. & CHANG, E. F. 2012. Rates and predictors of long-term seizure freedom after frontal lobe epilepsy surgery: a systematic review and meta-analysis. *J Neurosurg,* 116**,** 1042-8.

44. FALCO-WALTER, J. 2020. Epilepsy-Definition, Classification, Pathophysiology, and Epidemiology. *Semin Neurol,* 40**,** 617-623.

45. FARRELL, J. S., COLANGELI, R., WOLFF, M. D., WALL, A. K., PHILLIPS, T. J., GEORGE, A., FEDERICO, P. & TESKEY, G. C. 2017. Postictal hypoperfusion/hypoxia provides the

foundation for a unified theory of seizure-induced brain abnormalities and behavioral dysfunction. *Epilepsia,* 58**,** 1493-1501.

46. FARRELL, J. S., GAXIOLA-VALDEZ, I., WOLFF, M. D., DAVID, L. S., DIKA, H. I., GEERAERT, B. L., RACHEL WANG, X., SINGH, S., SPANSWICK, S. C., DUNN, J. F., ANTLE, M. C., FEDERICO, P. & TESKEY, G. C. 2016. Postictal behavioural impairments are due to a severe prolonged hypoperfusion/hypoxia event that is COX-2 dependent. *Elife,* 5.

47. FARRER, L. A., CUPPLES, L. A., HAINES, J. L., HYMAN, B., KUKULL, W. A., MAYEUX, R., MYERS, R. H., PERICAK-VANCE, M. A., RISCH, N. & VAN DUIJN, C. M. 1997. Effects of age, sex, and ethnicity on the association between apolipoprotein E genotype and Alzheimer disease. A meta-analysis. APOE and Alzheimer Disease Meta Analysis Consortium. *Jama,* 278**,** 1349-56.

48. FEDINEC, A. L., LIU, J., ZHANG, R., HARSONO, M., POURCYROUS, M. & PARFENOVA, H. 2021. The cold receptor TRPM8 activation leads to attenuation of endothelium-dependent cerebral vascular functions during head cooling. *J Cereb Blood Flow Metab,* 41**,** 2897-2906.

49. FERNÁNDEZ-KLETT, F., OFFENHAUSER, N., DIRNAGL, U., PRILLER, J. & LINDAUER, U. 2010. Pericytes in capillaries are contractile in vivo, but arterioles mediate functional hyperemia in the mouse brain. *Proc Natl Acad Sci U S A,* 107**,** 22290-5.

50. FINET, P., SANTOS, L. P., EL TAHRY, R., SANTOS, S. F., VAZ, G. R. & RAFTOPOULOS, C. 2019. Clinical Outcome of Radiating Multiple Subpial Transections Alone for Drug Resistant Epilepsy After More Than 5 Years Follow-Up. *World Neurosurg,* 126**,** e1155-e1159.

51. FISHER, R., SALANOVA, V., WITT, T., WORTH, R., HENRY, T., GROSS, R., OOMMEN, K., OSORIO, I., NAZZARO, J., LABAR, D., KAPLITT, M., SPERLING, M., SANDOK, E., NEAL, J., HANDFORTH, A., STERN, J., DESALLES, A., CHUNG, S., SHETTER, A., BERGEN, D., BAKAY, R., HENDERSON, J., FRENCH, J., BALTUCH, G., ROSENFELD, W., YOUKILIS, A., MARKS, W., GARCIA, P., BARBARO, N., FOUNTAIN, N., BAZIL, C., GOODMAN, R., MCKHANN, G., BABU KRISHNAMURTHY, K., PAPAVASSILIOU, S., EPSTEIN, C., POLLARD, J., TONDER, L., GREBIN, J., COFFEY, R. & GRAVES, N. 2010. Electrical stimulation of the anterior nucleus of thalamus for treatment of refractory epilepsy. *Epilepsia,* 51**,** 899-908.

52. FISHER, R. S., ACEVEDO, C., ARZIMANOGLOU, A., BOGACZ, A., CROSS, J. H., ELGER, C. E., ENGEL, J., JR., FORSGREN, L., FRENCH, J. A., GLYNN, M., HESDORFFER, D. C., LEE, B. I., MATHERN, G. W., MOSHÉ, S. L., PERUCCA, E., SCHEFFER, I. E., TOMSON, T., WATANABE, M. & WIEBE, S. 2014. ILAE official report: a practical clinical definition of epilepsy. *Epilepsia,* 55**,** 475-82.

53. FISHER, R. S., BOAS, W. V. E., BLUME, W., ELGER, C., GENTON, P., LEE, P. & ENGEL JR., J. 2005. Epileptic Seizures and Epilepsy: Definitions Proposed by the International League Against Epilepsy (ILAE) and the International Bureau for Epilepsy (IBE). *Epilepsia,* 46**,** 470-472.

54. FISHER, R. S., CROSS, J. H., D'SOUZA, C., FRENCH, J. A., HAUT, S. R., HIGURASHI, N., HIRSCH, E., JANSEN, F. E., LAGAE, L., MOSHÉ, S. L., PELTOLA, J., ROULET PEREZ, E., SCHEFFER, I. E., SCHULZE-BONHAGE, A., SOMERVILLE, E., SPERLING, M., YACUBIAN, E. M. & ZUBERI, S. M. 2017. Instruction manual for the ILAE 2017 operational classification of seizure types. *Epilepsia,* 58**,** 531-542.

55. FONG, G. C. Y., FONG, K. Y., MAK, W., TSANG, K. L., CHAN, K. H., CHEUNG, R. T. F., HO, S. L. & HO, W. Y. 2000. Postictal psychosis related regional cerebral hyperperfusion. *Journal of Neurology, Neurosurgery & Psychiatry,* 68**,** 100-101.

56. FORSYTH, R., ALLEN, M., BEDSON, E., DOWNES, A., GOUGH, C., HARTSHORN, S., LAWTON, K., LYTTLE, M. D., MESSAHEL, S., MULLEN, N., RAPER, J., ROSALA-HARRIS, A., TAGGART, L., URRON, J., WALTON, E. & GAMBLE, C. 2024. Seizure control via pH manipulation: a phase II double-blind randomised controlled trial of inhaled carbogen as adjunctive treatment of paediatric convulsive status epilepticus (Carbogen for Status Epilepticus in Children Trial (CRESCENT)). *Trials,* 25**,** 349.

57. FOWLER, S. B. 2012. Carbogen in the management of a central retinal artery occlusion. *Insight,* 37**,** 10-1.

58. FRIEDLAND, R. P. & IADECOLA, C. 1991. Roy and Sherrington (1890). *Neurology,* 41**,** 10-10.

59. FUJII, M., FUJIOKA, H., OKU, T., TANAKA, N., IMOTO, H., MARUTA, Y., NOMURA, S., KAJIWARA, K., SAITO, T., YAMAKAWA, T., YAMAKAWA, T. & SUZUKI, M. 2010. Application of focal cerebral cooling for the treatment of intractable epilepsy. *Neurol Med Chir (Tokyo),* 50**,** 839-44.

60. GARLICK, R. E. 1992. Cerebral Blood Flow and Metabolism. *In:* TINKER, J. & ZAPOL, W. M. (eds.) *Care of the Critically Ill Patient.* London: Springer London.

61. GENIN, E., HANNEQUIN, D., WALLON, D., SLEEGERS, K., HILTUNEN, M., COMBARROS, O., BULLIDO, M. J., ENGELBORGHS, S., DE DEYN, P., BERR, C., PASQUIER, F., DUBOIS, B., TOGNONI, G., FIÉVET, N., BROUWERS, N., BETTENS, K., AROSIO, B., COTO, E., DEL

ZOMPO, M., MATEO, I., EPELBAUM, J., FRANK-GARCIA, A., HELISALMI, S., PORCELLINI, E., PILOTTO, A., FORTI, P., FERRI, R., SCARPINI, E., SICILIANO, G., SOLFRIZZI, V., SORBI, S., SPALLETTA, G., VALDIVIESO, F., VEPSÄLÄINEN, S., ALVAREZ, V., BOSCO, P., MANCUSO, M., PANZA, F., NACMIAS, B., BOSSÙ, P., HANON, O., PICCARDI, P., ANNONI, G., SERIPA, D., GALIMBERTI, D., LICASTRO, F., SOININEN, H., DARTIGUES, J. F., KAMBOH, M. I., VAN BROECKHOVEN, C., LAMBERT, J. C., AMOUYEL, P. & CAMPION, D. 2011. APOE and Alzheimer disease: a major gene with semi-dominant inheritance. *Mol Psychiatry,* 16**,** 903-7.

62. GEORGE, A. G., FARRELL, J. S., COLANGELI, R., WALL, A. K., GOM, R. C., KESLER, M. T., RODRIGUEZ DE LA HOZ, C., VILLA, B. R., PERERA, T., RHO, J. M., KURRASCH, D. & TESKEY, G. C. 2023. Sudden unexpected death in epilepsy is prevented by blocking postictal hypoxia. *Neuropharmacology,* 231**,** 109513.

63. GODDARD, G. V., MCINTYRE, D. C. & LEECH, C. K. 1969. A permanent change in brain function resulting from daily electrical stimulation. *Exp Neurol,* 25**,** 295-330.

64. GOEDERT, M. & SPILLANTINI, M. G. 2000. Tau mutations in frontotemporal dementia FTDP-17 and their relevance for Alzheimer's disease. *Biochimica et Biophysica Acta (BBA) - Molecular Basis of Disease,* 1502**,** 110-121.

65. GOHEL, D., ZHANG, P., GUPTA, A. K., LI, Y., CHIANG, C. W., LI, L., HOU, Y., PIEPER, A. A., CUMMINGS, J. & CHENG, F. 2024. Sildenafil as a Candidate Drug for Alzheimer's Disease: Real-World Patient Data Observation and Mechanistic Observations from Patient-Induced Pluripotent Stem Cell-Derived Neurons. *J Alzheimers Dis,* 98**,** 643-657.

66. GONZÁLEZ, H. F. J., YENGO-KAHN, A. & ENGLOT, D. J. 2019. Vagus Nerve Stimulation for the Treatment of Epilepsy. *Neurosurg Clin N Am,* 30**,** 219-230.

67. GRAHAM, D., TISDALL, M. M. & GILL, D. 2016. Corpus callosotomy outcomes in pediatric patients: A systematic review. *Epilepsia,* 57**,** 1053-1068.

68. GRIESSENAUER, C. J., SALAM, S., HENDRIX, P., PATEL, D. M., TUBBS, R. S., BLOUNT, J. P. & WINKLER, P. A. 2015. Hemispherectomy for treatment of refractory epilepsy in the pediatric age group: a systematic review. *J Neurosurg Pediatr,* 15**,** 34-44.

69. GUBERMAN, A. 1998. Monotherapy or polytherapy for epilepsy? *Can J Neurol Sci,* 25**,** S3-8.

70. GUILLIAMS, K., ROSEN, M., BUTTRAM, S., ZEMPEL, J., PINEDA, J., MILLER, B. & SHOYKHET, M. 2013. Hypothermia for pediatric refractory status epilepticus. *Epilepsia,* 54**,** 1586-94.

71. GUTTMAN, R. 1962. Effect of temperature on the potential and current thresholds of axon membrane. *J Gen Physiol,* 46**,** 257-66.

72. HALL, C. N., REYNELL, C., GESSLEIN, B., HAMILTON, N. B., MISHRA, A., SUTHERLAND, B. A., O'FARRELL, F. M., BUCHAN, A. M., LAURITZEN, M. & ATTWELL, D. 2014. Capillary pericytes regulate cerebral blood flow in health and disease. *Nature,* 508**,** 55-60.

73. HAMER, M. & CHIDA, Y. 2009. Physical activity and risk of neurodegenerative disease: a systematic review of prospective evidence. *Psychol Med,* 39**,** 3-11.

74. HARCH, P. G. & FOGARTY, E. F. 2018. Hyperbaric oxygen therapy for Alzheimer's dementia with positron emission tomography imaging: a case report. *Med Gas Res,* 8**,** 181-184.

75. HARDER, D. R., ZHANG, C. & GEBREMEDHIN, D. 2002. Astrocytes function in matching blood flow to metabolic activity. *News Physiol Sci,* 17**,** 27-31.

76. HARDY, J. & SELKOE, D. J. 2002. The Amyloid Hypothesis of Alzheimer's Disease: Progress and Problems on the Road to Therapeutics. *Science,* 297**,** 353-356.

77. HARRIS, S., BRUYNS-HAYLETT, M., KENNERLEY, A., BOORMAN, L., OVERTON, P. G., MA, H., ZHAO, M., SCHWARTZ, T. H. & BERWICK, J. 2013. The effects of focal epileptic activity on regional sensory-evoked neurovascular coupling and postictal modulation of bilateral sensory processing. *J Cereb Blood Flow Metab,* 33**,** 1595-604.

78. HARRIS, S. S., BOORMAN, L. W., DAS, D., KENNERLEY, A. J., SHARP, P. S., MARTIN, C., REDGRAVE, P., SCHWARTZ, T. H. & BERWICK, J. 2018. Physiological and Pathological Brain Activation in the Anesthetized Rat Produces Hemodynamic-Dependent Cortical Temperature Increases That Can Confound the BOLD fMRI Signal. *Frontiers in Neuroscience,* Volume 12 - 2018.

79. HARSONO, M., POURCYROUS, M., JOLLY, E. J., DE JONGH CURRY, A., FEDINEC, A. L., LIU, J., BASUROY, S., ZHUANG, D., LEFFLER, C. W. & PARFENOVA, H. 2016. Selective head cooling during neonatal seizures prevents postictal cerebral vascular dysfunction without reducing epileptiform activity. *Am J Physiol Heart Circ Physiol,* 311**,** H1202-h1213.

80. HAUGLUND, N. L., ANDERSEN, M., TOKARSKA, K., RADOVANOVIC, T., KJAERBY, C., SØRENSEN, F. L., BOJAROWSKA, Z., UNTIET, V., BALLESTERO, S. B., KOLMOS, M. G., WEIKOP, P., HIRASE, H. & NEDERGAARD, M. 2025. Norepinephrine-mediated slow vasomotion drives glymphatic clearance during sleep. *Cell,* 188**,** 606-622.e17.

81. HAYS, C. C., ZLATAR, Z. Z. & WIERENGA, C. E. 2016. The Utility of Cerebral Blood Flow as a Biomarker of Preclinical Alzheimer's Disease. *Cell Mol Neurobiol,* 36**,** 167-79.

82. HECK, C. N., KING-STEPHENS, D., MASSEY, A. D., NAIR, D. R., JOBST, B. C., BARKLEY, G. L., SALANOVA, V., COLE, A. J., SMITH, M. C., GWINN, R. P., SKIDMORE, C., VAN NESS, P. C., BERGEY, G. K., PARK, Y. D., MILLER, I., GELLER, E., RUTECKI, P. A., ZIMMERMAN, R., SPENCER, D. C., GOLDMAN, A., EDWARDS, J. C., LEIPHART, J. W., WHAREN, R. E., FESSLER, J., FOUNTAIN, N. B., WORRELL, G. A., GROSS, R. E., EISENSCHENK, S., DUCKROW, R. B., HIRSCH, L. J., BAZIL, C., O'DONOVAN, C. A., SUN, F. T., COURTNEY, T. A., SEALE, C. G. & MORRELL, M. J. 2014. Two-year seizure reduction in adults with medically intractable partial onset epilepsy treated with responsive neurostimulation: final results of the RNS System Pivotal trial. *Epilepsia,* 55**,** 432-41.

83. HERRMANN, M., PUSCEDDU, I., MÄRZ, W. & HERRMANN, W. 2018. Telomere biology and age-related diseases. *Clin Chem Lab Med,* 56**,** 1210-1222.

84. HEUZEROTH, H., WAWRA, M., FIDZINSKI, P., DAG, R. & HOLTKAMP, M. 2019. The 4-Aminopyridine Model of Acute Seizures in vitro Elucidates Efficacy of New Antiepileptic Drugs. *Front Neurosci,* 13**,** 677.

85. HILDEBRAND, M. S., DAHL, H.-H. M., DAMIANO, J. A., SMITH, R. J. H., SCHEFFER, I. E. & BERKOVIC, S. F. 2013. Recent advances in the molecular genetics of epilepsy. *Journal of Medical Genetics,* 50**,** 271-279.

86. HILL, M. W., WONG, M., AMARAKONE, A. & ROTHMAN, S. M. 2000. Rapid cooling aborts seizure-like activity in rodent hippocampal-entorhinal slices. *Epilepsia,* 41**,** 1241-8.

87. HILL, R. A., TONG, L., YUAN, P., MURIKINATI, S., GUPTA, S. & GRUTZENDLER, J. 2015. Regional Blood Flow in the Normal and Ischemic Brain Is Controlled by Arteriolar Smooth Muscle Cell Contractility and Not by Capillary Pericytes. *Neuron,* 87**,** 95-110.

88. HOREL, J. A., VOYTKO, M. L. & SALSBURY, K. G. 1984. Visual learning suppressed by cooling the temporal pole. *Behav Neurosci,* 98**,** 310-24.

89. HOU, Y., DAN, X., BABBAR, M., WEI, Y., HASSELBALCH, S. G., CROTEAU, D. L. & BOHR, V. A. 2019. Ageing as a risk factor for neurodegenerative disease. *Nature Reviews Neurology,* 15**,** 565-581.

90. HUANG, E. J. & REICHARDT, L. F. 2001. Neurotrophins: roles in neuronal development and function. *Annu Rev Neurosci,* 24**,** 677-736.

91. HUGHES, T. M., KULLER, L. H., BARINAS-MITCHELL, E. J., MCDADE, E. M., KLUNK, W. E., COHEN, A. D., MATHIS, C. A., DEKOSKY, S. T., PRICE, J. C. & LOPEZ, O. L. 2014. Arterial stiffness and β-amyloid progression in nondemented elderly adults. *JAMA Neurol,* 71**,** 562-8.

92. HUGHES, T. M., WAGENKNECHT, L. E., CRAFT, S., MINTZ, A., HEISS, G., PALTA, P., WONG, D., ZHOU, Y., KNOPMAN, D., MOSLEY, T. H. & GOTTESMAN, R. F. 2018. Arterial

stiffness and dementia pathology: Atherosclerosis Risk in Communities (ARIC)-PET Study. *Neurology,* 90**,** e1248-e1256.

93. IACCARINO, H. F., SINGER, A. C., MARTORELL, A. J., RUDENKO, A., GAO, F., GILLINGHAM, T. Z., MATHYS, H., SEO, J., KRITSKIY, O., ABDURROB, F., ADAIKKAN, C., CANTER, R. G., RUEDA, R., BROWN, E. N., BOYDEN, E. S. & TSAI, L.-H. 2016. Gamma frequency entrainment attenuates amyloid load and modifies microglia. *Nature,* 540**,** 230-235.

94. IADECOLA, C. 1993. Regulation of the cerebral microcirculation during neural activity: is nitric oxide the missing link? *Trends Neurosci,* 16**,** 206-14.

95. IADECOLA, C. 2004. Neurovascular regulation in the normal brain and in Alzheimer's disease. *Nature Reviews Neuroscience,* 5**,** 347-360.

96. IADECOLA, C. 2013. The pathobiology of vascular dementia. *Neuron,* 80**,** 844-66.

97. IADECOLA, C. 2017. The Neurovascular Unit Coming of Age: A Journey through Neurovascular Coupling in Health and Disease. *Neuron,* 96**,** 17-42.

98. IMOTO, H., FUJII, M., UCHIYAMA, J., FUJISAWA, H., NAKANO, K., KUNITSUGU, I., NOMURA, S., SAITO, T. & SUZUKI, M. 2006. Use of a Peltier chip with a newly devised local brain-cooling system for neocortical seizures in the rat. Technical note. *J Neurosurg,* 104**,** 150-6.

99. ITO, H., KANNO, I., IBARAKI, M., HATAZAWA, J. & MIURA, S. 2003. Changes in human cerebral blood flow and cerebral blood volume during hypercapnia and hypocapnia measured by positron emission tomography. *J Cereb Blood Flow Metab,* 23**,** 665-70.

100. ITURRIA-MEDINA, Y., SOTERO, R. C., TOUSSAINT, P. J., MATEOS-PÉREZ, J. M. & EVANS, A. C. 2016. Early role of vascular dysregulation on late-onset Alzheimer's disease based on multifactorial data-driven analysis. *Nat Commun,* 7**,** 11934.

101. JALLON, P., LOISEAU, P. & LOISEAU, J. 2001. Newly Diagnosed Unprovoked Epileptic Seizures: Presentation at Diagnosis in CAROLE Study. *Epilepsia,* 42**,** 464-475.

102. JEHI, L. 2018. The Epileptogenic Zone: Concept and Definition. *Epilepsy Curr,* 18**,** 12-16.

103. JEONG, S. W., LEE, S. K., KIM, K. K., KIM, H., KIM, J. Y. & CHUNG, C. K. 1999. Prognostic Factors in Anterior Temporal Lobe Resections for Mesial Temporal Lobe Epilepsy: Multivariate Analysis. *Epilepsia,* 40**,** 1735-1739.

104. JESSEN, N. A., MUNK, A. S., LUNDGAARD, I. & NEDERGAARD, M. 2015. The Glymphatic System: A Beginner's Guide. *Neurochem Res,* 40**,** 2583-99.

105. KANNER, A. M. & BICCHI, M. M. 2022. Antiseizure Medications for Adults With Epilepsy: A Review. *JAMA,* 327**,** 1269-1281.

106. KATYAYAN, A. & DIAZ-MEDINA, G. 2021. Epilepsy: Epileptic Syndromes and Treatment. *Neurologic Clinics,* 39**,** 779-795.

107. KELLEHER, R. J. & SOIZA, R. L. 2013. Evidence of endothelial dysfunction in the development of Alzheimer's disease: Is Alzheimer's a vascular disorder? *Am J Cardiovasc Dis,* 3**,** 197-226.

108. KELSEY, J. E., SANDERSON, K. L. & FRYE, C. A. 2000. Perforant path stimulation in rats produces seizures, loss of hippocampal neurons, and a deficit in spatial mapping which are reduced by prior MK-801. *Behav Brain Res,* 107**,** 59-69.

109. KITAGUCHI, H., TOMIMOTO, H., IHARA, M., SHIBATA, M., UEMURA, K., KALARIA, R. N., KIHARA, T., ASADA-UTSUGI, M., KINOSHITA, A. & TAKAHASHI, R. 2009. Chronic cerebral hypoperfusion accelerates amyloid β deposition in APPSwInd transgenic mice. *Brain Research,* 1294**,** 202-210.

110. KOLLER, A. & TOTH, P. 2012. Contribution of flow-dependent vasomotor mechanisms to the autoregulation of cerebral blood flow. *J Vasc Res,* 49**,** 375-89.

111. KOSSOFF, E. H. & DORWARD, J. L. 2008. The Modified Atkins Diet. *Epilepsia,* 49**,** 37-41.

112. KRAWUTSCHKE, C., KOESLING, D. & RUSSWURM, M. 2015. Cyclic GMP in Vascular Relaxation. *Arteriosclerosis, Thrombosis, and Vascular Biology,* 35**,** 2011-2019.

113. KRESS, B. T., ILIFF, J. J., XIA, M., WANG, M., WEI, H. S., ZEPPENFELD, D., XIE, L., KANG, H., XU, Q., LIEW, J. A., PLOG, B. A., DING, F., DEANE, R. & NEDERGAARD, M. 2014. Impairment of paravascular clearance pathways in the aging brain. *Ann Neurol,* 76**,** 845-61.

114. KWAN, P., ARZIMANOGLOU, A., BERG, A. T., BRODIE, M. J., ALLEN HAUSER, W., MATHERN, G., MOSHÉ, S. L., PERUCCA, E., WIEBE, S. & FRENCH, J. 2010. Definition of drug resistant epilepsy: consensus proposal by the ad hoc Task Force of the ILAE Commission on Therapeutic Strategies. *Epilepsia,* 51**,** 1069-77.

115. KWAN, P. & BRODIE, M. J. 2000. Early Identification of Refractory Epilepsy. *New England Journal of Medicine,* 342**,** 314-319.

116. KWAN, P. & BRODIE, M. J. 2001. Effectiveness of First Antiepileptic Drug. *Epilepsia,* 42**,** 1255-1260.

117. LANG, B., KAHNAU, P., HOHLBAUM, K., MIESKE, P., ANDRESEN, N. P., BOON, M. N., THÖNE-REINEKE, C., LEWEJOHANN, L. & DIEDERICH, K. 2023. Challenges and advanced concepts for the assessment of learning and memory function in mice. *Front Behav Neurosci,* 17**,** 1230082.

118. LAVRNJA, I., PARABUCKI, A., BRKIC, P., JOVANOVIC, T., DACIC, S., SAVIC, D., PANTIC, I., STOJILJKOVIC, M. & PEKOVIC, S. 2015. Repetitive hyperbaric oxygenation attenuates reactive astrogliosis and suppresses expression of inflammatory mediators in the rat model of brain injury. *Mediators Inflamm,* 2015**,** 498405.

119. LAZOW, S. P., THADANI, V. M., GILBERT, K. L., MORSE, R. P., BUJARSKI, K. A., KULANDAIVEL, K., ROTH, R. M., SCOTT, R. C., ROBERTS, D. W. & JOBST, B. C. 2012. Outcome of frontal lobe epilepsy surgery. *Epilepsia,* 53**,** 1746-1755.

120. LECRUX, C., TOUSSAY, X., KOCHARYAN, A., FERNANDES, P., NEUPANE, S., LÉVESQUE, M., PLAISIER, F., SHMUEL, A., CAULI, B. & HAMEL, E. 2011. Pyramidal neurons are "neurogenic hubs" in the neurovascular coupling response to whisker stimulation. *J Neurosci,* 31**,** 9836-47.

121. LEE, H. J., PARK, C. Y., LEE, J. H., YANG, H. S., KIM, J. H., BAN, M. J. & MOON, I. S. 2012. Therapeutic effects of carbogen inhalation and lipo-prostaglandin E1 in sudden hearing loss. *Yonsei Med J,* 53**,** 999-1004.

122. LEW, S. M. 2014. Hemispherectomy in the treatment of seizures: a review. *Transl Pediatr,* 3**,** 208-17.

123. LEW, S. M., MATTHEWS, A. E., HARTMAN, A. L. & HARANHALLI, N. 2013. Posthemispherectomy hydrocephalus: results of a comprehensive, multiinstitutional review. *Epilepsia,* 54**,** 383-9.

124. LIU, H., YANG, Y., WANG, Y., TANG, H., ZHANG, F., ZHANG, Y. & ZHAO, Y. 2018. Ketogenic diet for treatment of intractable epilepsy in adults: A meta-analysis of observational studies. *Epilepsia Open,* 3**,** 9-17.

125. LOMBER, S. G., PAYNE, B. R. & HOREL, J. A. 1999. The cryoloop: an adaptable reversible cooling deactivation method for behavioral or electrophysiological assessment of neural function. *J Neurosci Methods,* 86**,** 179-94.

126. LONGDEN, T. A., DABERTRAND, F., KOIDE, M., GONZALES, A. L., TYKOCKI, N. R., BRAYDEN, J. E., HILL-EUBANKS, D. & NELSON, M. T. 2017. Capillary K(+)-sensing initiates retrograde hyperpolarization to increase local cerebral blood flow. *Nat Neurosci,* 20**,** 717-726.

127. LONGDEN, T. A., HILL-EUBANKS, D. C. & NELSON, M. T. 2016. Ion channel networks in the control of cerebral blood flow. *J Cereb Blood Flow Metab,* 36**,** 492-512.

128. LÓPEZ-OTÍN, C., BLASCO, M. A., PARTRIDGE, L., SERRANO, M. & KROEMER, G. 2013. The hallmarks of aging. *Cell,* 153**,** 1194-217.

129. LÖSCHER, W. & KLEIN, P. 2021. The Pharmacology and Clinical Efficacy of Antiseizure Medications: From Bromide Salts to Cenobamate and Beyond. *CNS Drugs,* 35**,** 935-963.

130. LOVE, S. & MINERS, J. S. 2016. Cerebrovascular disease in ageing and Alzheimer's disease. *Acta Neuropathol,* 131**,** 645-58.

131. MAGGI, C. A. & MELI, A. 1986. Suitability of urethane anesthesia for physiopharmacological investigations in various systems. Part 1: General considerations. *Experientia,* 42**,** 109-14.

132. MAHLER, B., CARLSSON, S., ANDERSSON, T. & TOMSON, T. 2018. Risk for injuries and accidents in epilepsy: A prospective population-based cohort study. *Neurology,* 90**,** e779-e789.

133. MANIPPA, V., PALMISANO, A., FILARDI, M., VILELLA, D., NITSCHE, M. A., RIVOLTA, D. & LOGROSCINO, G. 2022. An update on the use of gamma (multi)sensory stimulation for Alzheimer's disease treatment. *Frontiers in Aging Neuroscience,* 14.

134. MARROSU, F., SERRA, A., MALECI, A., PULIGHEDDU, M., BIGGIO, G. & PIGA, M. 2003. Correlation between GABAA receptor density and vagus nerve stimulation in individuals with drug-resistant partial epilepsy. *Epilepsy Research,* 55**,** 59-70.

135. MASTERSON, K., VARGAS, M. I. & DELAVELLE, J. 2009. Postictal deficit mimicking stroke: role of perfusion CT. *J Neuroradiol,* 36**,** 48-51.

136. MEREDITH, M. A., KRYKLYWY, J., MCMILLAN, A. J., MALHOTRA, S., LUM-TAI, R. & LOMBER, S. G. 2011. Crossmodal reorganization in the early deaf switches sensory, but not behavioral roles of auditory cortex. *Proc Natl Acad Sci U S A,* 108**,** 8856-61.

137. MILLER, D. L., PAPAYANNOPOULOS, I. A., STYLES, J., BOBIN, S. A., LIN, Y. Y., BIEMANN, K. & IQBAL, K. 1993. Peptide compositions of the cerebrovascular and senile plaque core amyloid deposits of Alzheimer's disease. *Arch Biochem Biophys,* 301**,** 41-52.

138. MILOVANOVIĆ, J. R., JANKOVIĆ, S. M., MILOVANOVIĆ, D., RUŽIĆ ZEČEVIĆ, D., FOLIĆ, M., KOSTIĆ, M., RANKOVIĆ, G. & STEFANOVIĆ, S. 2020. Contemporary surgical management of drug-resistant focal epilepsy. *Expert Rev Neurother,* 20**,** 23-40.

139. MOHANRAJ, R. & BRODIE, M. J. 2006. Diagnosing refractory epilepsy: response to sequential treatment schedules. *Eur J Neurol,* 13**,** 277-82.

140. MORIYAMA, H., NOMURA, S., KIDA, H., INOUE, T., IMOTO, H., MARUTA, Y., FUJIYAMA, Y., MITSUSHIMA, D. & SUZUKI, M. 2019. Suppressive Effects of Cooling Compounds Icilin on Penicillin G-Induced Epileptiform Discharges in Anesthetized Rats. *Front Pharmacol,* 10**,** 652.

141. MORIYAMA, S., ICHINOSE, M., DOBASHI, K., MATSUTAKE, R., SAKAMOTO, M., FUJII, N. & NISHIYASU, T. 2022. Hypercapnia elicits differential vascular and blood flow responses in the cerebral circulation and active skeletal muscles in exercising humans. *Physiol Rep,* 10**,** e15274.

142. MOTAMEDI, G. K., SALAZAR, P., SMITH, E. L., LESSER, R. P., WEBBER, W. R. S., ORTINSKI, P. I., VICINI, S. & ROGAWSKI, M. A. 2006. Termination of epileptiform activity by cooling in rat hippocampal slice epilepsy models. *Epilepsy Research,* 70**,** 200-210.

143. MURDOCK, M. H., YANG, C.-Y., SUN, N., PAO, P.-C., BLANCO-DUQUE, C., KAHN, M. C., KIM, T., LAVOIE, N. S., VICTOR, M. B., ISLAM, M. R., GALIANA, F., LEARY, N., WANG, S., BUBNYS, A., MA, E., AKAY, L. A., SNEVE, M., QIAN, Y., LAI, C., MCCARTHY, M. M., KOPELL, N., KELLIS, M., PIATKEVICH, K. D., BOYDEN, E. S. & TSAI, L.-H. 2024. Multisensory gamma stimulation promotes glymphatic clearance of amyloid. *Nature,* 627**,** 149-156.

144. MURRAY, K. J. 1990. Cyclic AMP and mechanisms of vasodilation. *Pharmacol Ther,* 47**,** 329-45.

145. NAIR, D. R., LAXER, K. D., WEBER, P. B., MURRO, A. M., PARK, Y. D., BARKLEY, G. L., SMITH, B. J., GWINN, R. P., DOHERTY, M. J., NOE, K. H., ZIMMERMAN, R. S., BERGEY, G. K., ANDERSON, W. S., HECK, C., LIU, C. Y., LEE, R. W., SADLER, T., DUCKROW, R. B., HIRSCH, L. J., WHAREN, R. E., JR., TATUM, W., SRINIVASAN, S., MCKHANN, G. M., AGOSTINI, M. A., ALEXOPOULOS, A. V., JOBST, B. C., ROBERTS, D. W., SALANOVA, V., WITT, T. C., CASH, S. S., COLE, A. J., WORRELL, G. A., LUNDSTROM, B. N., EDWARDS, J. C., HALFORD, J. J., SPENCER, D. C., ERNST, L., SKIDMORE, C. T., SPERLING, M. R., MILLER, I., GELLER, E. B., BERG, M. J., FESSLER, A. J., RUTECKI, P., GOLDMAN, A. M., MIZRAHI, E. M., GROSS, R. E., SHIELDS, D. C., SCHWARTZ, T. H., LABAR, D. R., FOUNTAIN, N. B., ELIAS, W. J., OLEJNICZAK, P. W., VILLEMARETTE-PITTMAN, N. R., EISENSCHENK, S., ROPER, S. N., BOGGS, J. G., COURTNEY, T. A., SUN, F. T., SEALE, C. G., MILLER, K. L., SKARPAAS, T. L. & MORRELL, M. J. 2020. Nine-year prospective efficacy and safety of brain-responsive neurostimulation for focal epilepsy. *Neurology,* 95**,** e1244-e1256.

146. NASERI, N. N., WANG, H., GUO, J., SHARMA, M. & LUO, W. 2019. The complexity of tau in Alzheimer's disease. *Neurosci Lett,* 705**,** 183-194.

147. NEAL, E. G., CHAFFE, H., SCHWARTZ, R. H., LAWSON, M. S., EDWARDS, N., FITZSIMMONS, G., WHITNEY, A. & CROSS, J. H. 2008. The ketogenic diet for the treatment of childhood epilepsy: a randomised controlled trial. *Lancet Neurol,* 7**,** 500-6.

148. NEDERGAARD, M. & GOLDMAN, S. A. 2020. Glymphatic failure as a final common pathway to dementia. *Science,* 370**,** 50-56.

149. NGAI, A. C., KO, K. R., MORII, S. & WINN, H. R. 1988. Effect of sciatic nerve stimulation on pial arterioles in rats. *Am J Physiol,* 254**,** H133-9.

150. NIESVIZKY-KOGAN, I., BASS, M., GOLDENHOLZ, S. R. & GOLDENHOLZ, D. M. 2022. Focal Cooling for Drug-Resistant Epilepsy: A Review. *JAMA Neurol,* 79**,** 937-944.

151. NIPPERT, A. R., BIESECKER, K. R. & NEWMAN, E. A. 2018. Mechanisms Mediating Functional Hyperemia in the Brain. *Neuroscientist,* 24**,** 73-83.

152. NOGUEIRA, J., GERARDO, B., SANTANA, I., SIMÕES, M. R. & FREITAS, S. 2022. The Assessment of Cognitive Reserve: A Systematic Review of the Most Used Quantitative Measurement Methods of Cognitive Reserve for Aging. *Front Psychol,* 13**,** 847186.

153. NOMURA, S., FUJII, M., INOUE, T., HE, Y., MARUTA, Y., KOIZUMI, H., SUEHIRO, E., IMOTO, H., ISHIHARA, H., OKA, F., MATSUMOTO, M., OWADA, Y., YAMAKAWA, T. & SUZUKI, M. 2014. Changes in glutamate concentration, glucose metabolism, and

cerebral blood flow during focal brain cooling of the epileptogenic cortex in humans. *Epilepsia,* 55**,** 770-776.

154. NORTLEY, R., KORTE, N., IZQUIERDO, P., HIRUNPATTARASILP, C., MISHRA, A., JAUNMUKTANE, Z., KYRARGYRI, V., PFEIFFER, T., KHENNOUF, L., MADRY, C., GONG, H., RICHARD-LOENDT, A., HUANG, W., SAITO, T., SAIDO, T. C., BRANDNER, S., SETHI, H. & ATTWELL, D. 2019. Amyloid β oligomers constrict human capillaries in Alzheimer's disease via signaling to pericytes. *Science,* 365**,** eaav9518.

155. NTSAMBI-EBA, G., VAZ, G., DOCQUIER, M. A., VAN RIJCKEVORSEL, K. & RAFTOPOULOS, C. 2013. Patients with refractory epilepsy treated using a modified multiple subpial transection technique. *Neurosurgery,* 72**,** 890-7; discussion 897-8.

156. O'REGAN, M. 2005. Adenosine and the regulation of cerebral blood flow. *Neurol Res,* 27**,** 175-81.

157. OMMAYA, A. K. & BALDWIN, M. 1963. Extravascular Local Cooling of the Brain in Man. *Journal of Neurosurgery,* 20**,** 8-20.

158. ORLOWSKI, J. P., ERENBERG, G., LUEDERS, H. & CRUSE, R. P. 1984. Hypothermia and barbiturate coma for refractory status epilepticus. *Crit Care Med,* 12**,** 367-72.

159. PADAMSEY, Z. & ROCHEFORT, N. L. 2023. Paying the brain's energy bill. *Current Opinion in Neurobiology,* 78**,** 102668.

160. PAILLARD, T., ROLLAND, Y. & DE SOUTO BARRETO, P. 2015. Protective Effects of Physical Exercise in Alzheimer's Disease and Parkinson's Disease: A Narrative Review. *J Clin Neurol,* 11**,** 212-9.

161. PAULSON, O. B., STRANDGAARD, S. & EDVINSSON, L. 1990. Cerebral autoregulation. *Cerebrovascular and brain metabolism reviews,* 2**,** 161-192.

162. PENG, W., ACHARIYAR, T. M., LI, B., LIAO, Y., MESTRE, H., HITOMI, E., REGAN, S., KASPER, T., PENG, S., DING, F., BENVENISTE, H., NEDERGAARD, M. & DEANE, R. 2016. Suppression of glymphatic fluid transport in a mouse model of Alzheimer's disease. *Neurobiol Dis,* 93**,** 215-25.

163. PEPPIATT, C. M., HOWARTH, C., MOBBS, P. & ATTWELL, D. 2006. Bidirectional control of CNS capillary diameter by pericytes. *Nature,* 443**,** 700-4.

164. PFEIFER, H. H. & THIELE, E. A. 2005. Low-glycemic-index treatment: A liberalized ketogenic diet for treatment of intractable epilepsy. *Neurology,* 65**,** 1810-1812.

165. POLDERMAN, K. H. & HEROLD, I. 2009. Therapeutic hypothermia and controlled normothermia in the intensive care unit: Practical considerations, side effects, and cooling methods*. *Critical Care Medicine,* 37.

166. POLLANDT, S. & BLECK, T. P. 2018. Chapter 45 - Thermoregulation in epilepsy. *In:* ROMANOVSKY, A. A. (ed.) *Handbook of Clinical Neurology.* Elsevier.

167. PONCE, C. R., LOMBER, S. G. & BORN, R. T. 2008. Integrating motion and depth via parallel pathways. *Nat Neurosci,* 11**,** 216-23.

168. PUGLIATTI, M., BEGHI, E., FORSGREN, L., EKMAN, M. & SOBOCKI, P. 2007. Estimating the cost of epilepsy in Europe: a review with economic modeling. *Epilepsia,* 48**,** 2224-33.

169. QIU, L., NG, G., TAN, E. K., LIAO, P., KANDIAH, N. & ZENG, L. 2016. Chronic cerebral hypoperfusion enhances Tau hyperphosphorylation and reduces autophagy in Alzheimer's disease mice. *Sci Rep,* 6**,** 23964.

170. RAZ, L., BHASKAR, K., WEAVER, J., MARINI, S., ZHANG, Q., THOMPSON, J. F., ESPINOZA, C., IQBAL, S., MAPHIS, N. M., WESTON, L., SILLERUD, L. O., CAPRIHAN, A., PESKO, J. C., ERHARDT, E. B. & ROSENBERG, G. A. 2019. Hypoxia promotes tau hyperphosphorylation with associated neuropathology in vascular dysfunction. *Neurobiol Dis,* 126**,** 124-136.

171. REKHA, L., FARID, S. & ASHOK, P. 2013. Therapeutic Hypothermia: Adverse Events, Recognition, Prevention and Treatment Strategies. *In:* FARID, S. (ed.) *Therapeutic Hypothermia in Brain Injury.* Rijeka: IntechOpen.

172. REN, G., YAN, J., TAO, G., GAN, Y., LI, D., YAN, X., FU, Y., WANG, L., WANG, W., ZHANG, Z., YUE, F. & YANG, X. 2017. Rapid focal cooling attenuates cortical seizures in a primate epilepsy model. *Experimental Neurology,* 295**,** 202-210.

173. ROLSTON, J. D., DENG, H., WANG, D. D., ENGLOT, D. J. & CHANG, E. F. 2018. Multiple Subpial Transections for Medically Refractory Epilepsy: A Disaggregated Review of Patient-Level Data. *Neurosurgery,* 82**,** 613-620.

174. ROTHMAN, S. & YANG, X. F. 2003. Local Cooling: A Therapy for Intractable Neocortical Epilepsy. *Epilepsy Curr,* 3**,** 153-156.

175. ROY, C. S. & SHERRINGTON, C. S. 1890. On the Regulation of the Blood-supply of the Brain. *J Physiol,* 11**,** 85-158.17.

176. RUBINSKI, A., TOSUN, D., FRANZMEIER, N., NEITZEL, J., FRONTZKOWSKI, L., WEINER, M. & EWERS, M. 2021. Lower cerebral perfusion is associated with tau-PET in the entorhinal cortex across the Alzheimer's continuum. *Neurobiol Aging,* 102**,** 111-118.

177. RYVLIN, P., RHEIMS, S. & LHATOO, S. D. 2019. Risks and predictive biomarkers of sudden unexpected death in epilepsy patient. *Curr Opin Neurol,* 32**,** 205-212.

178. SAGARE, A. P., BELL, R. D. & ZLOKOVIC, B. V. 2012. Neurovascular dysfunction and faulty amyloid β-peptide clearance in Alzheimer disease. *Cold Spring Harb Perspect Med,* 2.

179. SARTORIUS, C. J. & BERGER, M. S. 1998. Rapid termination of intraoperative stimulation-evoked seizures with application of cold Ringer's lactate to the cortex: Technical note. *Journal of Neurosurgery,* 88**,** 349-351.

180. SCARMEAS, N., LEVY, G., TANG, M. X., MANLY, J. & STERN, Y. 2001. Influence of leisure activity on the incidence of Alzheimer's disease. *Neurology,* 57**,** 2236-42.

181. SCHAEFFER, S. & IADECOLA, C. 2021. Revisiting the neurovascular unit. *Nat Neurosci,* 24**,** 1198-1209.

182. SCHAUMBURG, H., BYCK, R., HERMAN, R. & ROSENGART, C. 1967. Peripheral nerve damage by cold. *Arch Neurol,* 16**,** 103-9.

183. SCHEFFER, I. E., BERKOVIC, S., CAPOVILLA, G., CONNOLLY, M. B., FRENCH, J., GUILHOTO, L., HIRSCH, E., JAIN, S., MATHERN, G. W., MOSHÉ, S. L., NORDLI, D. R., PERUCCA, E., TOMSON, T., WIEBE, S., ZHANG, Y. H. & ZUBERI, S. M. 2017. ILAE

classification of the epilepsies: Position paper of the ILAE Commission for Classification and Terminology. *Epilepsia,* 58**,** 512-521.

184. SCHMIDT, S. D., MAZZELLA, M. J., NIXON, R. A. & MATHEWS, P. M. 2012. Aβ measurement by enzyme-linked immunosorbent assay. *Methods Mol Biol,* 849**,** 507-27.

185. SEGAL, S. S. 2015. Integration and Modulation of Intercellular Signaling Underlying Blood Flow Control. *J Vasc Res,* 52**,** 136-57.

186. SEIFERT, G., CARMIGNOTO, G. & STEINHÄUSER, C. 2010. Astrocyte dysfunction in epilepsy. *Brain Research Reviews,* 63**,** 212-221.

187. SELKOE, D. J., YAMAZAKI, T., CITRON, M., PODLISNY, M. B., KOO, E. H., TEPLOW, D. B. & HAASS, C. 1996. The Role of APP Processing and Trafficking Pathways in the Formation of Amyloid β-Protein. *Annals of the New York Academy of Sciences,* 777**,** 57-64.

188. SHABIR, O., SHARP, P., REBOLLAR, M. A., BOORMAN, L., HOWARTH, C., WHARTON, S. B., FRANCIS, S. E. & BERWICK, J. 2020. Enhanced Cerebral Blood Volume under Normobaric Hyperoxia in the J20-hAPP Mouse Model of Alzheimer's Disease. *Scientific Reports,* 10**,** 7518.

189. SHAPIRA, R., SOLOMON, B., EFRATI, S., FRENKEL, D. & ASHERY, U. 2018. Hyperbaric oxygen therapy ameliorates pathophysiology of 3xTg-AD mouse model by attenuating neuroinflammation. *Neurobiol Aging,* 62**,** 105-119.

190. SHARMA, K. 2019. Cholinesterase inhibitors as Alzheimer's therapeutics (Review). *Mol Med Rep,* 20**,** 1479-1487.

191. SHARMA, S., RAKOCZY, S. & BROWN-BORG, H. 2010. Assessment of spatial memory in mice. *Life Sci,* 87**,** 521-36.

192. SHINNAR, S. & GLAUSER, T. A. 2002. Febrile seizures. *J Child Neurol,* 17 Suppl 1**,** S44-52.

193. SILVERMAN, A. & PETERSEN, N. H. 2024. Physiology, Cerebral Autoregulation. *StatPearls.* Treasure Island (FL): StatPearls Publishing

194. Copyright © 2024, StatPearls Publishing LLC.

195. SIMS, J. R., ZIMMER, J. A., EVANS, C. D., LU, M., ARDAYFIO, P., SPARKS, J., WESSELS, A. M., SHCHERBININ, S., WANG, H., MONKUL NERY, E. S., COLLINS, E. C., SOLOMON, P., SALLOWAY, S., APOSTOLOVA, L. G., HANSSON, O., RITCHIE, C., BROOKS, D. A., MINTUN, M., SKOVRONSKY, D. M. & INVESTIGATORS, T.-A. 2023. Donanemab in Early Symptomatic Alzheimer Disease: The TRAILBLAZER-ALZ 2 Randomized Clinical Trial. *JAMA,* 330**,** 512-527.

196. SOKOLOV, A. Y., MENGAL, M. & BERKOVICH, R. 2024. Menthol dural application alters meningeal arteries tone and enhances excitability of trigeminocervical neurons in rats. *Brain Research,* 1825**,** 148725.

197. SOURBRON, J., KLINKENBERG, S., VAN KUIJK, S. M. J., LAGAE, L., LAMBRECHTS, D., BRAAKMAN, H. M. H. & MAJOIE, M. 2020. Ketogenic diet for the treatment of pediatric epilepsy: review and meta-analysis. *Child's Nervous System,* 36**,** 1099-1109.

198. ŠOUREK, K. & TRÁVNÍČEK, V. 1970. General and local hypothermia of the brain in the treatment of intractable epilepsy. *Journal of Neurosurgery,* 33**,** 253-259.

199. SPENCER, S. & HUH, L. 2008. Outcomes of epilepsy surgery in adults and children. *Lancet Neurol,* 7**,** 525-37.

200. STERN, Y. 2002. What is cognitive reserve? Theory and research application of the reserve concept. *J Int Neuropsychol Soc,* 8**,** 448-60.

201. STERN, Y. 2009. Cognitive reserve. *Neuropsychologia,* 47**,** 2015-28.

202. STERN, Y., GURLAND, B., TATEMICHI, T. K., TANG, M. X., WILDER, D. & MAYEUX, R. 1994. Influence of education and occupation on the incidence of Alzheimer's disease. *Jama,* 271**,** 1004-10.

203. STRZELCZYK, A., GRIEBEL, C., LUX, W., ROSENOW, F. & REESE, J.-P. 2017. The Burden of Severely Drug-Refractory Epilepsy: A Comparative Longitudinal Evaluation of Mortality, Morbidity, Resource Use, and Cost Using German Health Insurance Data. *Frontiers in Neurology,* 8.

204. STUDY, N. G. M. R. C. C. F. A. A. 2001. Pathological correlates of late-onset dementia in a multicentre, community-based population in England and Wales. Neuropathology Group of the Medical Research Council Cognitive Function and Ageing Study (MRC CFAS). *Lancet,* 357**,** 169-75.

205. SUN, X., HE, G., QING, H., ZHOU, W., DOBIE, F., CAI, F., STAUFENBIEL, M., HUANG, L. E. & SONG, W. 2006. Hypoxia facilitates Alzheimer's disease pathogenesis by up-regulating BACE1 gene expression. *Proc Natl Acad Sci U S A,* 103**,** 18727-32.

206. SWEENEY, M. D., MONTAGNE, A., SAGARE, A. P., NATION, D. A., SCHNEIDER, L. S., CHUI, H. C., HARRINGTON, M. G., PA, J., LAW, M., WANG, D. J. J., JACOBS, R. E., DOUBAL, F. N., RAMIREZ, J., BLACK, S. E., NEDERGAARD, M., BENVENISTE, H.,

DICHGANS, M., IADECOLA, C., LOVE, S., BATH, P. M., MARKUS, H. S., AL-SHAHI SALMAN, R., ALLAN, S. M., QUINN, T. J., KALARIA, R. N., WERRING, D. J., CARARE, R. O., TOUYZ, R. M., WILLIAMS, S. C. R., MOSKOWITZ, M. A., KATUSIC, Z. S., LUTZ, S. E., LAZAROV, O., MINSHALL, R. D., REHMAN, J., DAVIS, T. P., WELLINGTON, C. L., GONZÁLEZ, H. M., YUAN, C., LOCKHART, S. N., HUGHES, T. M., CHEN, C. L. H., SACHDEV, P., O'BRIEN, J. T., SKOOG, I., PANTONI, L., GUSTAFSON, D. R., BIESSELS, G. J., WALLIN, A., SMITH, E. E., MOK, V., WONG, A., PASSMORE, P., BARKOF, F., MULLER, M., BRETELER, M. M. B., ROMÁN, G. C., HAMEL, E., SESHADRI, S., GOTTESMAN, R. F., VAN BUCHEM, M. A., ARVANITAKIS, Z., SCHNEIDER, J. A., DREWES, L. R., HACHINSKI, V., FINCH, C. E., TOGA, A. W., WARDLAW, J. M. & ZLOKOVIC, B. V. 2019. Vascular dysfunction-The disregarded partner of Alzheimer's disease. *Alzheimers Dement,* 15**,** 158-167.

207. SWINFORD, C. G., RISACHER, S. L., VOSMEIER, A., DEARDORFF, R., CHUMIN, E. J., DZEMIDZIC, M., WU, Y. C., GAO, S., MCDONALD, B. C., YODER, K. K., UNVERZAGT, F. W., WANG, S., FARLOW, M. R., BROSCH, J. R., CLARK, D. G., APOSTOLOVA, L. G., SIMS, J., WANG, D. J. & SAYKIN, A. J. 2023. Amyloid and tau pathology are associated with cerebral blood flow in a mixed sample of nondemented older adults with and without vascular risk factors for Alzheimer's disease. *Neurobiol Aging,* 130**,** 103-113.

208. TABET, N. 2006. Acetylcholinesterase inhibitors for Alzheimer's disease: anti-inflammatories in acetylcholine clothing! *Age Ageing,* 35**,** 336-8.

209. TAN, X. R., STEPHENSON, M. C., ALHADAD, S. B., LOH, K. W. Z., SOONG, T. W., LEE, J. K. W. & LOW, I. C. C. 2024. Elevated brain temperature under severe heat

exposure impairs cortical motor activity and executive function. *J Sport Health Sci,* 13**,** 233-244.

210. TANAKA, N., FUJII, M., IMOTO, H., UCHIYAMA, J., NAKANO, K., NOMURA, S., FUJISAWA, H., KUNITSUGU, I., SAITO, T. & SUZUKI, M. 2008. Effective suppression of hippocampal seizures in rats by direct hippocampal cooling with a Peltier chip. *J Neurosurg,* 108**,** 791-7.

211. TANZI, R. E. 2012. The genetics of Alzheimer disease. *Cold Spring Harb Perspect Med,* 2.

212. TCW, J. & GOATE, A. M. 2017. Genetics of β-Amyloid Precursor Protein in Alzheimer's Disease. *Cold Spring Harb Perspect Med,* 7.

213. THAKORE, P., ALI, S. & EARLEY, S. 2020. Chapter Five - Regulation of vascular tone by transient receptor potential ankyrin 1 channels. *In:* JACKSON, W. F. (ed.) *Current Topics in Membranes.* Academic Press.

214. THOMPSON, S. M., MASUKAWA, L. M. & PRINCE, D. A. 1985. Temperature dependence of intrinsic membrane properties and synaptic potentials in hippocampal CA1 neurons in vitro. *J Neurosci,* 5**,** 817-24.

215. THURMAN, D. J., LOGROSCINO, G., BEGHI, E., HAUSER, W. A., HESDORFFER, D. C., NEWTON, C. R., SCORZA, F. A., SANDER, J. W. & TOMSON, T. 2017. The burden of premature mortality of epilepsy in high-income countries: A systematic review from the Mortality Task Force of the International League Against Epilepsy. *Epilepsia,* 58**,** 17-26.

216. TRUNE, D. R. & NGUYEN-HUYNH, A. 2012. Vascular Pathophysiology in Hearing Disorders. *Semin Hear,* 33**,** 242-250.

217. VAN VLIET, E. A., DA COSTA ARAÚJO, S., REDEKER, S., VAN SCHAIK, R., ARONICA, E. & GORTER, J. A. 2007. Blood-brain barrier leakage may lead to progression of temporal lobe epilepsy. *Brain,* 130**,** 521-34.

218. VERROTTI, A., IAPADRE, G., DI FRANCESCO, L., ZAGAROLI, L. & FARELLO, G. 2020. Diet in the Treatment of Epilepsy: What We Know So Far. *Nutrients,* 12.

219. VEZZANI, A., FRENCH, J., BARTFAI, T. & BARAM, T. Z. 2011. The role of inflammation in epilepsy. *Nat Rev Neurol,* 7**,** 31-40.

220. VOLGUSHEV, M., KUDRYASHOV, I., CHISTIAKOVA, M., MUKOVSKI, M., NIESMANN, J. & EYSEL, U. T. 2004. Probability of transmitter release at neocortical synapses at different temperatures. *J Neurophysiol,* 92**,** 212-20.

221. WAKUYA, M., INOUE, T., IMOTO, H., MARUTA, Y., NOMURA, S., SUZUKI, M. & YAMAKAWA, T. 2022. Epileptic seizure-related changes in electrocorticogram, cortical temperature, and cerebral hemodynamics obtained via an implantable multimodal multichannel probe during preoperative monitoring: illustrative case. *J Neurosurg Case Lessons,* 3.

222. WANG, H., ZHANG, Y., TAN, G., CHEN, D., FU, Y. & LIU, L. 2023. Suicidality and epilepsy: A systematic review and meta-analysis. *Front Psychiatry,* 14**,** 1097516.

223. WANG, R. & REDDY, P. H. 2017. Role of Glutamate and NMDA Receptors in Alzheimer's Disease. *J Alzheimers Dis,* 57**,** 1041-1048.

224. WANG, Y., WEI, P., YAN, F., LUO, Y. & ZHAO, G. 2022. Animal Models of Epilepsy: A Phenotype-oriented Review. *Aging Dis,* 13**,** 215-231.

225. WATILA, M. M., BALARABE, S. A., OJO, O., KEEZER, M. R. & SANDER, J. W. 2018. Overall and cause-specific premature mortality in epilepsy: A systematic review. *Epilepsy & Behavior,* 87**,** 213-225.

226. WEBB, A. J. S., BIRKS, J. S., FEAKINS, K. A., LAWSON, A., DAWSON, J., ROTHMAN, A. M. K., WERRING, D. J., LLWYD, O., STEWART, C. R. & THOMAS, J. 2024. Cerebrovascular Effects of Sildenafil in Small Vessel Disease: The OxHARP Trial. *Circulation Research,* 135**,** 320-331.

227. WEINGARTEN, M. D., LOCKWOOD, A. H., HWO, S. Y. & KIRSCHNER, M. W. 1975. A protein factor essential for microtubule assembly. *Proc Natl Acad Sci U S A,* 72**,** 1858-62.

228. WELLER, R. O., SUBASH, M., PRESTON, S. D., MAZANTI, I. & CARARE, R. O. 2008. Perivascular drainage of amyloid-beta peptides from the brain and its failure in cerebral amyloid angiopathy and Alzheimer's disease. *Brain Pathol,* 18**,** 253-66.

229. WIBISONO, C., ROWE, N., BEAVIS, E., KEPREOTES, H., MACKIE, F. E., LAWSON, J. A. & CARDAMONE, M. 2015. Ten-year single-center experience of the ketogenic diet: factors influencing efficacy, tolerability, and compliance. *J Pediatr,* 166**,** 1030-6.e1.

230. WIESER, H., BLUME, W., FISH, D., GOLDENSOHN, E., HUFNAGEL, A., KING, D., SPERLING, M. & LUDERS, H. 2001. Proposal for a new classification of outcome with respect to epileptic seizures following epilepsy surgery. *Epilepsia (Series 4),* 42.

231. XIU, G., LI, X., LI, Q., YIN, Y., TANG, Q., LI, J., LING, J., LING, B. & YANG, Y. 2023. Role of hyperbaric oxygen therapy in PDGF-BB-mediated astrogliosis in traumatic brain injury rats associated with ERK1/2 signaling pathway inhibition. *European Journal of Medical Research,* 28**,** 99.

232. YANG, X.-F., KENNEDY, B. R., LOMBER, S. G., SCHMIDT, R. E. & ROTHMAN, S. M. 2006. Cooling produces minimal neuropathology in neocortex and hippocampus. *Neurobiology of Disease,* 23**,** 637-643.

233. YANG, X. F., OUYANG, Y., KENNEDY, B. R. & ROTHMAN, S. M. 2005. Cooling blocks rat hippocampal neurotransmission by a presynaptic mechanism: observations using 2-photon microscopy. *J Physiol,* 567**,** 215-24.

234. ZHANG, F., ECKMAN, C., YOUNKIN, S., HSIAO, K. K. & IADECOLA, C. 1997. Increased susceptibility to ischemic brain damage in transgenic mice overexpressing the amyloid precursor protein. *J Neurosci,* 17**,** 7655-61.

235. ZHANG, Z. H., FANG, X. B., XI, G. M., LI, W. C., LING, H. Y. & QU, P. 2010. Calcitonin gene-related peptide enhances CREB phosphorylation and attenuates tau protein phosphorylation in rat brain during focal cerebral ischemia/reperfusion. *Biomed Pharmacother,* 64**,** 430-6.

236. ZONTA, M., ANGULO, M. C., GOBBO, S., ROSENGARTEN, B., HOSSMANN, K.-A., POZZAN, T. & CARMIGNOTO, G. 2003. Neuron-to-astrocyte signaling is central to the dynamic control of brain microcirculation. *Nature Neuroscience,* 6**,** 43-50.